

COMPARATIVE STUDY IN THE USE OF 316SS, V-20Ti, AND Nb-1Zr AS A STRUCTURAL MATERIAL IN THE FIRST-WALL OF A TOKAMAK REACTOR	العنوان:
Al Morished, Mutlaq Hamad	المؤلف الرئيسي:
Johnson, Ernest F.(Super.)	مؤلفين آخرين:
1981	التاريخ الميلادي:
Princeton	موقع:
1 - 161	الصفحات:
617900	رقم MD:
رسائل جامعية	نوع المحتوى:
English	اللغة:
رسالة ماجستير	الدرجة العلمية:
Princeton University	الجامعة:
School of Engineering and Applied Science	الكلية:
الولايات المتحدة الأمريكية	الدولة:
Dissertations	قواعد المعلومات:
الهندسة النووية، فيزياء البلازما، المفاعلات النووية	مواضيع:
<a href="https://search.mandumah.com/Record/617900">https://search.mandumah.com/Record/617900</a>	رابط:

COMPARATIVE STUDY IN THE USE OF 316SS, V-20Ti, AND  
Nb-1Zr AS A STRUCTURAL MATERIAL IN THE FIRST-WALL OF  
A TOKAMAK REACTOR

by

MUTLAQ HAMAD ALMORISHED  
//

A Thesis Submitted to the Faculty  
of Princeton University in Partial  
Fulfillment of the Requirements  
for the Degree of Master of Science  
in Engineering

Advisor  
Ernest F. Johnson

Recommended for Acceptance by  
The Department of Chemical Engineering

June, 1981

COMPARATIVE STUDY IN THE USE OF 316SS, V-20Ti, AND Nb-1Zr AS A STRUCTURAL MATERIAL IN THE FIRST-WALL OF A TOKAMAK REACTOR	العنوان:
Al Morished, Mutlaq Hamad	المؤلف الرئيسي:
Johnson, Ernest F.(Super.)	مؤلفين آخرين:
1981	التاريخ الميلادي:
Princeton	موقع:
1 - 161	الصفحات:
617900	رقم MD:
رسائل جامعية	نوع المحتوى:
English	اللغة:
رسالة ماجستير	الدرجة العلمية:
Princeton University	الجامعة:
School of Engineering and Applied Science	الكلية:
الولايات المتحدة الأمريكية	الدولة:
Dissertations	قواعد المعلومات:
الهندسة النووية، فيزياء البلازما، المفاعلات النووية	مواضيع:
<a href="https://search.mandumah.com/Record/617900">https://search.mandumah.com/Record/617900</a>	رابط:

COMPARATIVE STUDY IN THE USE OF 316SS, V-20Ti, AND  
Nb-1Zr AS A STRUCTURAL MATERIAL IN THE FIRST-WALL OF  
A TOKAMAK REACTOR

by

MUTLAQ HAMAD ALMORISHED  
//

A Thesis Submitted to the Faculty  
of Princeton University in Partial  
Fulfillment of the Requirements  
for the Degree of Master of Science  
in Engineering

Advisor  
Ernest F. Johnson

Recommended for Acceptance by  
The Department of Chemical Engineering

June, 1981

To My Uncle

ABDULLA MUTLAQ ALMORISHED ALKHALDI

### Acknowledgements

It is a pleasure to thank my advisor, Dr. Ernest F. Johnson, for his great help in finishing this thesis. I would also like to thank Drs. F.W. Wiffen and J. Devan for their help in sending me helpful materials.

## TABLE OF CONTENTS

	<u>Page</u>
CHAPTER ONE	
1. Abstract . . . . .	1
2. General Introduction . . . . .	2
3. Ideal First-Wall . . . . .	4
4. Load to the Materials . . . . .	4
CHAPTER TWO	
Surface Radiation Damage . . . . .	10
1. Sputtering . . . . .	11
2. Blistering . . . . .	28
CHAPTER THREE	
Bulk Radiation Damage . . . . .	41
1. Swelling . . . . .	42
2. Embrittlement (Loss of Ductility) . . . . .	57
3. Transmutation . . . . .	64
4. Effect of Radiation in General on a Power Producing Tokamak . . . . .	67
CHAPTER FOUR	
Compatibility of the First-Wall Materials With Coolants . . . . .	70
1. Liquid Lithium . . . . .	70
2. Helium . . . . .	72
3. Molten Salt . . . . .	74
4. Water (H <sub>2</sub> O) . . . . .	74
Compatibility of the First-Wall Materials With Breeders . . . . .	78
1. Liquid Lithium . . . . .	78
2. Molten Salt . . . . .	79
3. Solid Breeder . . . . .	80
CHAPTER FIVE	
Mechanical and Thermal Properties (Irradiated) . . . . .	81
1. Yield Strength . . . . .	82
2. Creep Strength . . . . .	85
3. Fatigue . . . . .	94
4. Thermal Stress Parameter . . . . .	106
CHAPTER SIX	
Some General Properties of the Structural Materials . . . . .	
1. Fabricability and Joining . . . . .	108
2. Induced Radioactivity . . . . .	111

3. Cost . . . . .	117
4. Resources Availability (U.S.A.) . . . . .	118

CHAPTER SEVEN

Short Look Into how the Choice and Lifetime of the Structural Material will Influence the Economics of the Tokamak as a Power Producing Plant . . . . .	120
---	-----

CHAPTER EIGHT

Conclusion . . . . .	133
----------------------	-----

CHAPTER NINE

Appendix . . . . .	134
Hazards and Waste of Tokamak Fusion Reactors . . . . .	134



## Chapter One

1. Abstract
2. General Introduction
3. Ideal First-Wall
4. Load to the Materials

## 1. Abstract

The first-wall problem in Tokamak fusion reactors is of great importance to the nuclear fusion community, and it may be second in difficulty only to the plasma physics problem. In the last few years there has been great progress in the study of materials for use in the reactor first-wall. Most of these studies have been concerned with the use of 316SS. In this thesis two materials (Nb-1Zr and V-20Ti) are compared to 316SS as candidate structural materials for the first wall. The comparison includes insofar as available information permits, all of the relevant properties.

The factors which argue most strongly for the use of refractory metal alloys (V-20Ti and Nb-1Zr) in fusion reactor first-walls are: better surface performance in the presence of a plasma at temperatures of interest, their superior mechanical properties at temperatures above about 600°C, improved radiation resistance, much better physical and thermal properties, and potentially superior operation in liquid lithium cooled systems at high temperatures (especially Nb-1Zr).

Factors for which refractory metal alloys (V-20Ti and Nb-1Zr) are at a disadvantage relative to conventional structural alloys (316SS) include cost, more difficult fabrication and joining requirements, availability (especially in the United States), lack of an established industry, and in the area of gas - metal interactions.

The increased costs associated with the use of V-20Ti and Nb-1Zr (especially V-20Ti), both the raw material costs and fabricated structural costs and any additional costs associated with special hardware or systems which might be required to permit their use must be recoverable by permitting greater system efficiencies. If they are not, V-20Ti and Nb-1Zr will not likely be competitive with 316SS.

## 2. General Introduction

It is easy to strengthen the value judgment about the importance of materials development by examining the history of engineering. Modern heat engineering, commencing with Watt's steam engine and passing through the introduction of high speed transportation in the form of railroads and automobiles, would, of course, have been totally impossible without the development and wide use of ferrous metals. Modern aviation would have been equally impossible without aluminum and its alloys; jet engine engineering would not possible except for new high temperature alloys; and finally, fission reactors would have had a difficult time being economically useful without significant materials development in zirconium and stainless steel.<sup>1</sup>

We are equally dependent upon materials development for fusion. The materials problem of fusion will not be simply the development of one material which can withstand the intense bombardment of high energy fusion neutrons. They will include new and innovative developments in such specifically fusion areas as the effect of plasma radiation on surface, bulk, thermal, and mechanical properties of the materials.

In the last few years, there has been a great deal of progress in the study of first wall structural materials. Most of these studies have been concerned with two kinds of materials - stainless steel and refractory metal alloys.

Stainless steels have been around for more than twenty years, and we have a considerable knowledge of their properties from their use in the fission reactors.

In the case of refractory metal alloys, the information we have about them is small compared with stainless steel. The reasons for choosing the refractory metal alloys as first wall structural materials are: higher temperature capability, good compatibility with liquid alkali metal working fluids (liquid lithium), preliminary, but promising, radiation effects data, and more attractive physical and thermal properties (high melting point, high thermal stress parameter, high thermal conductivity and low thermal expansion).

The objective of this thesis is to examine the practicality of the refractory metal alloys (Nb-1Zr or V-20Ti) as a first wall structural materials in comparison with 316SS.

### 3. Ideal First-Wall

The first-wall of a fusion reactor is a critical component because it is exposed to a harsh environment and still has to maintain a near vacuum.

Ideally, one would like the structural members of a fusion reactor first-wall to retain the following properties during irradiation in order to assure vacuum tightness for the plasma and containment of the reactor coolant.

1. Reasonable ductility<sup>2</sup> ( $\geq 1\%$  uniform elongation)
2. Low creep rate<sup>2</sup> ( $\leq 10^{-7} \text{ hr}^{-1}$ )
3. Acceptable stress rupture life at reactor operating conditions<sup>2</sup> ( $\sim 10^5 \text{ hr}$ )
4. Long fatigue life during  $10^4 - 10^8$  thermal cycles.
5. Dimension stability (swelling  $\sim 10\%$  or less)

The above properties are assumed for a fusion reactor first-wall by comparing the first-wall of a fusion reactor to a fuel cladding material in a fission reactor. All the properties shown above (1-5) will be discussed in greater detail in the bulk radiation damage and the mechanical and thermal properties, chapters three and five respectively.

### 4. Loads on First-Wall Materials

The materials of the first-wall will be subjected to the following loads:

a) Neutrons close to the first wall:

neutrons from thermonuclear reactions:

energy: 14.1 MeV

flux:  $2 - 3 \times 10^{14} \text{ neutrons/cm}^2 \text{ sec}$

Neutron-back-shine from the blanket:<sup>3</sup>

energy: neutrons at all energy levels up to almost 14 MeV,  
peaking close to 0.1 MeV.

total flux:  $1 - 2 \times 10^{15}$  neutrons/cm<sup>2</sup> sec

flux close to 0.1 MeV:  $10^{14}$  neutrons/cm<sup>2</sup> sec

flux for neutrons with  $E > 1$  MeV: 40% of the total flux.

- b)  $\gamma$ -back-shine of the blanket on the first wall: most of the  $\gamma$ -radiation is produced by scattering processes of the neutrons inside the blanket:<sup>3</sup>

energy: up to 14 MeV

deposited power in the first wall:  $100 - 200$  W/cm<sup>3</sup> for the total neutron flux given in a.

- c) Bremsstrahlung of the plasma:

energy: covering the entire spectral range from close to  $1\text{\AA}$ <sup>o</sup> up to the plasma frequency of the reactor core, with peaking in the soft x-ray region.

deposited power on the first wall:  $40 - 50$  W/cm<sup>3</sup>.

- d) Synchrotron radiation:

energy: centered in the far infrared, total power of synchrotron radiation will exceed the power of bremsstrahlung considerably at high plasma temperatures (e.g. 50 keV). Deposited power at the first wall depends on the reflectivity of the first wall facing the plasma. The reflectivity is determined by the structure and composition of the damaged surface.

- e) Ions impinging on the first wall facing the plasma:  
energy: not well known, spectrum may be centered around 1-3 keV  
flux: not well known, may be  $10^{16}$  particles per  $\text{cm}^2$ , sec.  
composition: 48.4% D, 48.4% T, 3% He, 0.1 heavy ions from the wall.
- f) Pressure inside the vacuum vessel before ignition:  
 $10^{-3} - 10^{-2}$  torr ( $1.3 \times 10^{-6} - 1.3 \times 10^{-5}$  atm) D-T-mixture depending on reactor system.
- g) Temperature of the blanket:  
600 - 1000°C
- h) Pressure inside the cooling pipes:  
40 - 90 bar (39.5 - 88.8 atm) for gas-cooling
- i) Voltage at the H.F. coils:  
Up to 100 kV depending on the heating method by fast rising magnetic fields.

The numbers given for the different loads on the materials are taken from the European design.<sup>3</sup> Each design has different values; the ones given here are typical and provide a general idea of the loads on the first wall.

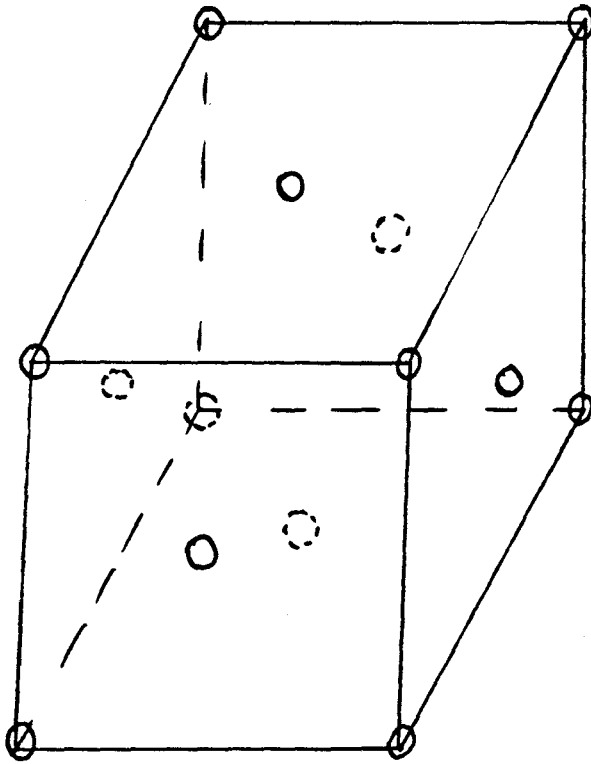
Table (1)

Some Important Properties of the Materials in Question

Property	Material		
	316SS	Nb-1Zr	V-20Ti
Thermal Conductivity <sup>4</sup> (k) W/m <sup>2</sup> °k at 500°C	22	31	26
Thermal Expansion <sup>4</sup> (α) 10 <sup>-6</sup> /°k at 500°C	18.3	7.9	10
Young's Modulus <sup>4</sup> (E) GW/m <sup>2</sup> at 500°C	160	65	112
Thermal Stress Coefficient <sup>4</sup> (αE/k) at 500°C	133	17	43
Density gm/cm <sup>3</sup> at 25°C	8.0	8.66	5.72
Crystal Structure	FCC	BCC	BCC
Melting Point, °C	1550	2400	1900
Hydrogen permeability Co- efficient (cm <sup>3</sup> (STP) mm/h cm <sup>2</sup> atm <sup>1/2</sup> )	0.02 at 500°C	200 at 1000°C	<200 at 800°C
Weldability	Excellent	Excellent	Good

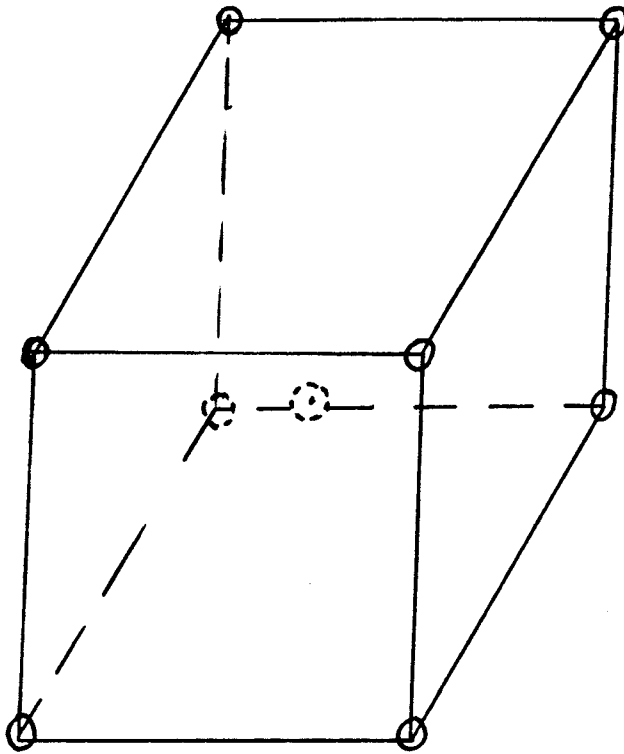


Figure (1)



Lattice of Face Centered Cubic (F.C.C.)

Figure (2)



Lattice of Body Centered Cubic (B.C.C.)

## Chapter Two

### Surface Radiation Damage

1. Sputtering
2. Blistering

## PLASMA MATERIALS INTERACTION

The burning of the D-T fuel in a fusion reactor results in three types of radiation that can strike the first wall; there are charged particles, electromagnetic radiation, and neutrons. The charged particles consist mostly of hydrogen isotopes, helium, and electrons. Other particles are created when atoms are sputtered off the surface of the first wall. The electromagnetic radiation is composed of line, synchrotron, bremsstrahlung, and recombination radiation. The first wall can also be struck by neutral atoms which are formed through a charge exchange at the plasma edge.<sup>5</sup>

The major consequence of the interaction of this radiation with the first wall is the introduction of unwanted impurities into the plasma. These impurities result in the production of line and or x-radiation which transport the energy out of the plasma, thereby cooling it. If impurities are present in sufficient quantities, the plasma may be quenched below the threshold temperature necessary for the fusion reaction to effectively sustain itself. These impurities can be a result of the sputtering of atoms from the free surface or from larger portions of material as a result of blister rupture or exfoliation. The number of sputtered atoms is essentially proportional to the number of incident particles, the energy of the particle, its mass, and its angle of incidence. As a result, sputtering yields for light ions will differ widely for the different target elements.

## 1. Sputtering

Sputtering is the removal of surface atoms due to the bombardment of a solid with energetic atoms, ions, electrons, and neutrons. It is caused by binary collisions between the incident particle and the atoms of the solid. The sputtering process can be regarded as radiation damage at the surface.

The most important quantity is the sputtering yield, defined as the mean number of atoms removed per incident particle - sputtering yield is not constant over the whole surface. It depends not only on the target material and ion energy, but also on the angle between the incident ion beam and the (local) surface normal, as well as on the orientation of the (local) crystal structure to the incident beam.

If  $\theta$  is the angle between the incident ion beam and the surface normal, then sputtering yield  $S(\theta)$ , defined as the number of sputtered atoms per incoming ion, can be expressed as a function of  $\theta$ . Using the theoretical work of Thompson and Stewart,<sup>6</sup> and Thompson,<sup>7</sup> one can write the following equation for the sputtering yield.

$$S(\theta) = (\pi^2/4) S_a^2 n E_a R \sec \theta \quad \dots \quad (1)$$

where

$S(\theta)$  = Sputtering yield, atoms/ion

$S$  = The crystal constant giving the number of atoms ejected per unit energy deposited in the surface layer of effective depth  $R$

$n$  = Density, atoms per unit volume

$E_a$  = The value of ion energy ( $E_i$ ) that allows the ion and atom to approach to a distance  $a$  in head on collision

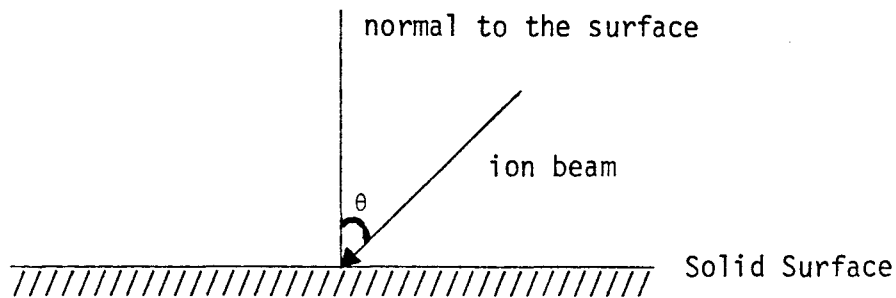
$$a = a_0(Z_1 Z_2)^{1/6}$$

$a_0$  = Bohr radius =  $0.53\text{\AA}$

$Z_1$  = Atomic number of the incoming ion

$Z_2$  = Atomic number of the solid surface atom

$\theta$  = Angle of sputtering



The angular dependence of sputtering is shown in Figure (1). At angles between  $70^\circ$  and  $80^\circ$  the sputtering yield increases to a maximum and then decreases to zero as  $\theta \rightarrow \frac{\pi}{2}$ .  $\theta_c$  represents the critical angle at which  $S(\theta)$  reaches its maximum value<sup>8</sup>. At this angle, reflection of incoming ions predominate over penetration and, therefore,  $S$  decreases rapidly. The critical angle for reflection was given by Lindhard,<sup>9</sup>

$$\frac{\pi}{2} - \theta_c = \frac{5a_0^2 n^{2/3} Z_1 Z_2 E_R}{(Z_1^{2/3} + Z_2^{2/3}) E_i} \dots \quad (2)$$

where

$E_R$  = Rydberg energy = 13.6 eV

$E_i$  = The energy of the incoming ion

It is understandable that  $\theta_c$  increases with increasing ion energy and decreases with either increasing  $Z_1$  or  $Z_2$ .

The exact form of the curve  $S(\theta)$  and the value of  $\theta_c$  depends not only on the ion type, energy and target material, but also undoubtedly on the depth distribution of the ion in the target. This parameter also includes crystal structure, grown-in impurities and many other factors. Data for sputtering yields are usually given as  $S_n$  at normal incidence ( $\theta = 0^\circ$ ).

Since in most cases we are interested in the thickness of material removed by sputtering (ion erosion process), we can express the depth  $d$  sputtered from a plane surface by:<sup>8</sup>

$$d = \frac{\phi t}{n} S(\theta) \cos \theta \quad \dots \quad (3)$$

where

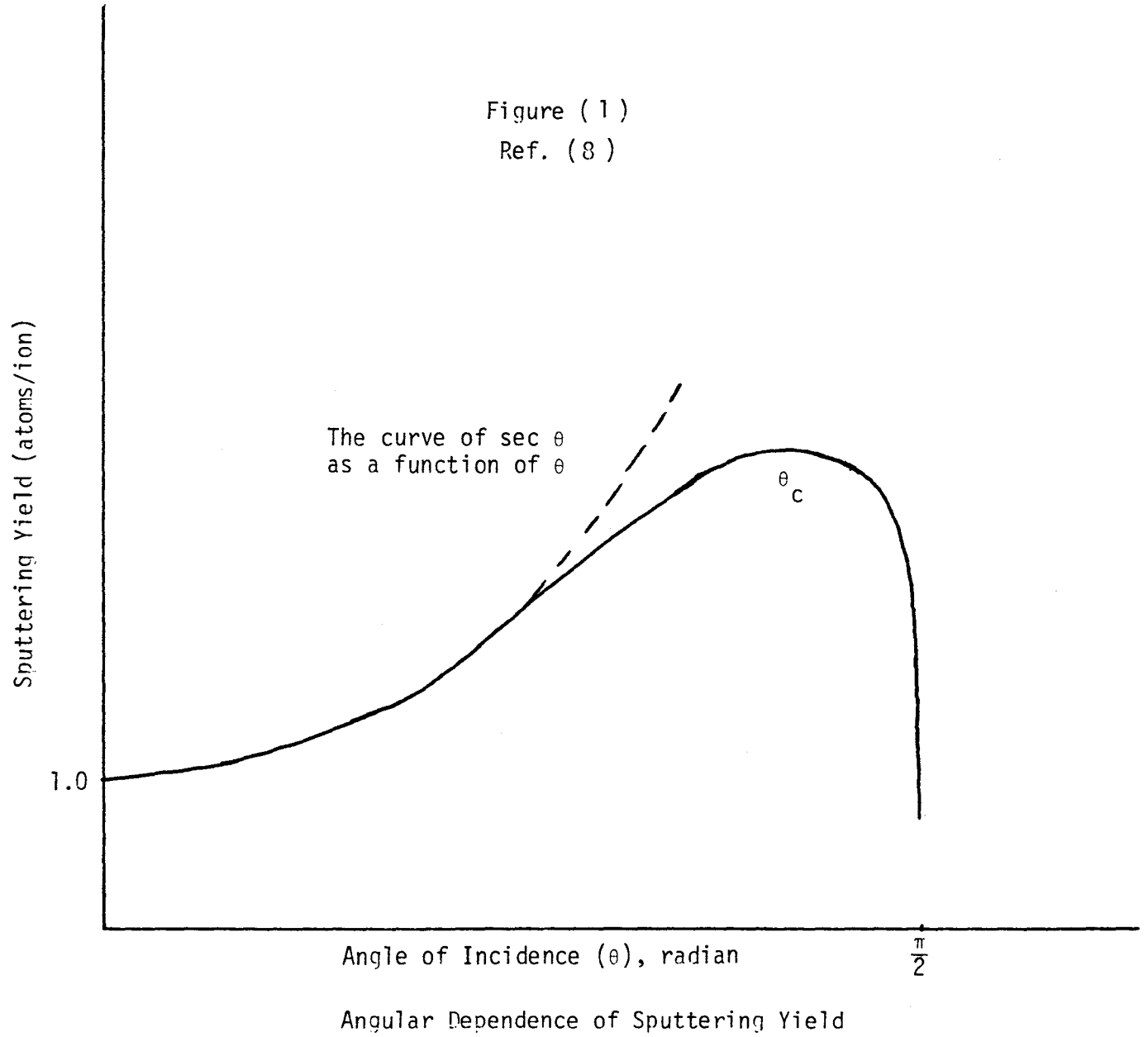
$\phi$  = number of ions per second striking unit area of surface normally

$t$  = time of bombardment

For normal incidence, the erosion depth is given by:<sup>8</sup>

$$d_n = \frac{\phi t}{n} S_n \quad \dots \quad (4)$$

Figure (1)  
Ref. (8)





### Sputtering and Tokamak

Sputtering of Tokamak first-wall by energetic particles and metal ions has at least two effects. First, adsorbed impurities are released into the plasma chamber and become a source of plasma contamination. Second, erosion of the wall material may occur after extensive sputtering. Although the magnitude of this erosion is unlikely to be so great as to cause structural weakening of the wall, alteration of the composition and microtopography could cause changes in the adsorption and sputtering characteristic of the wall.

Assuming a normal incidence, the energy dependent sputtering yield in Tokamak reactors is given by the following equation (from D.L. Smith,<sup>10</sup> TRANS AM NUC SOC).

$$S(E) = \frac{20}{U_0} Z_1^2 Z_2^2 \frac{M_1}{M_2} \frac{E}{(E+50 Z_1 Z_2)^2} \dots \quad (5)$$

where

$S(E)$  = Sputtering yield (atoms/ion)

$U_0$  = Surface binding energy (eV)

$Z_1$  = Incident particle atomic number

$Z_2$  = Material atomic number

$M_1$  = Incident particle mass number

$M_2$  = Material mass number

$E$  = Incident particle energy (eV)

It is assumed that no sputtering occurs below a threshold incident-particle energy. The threshold energy is the energy at which the maximum energy transferable is equivalent to the surface binding energy  $U_0$  of the target material.<sup>11</sup> The magnitude as a function of mass numbers of the projectile and target is given by

$$E_t = \frac{(M_1 + M_2)^2}{4M_1 M_2} U_0 \quad \dots \quad (6)$$

Therefore, the sputtering yield curves from Equation (5) are terminated at values given by Equation (6).

Parameter for Calculation of Sputtering Yields for 316SS, V-20Ti, and Nb-1Zr

Table (1)

Wall Material	Z	M	$U_0$ (eV)
316SS	26	55.9	4.3
V-20Ti	23	50.9	5.22
Nb-1Zr	41	92.9	7.6
Incident Particles			
H <sup>+</sup>	1	1	
D <sup>+</sup>	1	2	
T <sup>+</sup>	1	3	
He <sup>+</sup>	2	4	

Sputtering of 316SS

Using Equation (5), Equation (6), and Table (1)

$$H^+ \rightarrow E_t = \frac{(M_1 + M_2)^2}{4M_1 M_2} U_0 = 62.3 \text{ eV}$$

$$D^+ \rightarrow E_t = 32.2 \text{ eV}$$

$$T^+ \rightarrow E_t = 22.2 \text{ eV}$$

$$He^+ \rightarrow E_t = 17.3 \text{ eV}$$

$$Fe^+ \rightarrow E_t = 4.3 \text{ eV}$$

$$S(E) = \frac{20}{U_0} Z_1^2 Z_2^2 \frac{M_1}{M_2} \frac{E}{(E + 50 Z_1 Z_2)^2}$$

$$H^+ \rightarrow S(E) = \frac{20}{4.3} 1(26)^2 \frac{1}{55.9} \frac{100}{(100 + 50(1)(26))^2}$$

All energies (E) are in eV

$$S(100) = 2.9 \times 10^{-3} \text{ atoms/ion}$$

$$S(1000) = 1.1 \times 10^{-2} \text{ atoms/ion}$$

$$S(10000) = 4.4 \times 10^{-3} \text{ atoms/ion}$$

$$S(100000) = 5.5 \times 10^{-4} \text{ atoms/ion}$$

COMPARATIVE STUDY IN THE USE OF 316SS, V-20Ti, AND Nb-1Zr AS A STRUCTURAL MATERIAL IN THE FIRST-WALL OF A TOKAMAK REACTOR	العنوان:
Al Morished, Mutlaq Hamad	المؤلف الرئيسي:
Johnson, Ernest F.(Super.)	مؤلفين آخرين:
1981	التاريخ الميلادي:
Princeton	موقع:
1 - 161	الصفحات:
617900	رقم MD:
رسائل جامعية	نوع المحتوى:
English	اللغة:
رسالة ماجستير	الدرجة العلمية:
Princeton University	الجامعة:
School of Engineering and Applied Science	الكلية:
الولايات المتحدة الأمريكية	الدولة:
Dissertations	قواعد المعلومات:
الهندسة النووية، فيزياء البلازما، المفاعلات النووية	مواضيع:
<a href="https://search.mandumah.com/Record/617900">https://search.mandumah.com/Record/617900</a>	رابط:

## TABLE OF CONTENTS

	<u>Page</u>
CHAPTER ONE	
1. Abstract . . . . .	1
2. General Introduction . . . . .	2
3. Ideal First-Wall . . . . .	4
4. Load to the Materials . . . . .	4
CHAPTER TWO	
Surface Radiation Damage . . . . .	10
1. Sputtering . . . . .	11
2. Blistering . . . . .	28
CHAPTER THREE	
Bulk Radiation Damage . . . . .	41
1. Swelling . . . . .	42
2. Embrittlement (Loss of Ductility) . . . . .	57
3. Transmutation . . . . .	64
4. Effect of Radiation in General on a Power Producing Tokamak . . . . .	67
CHAPTER FOUR	
Compatibility of the First-Wall Materials With Coolants . . . . .	70
1. Liquid Lithium . . . . .	70
2. Helium . . . . .	72
3. Molten Salt . . . . .	74
4. Water (H <sub>2</sub> O) . . . . .	74
Compatibility of the First-Wall Materials With Breeders . . . . .	78
1. Liquid Lithium . . . . .	78
2. Molten Salt . . . . .	79
3. Solid Breeder . . . . .	80
CHAPTER FIVE	
Mechanical and Thermal Properties (Irradiated) . . . . .	81
1. Yield Strength . . . . .	82
2. Creep Strength . . . . .	85
3. Fatigue . . . . .	94
4. Thermal Stress Parameter . . . . .	106
CHAPTER SIX	
Some General Properties of the Structural Materials . . . . .	
1. Fabricability and Joining . . . . .	108
2. Induced Radioactivity . . . . .	111

3. Cost . . . . .	117
4. Resources Availability (U.S.A.) . . . . .	118

CHAPTER SEVEN

Short Look Into how the Choice and Lifetime of the Structural Material will Influence the Economics of the Tokamak as a Power Producing Plant . . . . .	120
---	-----

CHAPTER EIGHT

Conclusion . . . . .	133
----------------------	-----

CHAPTER NINE

Appendix . . . . .	134
Hazards and Waste of Tokamak Fusion Reactors . . . . .	134

COMPARATIVE STUDY IN THE USE OF 316SS, V-20Ti, AND Nb-1Zr AS A STRUCTURAL MATERIAL IN THE FIRST-WALL OF A TOKAMAK REACTOR	العنوان:
Al Morished, Mutlaq Hamad	المؤلف الرئيسي:
Johnson, Ernest F.(Super.)	مؤلفين آخرين:
1981	التاريخ الميلادي:
Princeton	موقع:
1 - 161	الصفحات:
617900	رقم MD:
رسائل جامعية	نوع المحتوى:
English	اللغة:
رسالة ماجستير	الدرجة العلمية:
Princeton University	الجامعة:
School of Engineering and Applied Science	الكلية:
الولايات المتحدة الأمريكية	الدولة:
Dissertations	قواعد المعلومات:
الهندسة النووية، فيزياء البلازما، المفاعلات النووية	مواضيع:
<a href="https://search.mandumah.com/Record/617900">https://search.mandumah.com/Record/617900</a>	رابط:

## Chapter One

1. Abstract
2. General Introduction
3. Ideal First-Wall
4. Load to the Materials



## 1. Abstract

The first-wall problem in Tokamak fusion reactors is of great importance to the nuclear fusion community, and it may be second in difficulty only to the plasma physics problem. In the last few years there has been great progress in the study of materials for use in the reactor first-wall. Most of these studies have been concerned with the use of 316SS. In this thesis two materials (Nb-1Zr and V-20Ti) are compared to 316SS as candidate structural materials for the first wall. The comparison includes insofar as available information permits, all of the relevant properties.

The factors which argue most strongly for the use of refractory metal alloys (V-20Ti and Nb-1Zr) in fusion reactor first-walls are: better surface performance in the presence of a plasma at temperatures of interest, their superior mechanical properties at temperatures above about 600°C, improved radiation resistance, much better physical and thermal properties, and potentially superior operation in liquid lithium cooled systems at high temperatures (especially Nb-1Zr).

Factors for which refractory metal alloys (V-20Ti and Nb-1Zr) are at a disadvantage relative to conventional structural alloys (316SS) include cost, more difficult fabrication and joining requirements, availability (especially in the United States), lack of an established industry, and in the area of gas - metal interactions.

The increased costs associated with the use of V-20Ti and Nb-1Zr (especially V-20Ti), both the raw material costs and fabricated structural costs and any additional costs associated with special hardware or systems which might be required to permit their use must be recoverable by permitting greater system efficiencies. If they are not, V-20Ti and Nb-1Zr will not likely be competitive with 316SS.

## 2. General Introduction

It is easy to strengthen the value judgment about the importance of materials development by examining the history of engineering. Modern heat engineering, commencing with Watt's steam engine and passing through the introduction of high speed transportation in the form of railroads and automobiles, would, of course, have been totally impossible without the development and wide use of ferrous metals. Modern aviation would have been equally impossible without aluminum and its alloys; jet engine engineering would not possible except for new high temperature alloys; and finally, fission reactors would have had a difficult time being economically useful without significant materials development in zirconium and stainless steel.<sup>1</sup>

We are equally dependent upon materials development for fusion. The materials problem of fusion will not be simply the development of one material which can withstand the intense bombardment of high energy fusion neutrons. They will include new and innovative developments in such specifically fusion areas as the effect of plasma radiation on surface, bulk, thermal, and mechanical properties of the materials.

In the last few years, there has been a great deal of progress in the study of first wall structural materials. Most of these studies have been concerned with two kinds of materials - stainless steel and refractory metal alloys.

Stainless steels have been around for more than twenty years, and we have a considerable knowledge of their properties from their use in the fission reactors.

In the case of refractory metal alloys, the information we have about them is small compared with stainless steel. The reasons for choosing the refractory metal alloys as first wall structural materials are: higher temperature capability, good compatibility with liquid alkali metal working fluids (liquid lithium), preliminary, but promising, radiation effects data, and more attractive physical and thermal properties (high melting point, high thermal stress parameter, high thermal conductivity and low thermal expansion).

The objective of this thesis is to examine the practicality of the refractory metal alloys (Nb-1Zr or V-20Ti) as a first wall structural materials in comparison with 316SS.

### 3. Ideal First-Wall

The first-wall of a fusion reactor is a critical component because it is exposed to a harsh environment and still has to maintain a near vacuum.

Ideally, one would like the structural members of a fusion reactor first-wall to retain the following properties during irradiation in order to assure vacuum tightness for the plasma and containment of the reactor coolant.

1. Reasonable ductility<sup>2</sup> ( $\geq 1\%$  uniform elongation)
2. Low creep rate<sup>2</sup> ( $\leq 10^{-7} \text{ hr}^{-1}$ )
3. Acceptable stress rupture life at reactor operating conditions<sup>2</sup> ( $\sim 10^5 \text{ hr}$ )
4. Long fatigue life during  $10^4 - 10^8$  thermal cycles.
5. Dimension stability (swelling  $\sim 10\%$  or less)

The above properties are assumed for a fusion reactor first-wall by comparing the first-wall of a fusion reactor to a fuel cladding material in a fission reactor. All the properties shown above (1-5) will be discussed in greater detail in the bulk radiation damage and the mechanical and thermal properties, chapters three and five respectively.

### 4. Loads on First-Wall Materials

The materials of the first-wall will be subjected to the following loads:

a) Neutrons close to the first wall:

neutrons from thermonuclear reactions:

energy: 14.1 MeV

flux:  $2 - 3 \times 10^{14} \text{ neutrons/cm}^2 \text{ sec}$

Neutron-back-shine from the blanket:<sup>3</sup>

energy: neutrons at all energy levels up to almost 14 MeV,  
peaking close to 0.1 MeV.

total flux:  $1 - 2 \times 10^{15}$  neutrons/cm<sup>2</sup> sec

flux close to 0.1 MeV:  $10^{14}$  neutrons/cm<sup>2</sup> sec

flux for neutrons with  $E > 1$  MeV: 40% of the total flux.

- b)  $\gamma$ -back-shine of the blanket on the first wall: most of the  $\gamma$ -radiation is produced by scattering processes of the neutrons inside the blanket:<sup>3</sup>

energy: up to 14 MeV

deposited power in the first wall:  $100 - 200$  W/cm<sup>3</sup> for the total neutron flux given in a.

- c) Bremsstrahlung of the plasma:

energy: covering the entire spectral range from close to  $1\text{\AA}$ <sup>o</sup> up to the plasma frequency of the reactor core, with peaking in the soft x-ray region.

deposited power on the first wall:  $40 - 50$  W/cm<sup>3</sup>.

- d) Synchrotron radiation:

energy: centered in the far infrared, total power of synchrotron radiation will exceed the power of bremsstrahlung considerably at high plasma temperatures (e.g. 50 keV). Deposited power at the first wall depends on the reflectivity of the first wall facing the plasma. The reflectivity is determined by the structure and composition of the damaged surface.

- e) Ions impinging on the first wall facing the plasma:  
energy: not well known, spectrum may be centered around 1-3 keV  
flux: not well known, may be  $10^{16}$  particles per  $\text{cm}^2$ , sec.  
composition: 48.4% D, 48.4% T, 3% He, 0.1 heavy ions from the wall.
- f) Pressure inside the vacuum vessel before ignition:  
 $10^{-3} - 10^{-2}$  torr ( $1.3 \times 10^{-6} - 1.3 \times 10^{-5}$  atm) D-T-mixture depending on reactor system.
- g) Temperature of the blanket:  
600 - 1000°C
- h) Pressure inside the cooling pipes:  
40 - 90 bar (39.5 - 88.8 atm) for gas-cooling
- i) Voltage at the H.F. coils:  
Up to 100 kV depending on the heating method by fast rising magnetic fields.

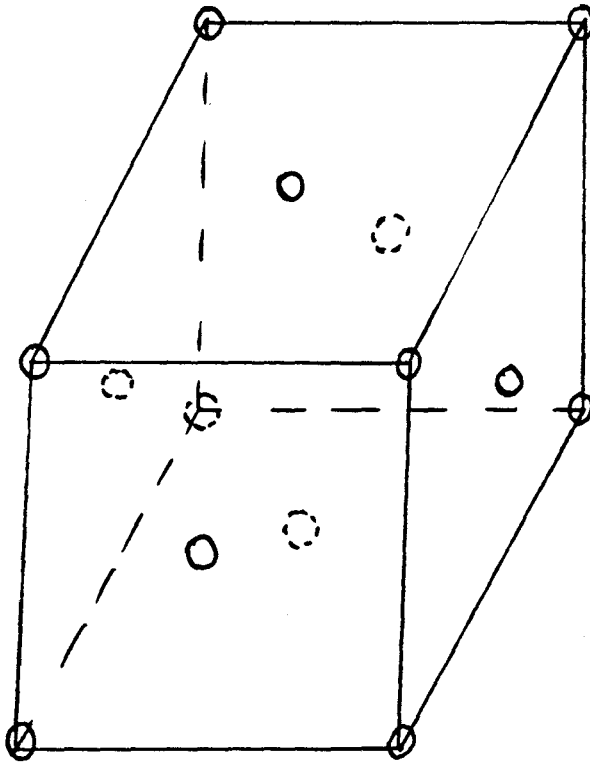
The numbers given for the different loads on the materials are taken from the European design.<sup>3</sup> Each design has different values; the ones given here are typical and provide a general idea of the loads on the first wall.

Table (1)

Some Important Properties of the Materials in Question

Property	Material		
	316SS	Nb-1Zr	V-20Ti
Thermal Conductivity <sup>4</sup> (k) W/m <sup>2</sup> °k at 500°C	22	31	26
Thermal Expansion <sup>4</sup> (α) 10 <sup>-6</sup> /°k at 500°C	18.3	7.9	10
Young's Modulus <sup>4</sup> (E) GW/m <sup>2</sup> at 500°C	160	65	112
Thermal Stress Coefficient <sup>4</sup> (αE/k) at 500°C	133	17	43
Density gm/cm <sup>3</sup> at 25°C	8.0	8.66	5.72
Crystal Structure	FCC	BCC	BCC
Melting Point, °C	1550	2400	1900
Hydrogen permeability Co- efficient (cm <sup>3</sup> (STP) mm/h cm <sup>2</sup> atm <sup>1/2</sup> )	0.02 at 500°C	200 at 1000°C	<200 at 800°C
Weldability	Excellent	Excellent	Good

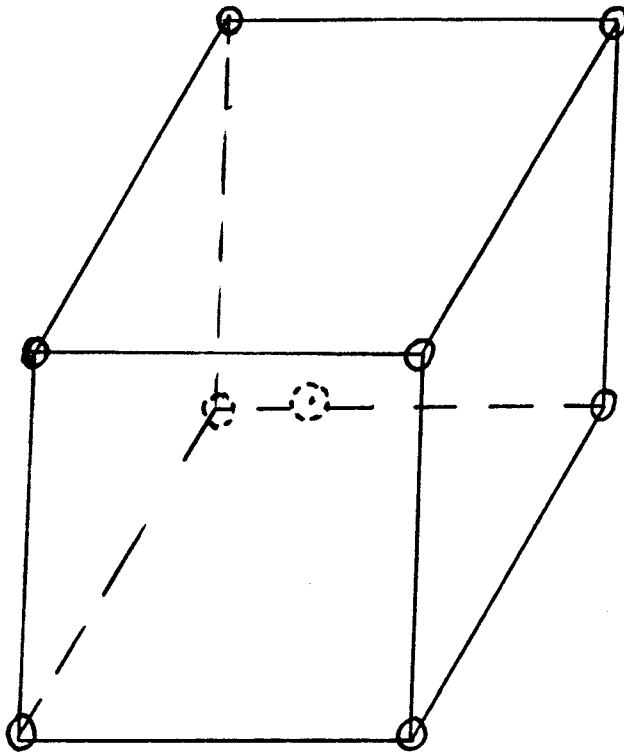
Figure (1)



Lattice of Face Centered Cubic (F.C.C.)



Figure (2)



Lattice of Body Centered Cubic (B.C.C.)

COMPARATIVE STUDY IN THE USE OF 316SS, V-20Ti, AND Nb-1Zr AS A STRUCTURAL MATERIAL IN THE FIRST-WALL OF A TOKAMAK REACTOR	العنوان:
Al Morished, Mutlaq Hamad	المؤلف الرئيسي:
Johnson, Ernest F.(Super.)	مؤلفين آخرين:
1981	التاريخ الميلادي:
Princeton	موقع:
1 - 161	الصفحات:
617900	رقم MD:
رسائل جامعية	نوع المحتوى:
English	اللغة:
رسالة ماجستير	الدرجة العلمية:
Princeton University	الجامعة:
School of Engineering and Applied Science	الكلية:
الولايات المتحدة الأمريكية	الدولة:
Dissertations	قواعد المعلومات:
الهندسة النووية، فيزياء البلازما، المفاعلات النووية	مواضيع:
<a href="https://search.mandumah.com/Record/617900">https://search.mandumah.com/Record/617900</a>	رابط:

## Chapter Two

### Surface Radiation Damage

1. Sputtering
2. Blistering

## PLASMA MATERIALS INTERACTION

The burning of the D-T fuel in a fusion reactor results in three types of radiation that can strike the first wall; there are charged particles, electromagnetic radiation, and neutrons. The charged particles consist mostly of hydrogen isotopes, helium, and electrons. Other particles are created when atoms are sputtered off the surface of the first wall. The electromagnetic radiation is composed of line, synchrotron, bremsstrahlung, and recombination radiation. The first wall can also be struck by neutral atoms which are formed through a charge exchange at the plasma edge.<sup>5</sup>

The major consequence of the interaction of this radiation with the first wall is the introduction of unwanted impurities into the plasma. These impurities result in the production of line and or x-radiation which transport the energy out of the plasma, thereby cooling it. If impurities are present in sufficient quantities, the plasma may be quenched below the threshold temperature necessary for the fusion reaction to effectively sustain itself. These impurities can be a result of the sputtering of atoms from the free surface or from larger portions of material as a result of blister rupture or exfoliation. The number of sputtered atoms is essentially proportional to the number of incident particles, the energy of the particle, its mass, and its angle of incidence. As a result, sputtering yields for light ions will differ widely for the different target elements.

## 1. Sputtering

Sputtering is the removal of surface atoms due to the bombardment of a solid with energetic atoms, ions, electrons, and neutrons. It is caused by binary collisions between the incident particle and the atoms of the solid. The sputtering process can be regarded as radiation damage at the surface.

The most important quantity is the sputtering yield, defined as the mean number of atoms removed per incident particle - sputtering yield is not constant over the whole surface. It depends not only on the target material and ion energy, but also on the angle between the incident ion beam and the (local) surface normal, as well as on the orientation of the (local) crystal structure to the incident beam.

If  $\theta$  is the angle between the incident ion beam and the surface normal, then sputtering yield  $S(\theta)$ , defined as the number of sputtered atoms per incoming ion, can be expressed as a function of  $\theta$ . Using the theoretical work of Thompson and Stewart,<sup>6</sup> and Thompson,<sup>7</sup> one can write the following equation for the sputtering yield.

$$S(\theta) = (\pi^2/4) S_a^2 n E_a R \sec \theta \quad \dots \quad (1)$$

where

$S(\theta)$  = Sputtering yield, atoms/ion

$S$  = The crystal constant giving the number of atoms ejected per unit energy deposited in the surface layer of effective depth  $R$

$n$  = Density, atoms per unit volume

$E_a$  = The value of ion energy ( $E_i$ ) that allows the ion and atom to approach to a distance  $a$  in head on collision

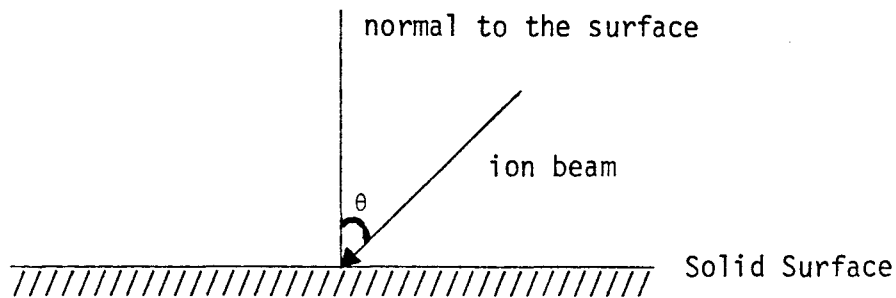
$$a = a_0(Z_1 Z_2)^{1/6}$$

$a_0$  = Bohr radius =  $0.53\text{\AA}$

$Z_1$  = Atomic number of the incoming ion

$Z_2$  = Atomic number of the solid surface atom

$\theta$  = Angle of sputtering



The angular dependence of sputtering is shown in Figure (1). At angles between  $70^\circ$  and  $80^\circ$  the sputtering yield increases to a maximum and then decreases to zero as  $\theta \rightarrow \frac{\pi}{2}$ .  $\theta_c$  represents the critical angle at which  $S(\theta)$  reaches its maximum value<sup>8</sup>. At this angle, reflection of incoming ions predominate over penetration and, therefore,  $S$  decreases rapidly. The critical angle for reflection was given by Lindhard,<sup>9</sup>

$$\frac{\pi}{2} - \theta_c = \frac{5a_0^2 n^{2/3} Z_1 Z_2 E_R}{(Z_1^{2/3} + Z_2^{2/3}) E_i} \dots \quad (2)$$

where

$E_R$  = Rydberg energy = 13.6 eV

$E_i$  = The energy of the incoming ion

It is understandable that  $\theta_c$  increases with increasing ion energy and decreases with either increasing  $Z_1$  or  $Z_2$ .

The exact form of the curve  $S(\theta)$  and the value of  $\theta_c$  depends not only on the ion type, energy and target material, but also undoubtedly on the depth distribution of the ion in the target. This parameter also includes crystal structure, grown-in impurities and many other factors. Data for sputtering yields are usually given as  $S_n$  at normal incidence ( $\theta = 0^\circ$ ).

Since in most cases we are interested in the thickness of material removed by sputtering (ion erosion process), we can express the depth  $d$  sputtered from a plane surface by:<sup>8</sup>

$$d = \frac{\phi t}{n} S(\theta) \cos \theta \quad \dots \quad (3)$$

where

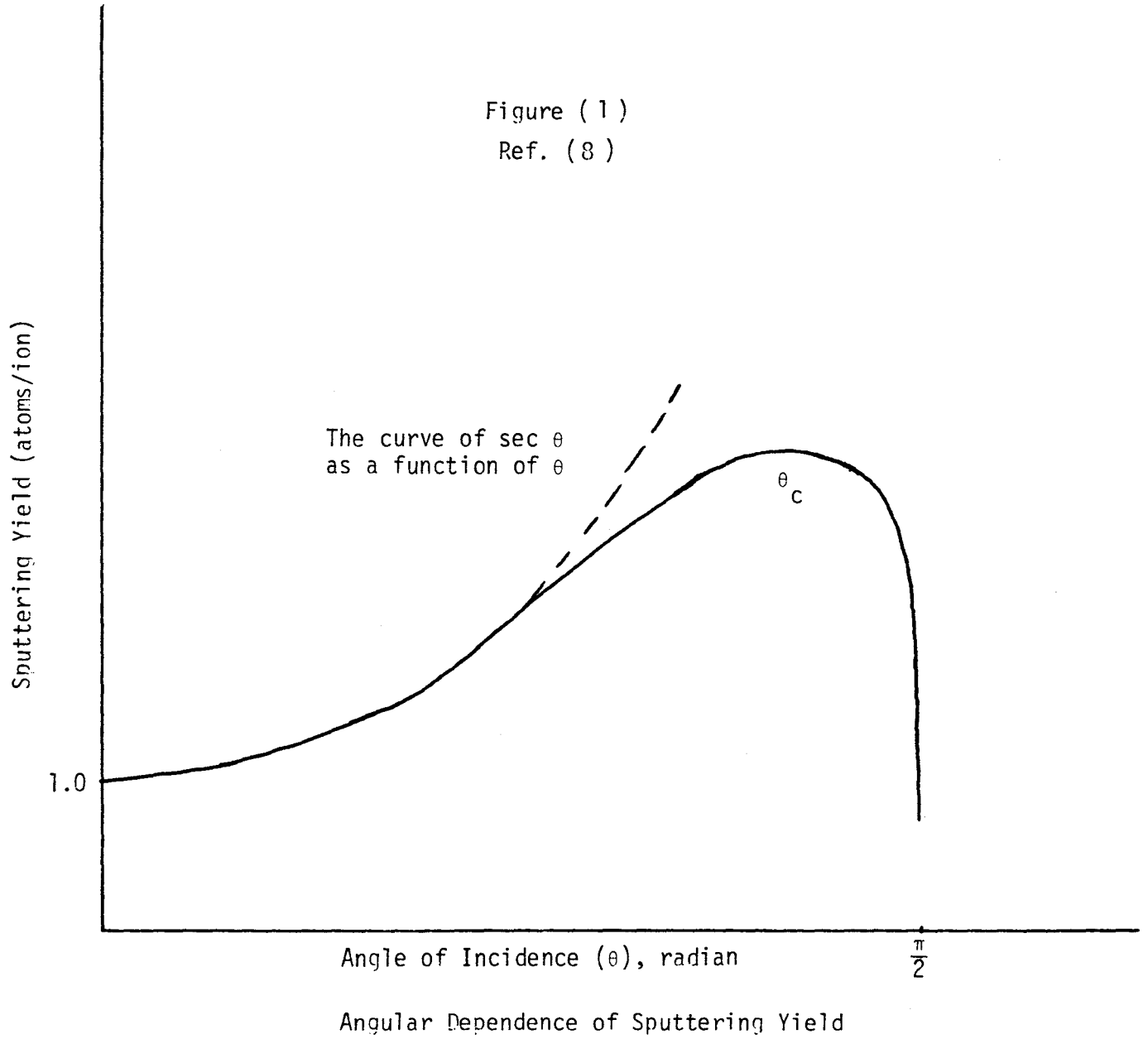
$\phi$  = number of ions per second striking unit area of surface normally

$t$  = time of bombardment

For normal incidence, the erosion depth is given by:<sup>8</sup>

$$d_n = \frac{\phi t}{n} S_n \quad \dots \quad (4)$$

Figure (1)  
Ref. (8)





### Sputtering and Tokamak

Sputtering of Tokamak first-wall by energetic particles and metal ions has at least two effects. First, adsorbed impurities are released into the plasma chamber and become a source of plasma contamination. Second, erosion of the wall material may occur after extensive sputtering. Although the magnitude of this erosion is unlikely to be so great as to cause structural weakening of the wall, alteration of the composition and microtopography could cause changes in the adsorption and sputtering characteristic of the wall.

Assuming a normal incidence, the energy dependent sputtering yield in Tokamak reactors is given by the following equation (from D.L. Smith,<sup>10</sup> TRANS AM NUC SOC).

$$S(E) = \frac{20}{U_0} Z_1^2 Z_2^2 \frac{M_1}{M_2} \frac{E}{(E+50 Z_1 Z_2)^2} \dots \quad (5)$$

where

$S(E)$  = Sputtering yield (atoms/ion)

$U_0$  = Surface binding energy (eV)

$Z_1$  = Incident particle atomic number

$Z_2$  = Material atomic number

$M_1$  = Incident particle mass number

$M_2$  = Material mass number

$E$  = Incident particle energy (eV)

It is assumed that no sputtering occurs below a threshold incident-particle energy. The threshold energy is the energy at which the maximum energy transferable is equivalent to the surface binding energy  $U_0$  of the target material.<sup>11</sup> The magnitude as a function of mass numbers of the projectile and target is given by

$$E_t = \frac{(M_1 + M_2)^2}{4M_1 M_2} U_0 \dots \quad (6)$$

Therefore, the sputtering yield curves from Equation (5) are terminated at values given by Equation (6).

Parameter for Calculation of Sputtering Yields for 316SS, V-20Ti, and Nb-1Zr

Table (1)

Wall Material	Z	M	$U_0$ (eV)
316SS	26	55.9	4.3
V-20Ti	23	50.9	5.22
Nb-1Zr	41	92.9	7.6
Incident Particles			
H <sup>+</sup>	1	1	
D <sup>+</sup>	1	2	
T <sup>+</sup>	1	3	
He <sup>+</sup>	2	4	

Sputtering of 316SS

Using Equation (5), Equation (6), and Table (1)

$$H^+ \rightarrow E_t = \frac{(M_1 + M_2)^2}{4M_1 M_2} U_0 = 62.3 \text{ eV}$$

$$D^+ \rightarrow E_t = 32.2 \text{ eV}$$

$$T^+ \rightarrow E_t = 22.2 \text{ eV}$$

$$He^+ \rightarrow E_t = 17.3 \text{ eV}$$

$$Fe^+ \rightarrow E_t = 4.3 \text{ eV}$$

$$S(E) = \frac{20}{U_0} Z_1^2 Z_2^2 \frac{M_1}{M_2} \frac{E}{(E + 50 Z_1 Z_2)^2}$$

$$H^+ \rightarrow S(E) = \frac{20}{4.3} 1(26)^2 \frac{1}{55.9} \frac{100}{(100 + 50(1)(26))^2}$$

All energies (E) are in eV

$$S(100) = 2.9 \times 10^{-3} \text{ atoms/ion}$$

$$S(1000) = 1.1 \times 10^{-2} \text{ atoms/ion}$$

$$S(10000) = 4.4 \times 10^{-3} \text{ atoms/ion}$$

$$S(100000) = 5.5 \times 10^{-4} \text{ atoms/ion}$$

$D^+ \rightarrow 316SS$

$$S = \frac{20}{4.3} (1)^2 (26)^2 \frac{2}{55.9} \frac{100}{(100+50(1)(26))^2}$$

$$S(100) = 5.7 \times 10^{-3} \text{ atoms/ion}$$

$$S(1000) = 2.1 \times 10^{-2} \text{ atoms/ion}$$

$$S(10000) = 8.8 \times 10^{-3} \text{ atoms/ion}$$

$$S(100000) = 1.1 \times 10^{-3} \text{ atoms/ion}$$

$T^+ \rightarrow 316SS$

$$S = \frac{20}{4.3} (1)^2 (26)^2 \frac{3}{55.9} \frac{100}{(100+50(26))^2}$$

$$S(100) = 8.6 \times 10^{-3} \text{ atoms/ion}$$

$$S(1000) = 3.2 \times 10^{-2} \text{ atoms/ion}$$

$$S(10000) = 1.3 \times 10^{-2} \text{ atoms/ion}$$

$$S(100000) = 1.6 \times 10^{-3} \text{ atoms/ion}$$

$He^+ \rightarrow 316SS$

$$S = \frac{20}{4.3} (2)^2 (26)^2 \frac{4}{55.9} \frac{100}{(100+50(2)(26))^2}$$

$$S(100) = 1.2 \times 10^{-2} \text{ atoms/ion}$$

$$S(1000) = 6.9 \times 10^{-2} \text{ atoms/ion}$$

$$S(10000) = 5.7 \times 10^{-2} \text{ atoms/ion}$$

$$S(100000) = 8.5 \times 10^{-3} \text{ atoms/ion}$$

Fe → 316SS (Self-Sputtering)

$$S(E) = \frac{20}{4.3} (26)^2 (26)^2 \frac{55.9}{55.9} \frac{100}{(100+50(26)(26))^2}$$

$$S(100) = 1.8 \times 10^{-1} \text{ atoms/ion}$$

$$S(1000) = 1.8 \text{ atoms/ion}$$

$$S(10000) = 11.1 \text{ atoms/ion}$$

$$S(100000) = 11.9 \text{ atoms/ion}$$

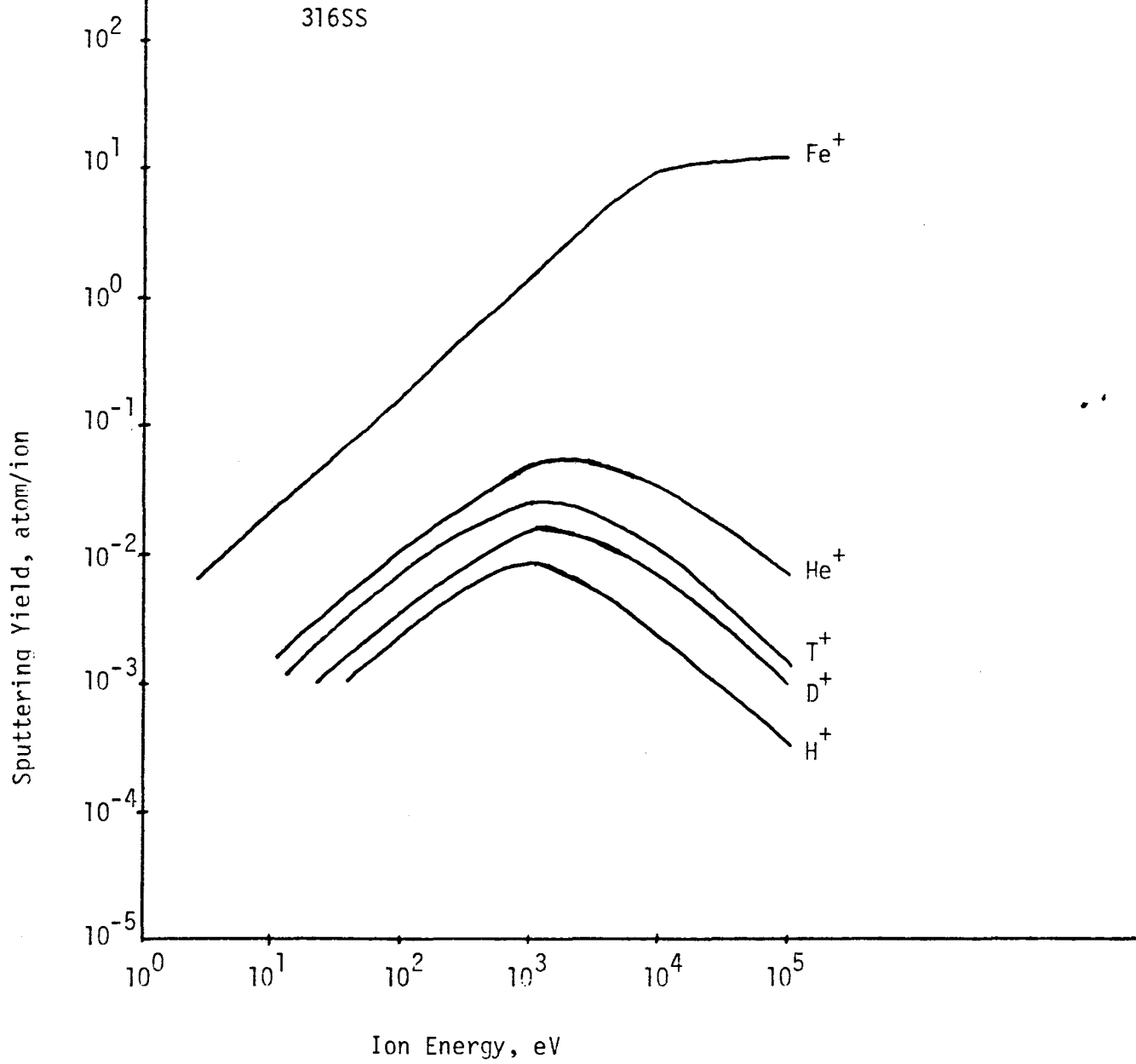
Theses values of sputtering yields are shown in Figure ( 2 ).

#### Sputtering of V-20Ti:

Using Equation ( 5 ), Equation ( 6 ), and Table ( 1 )

Incident Particle	Material	Terminated Values ( $E_t$ ) (eV)
H <sup>+</sup>	V-20Ti	69.1
D <sup>+</sup>	↓	35.9
T <sup>+</sup>		24.8
He <sup>+</sup>		19.3
V <sup>+</sup>		5.22

Figure ( 2 )



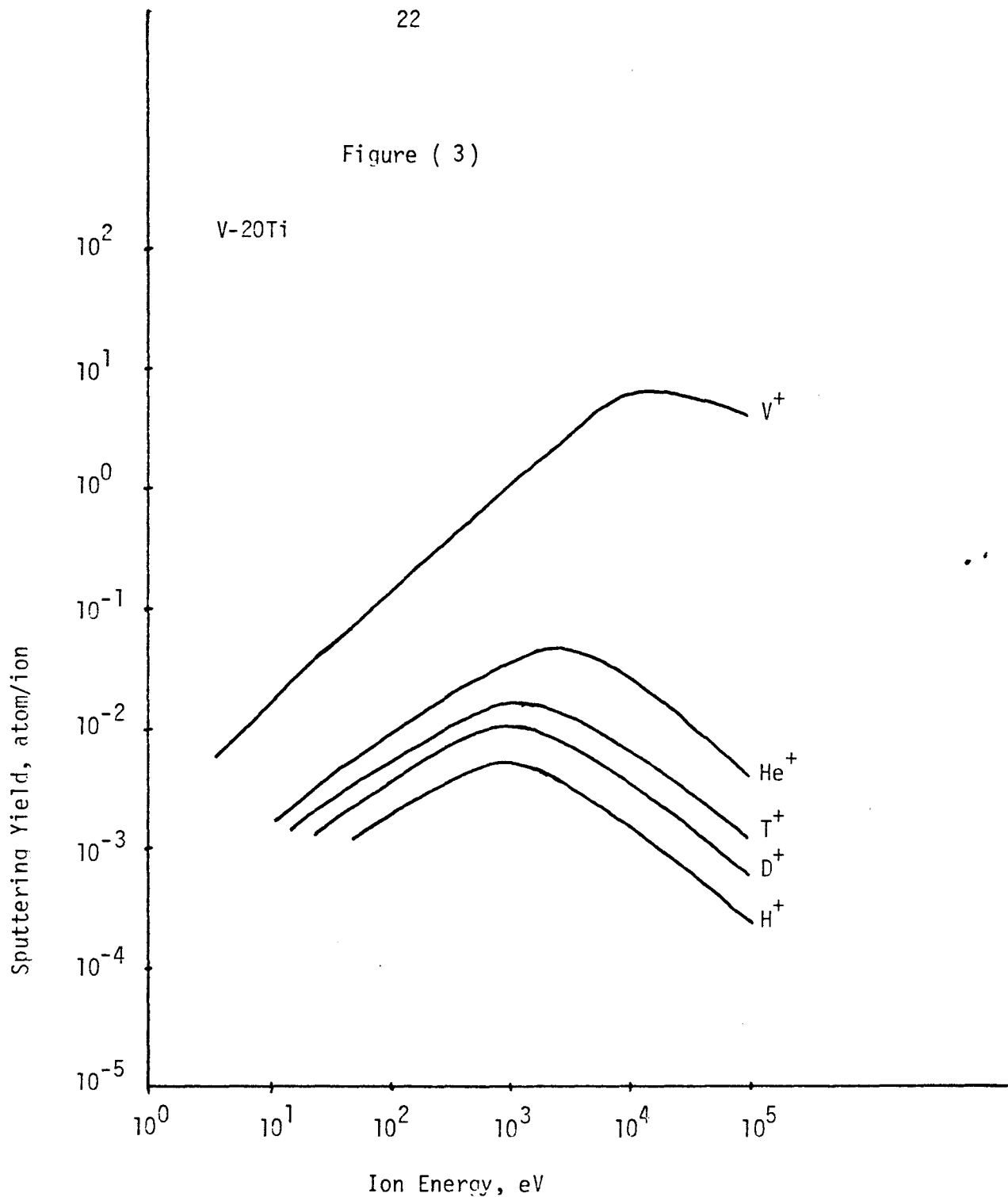
Plot of Calculated Energy-Dependent Sputtering Yield Curves for 316SS

## Sputtering of V-20Ti (continued)

Incident Particle	Particle Energy (eV)	Material	S(E) atoms/ion	
H <sup>+</sup>	100	V-20Ti ↓	$2.5 \times 10^{-3}$	
	1000		$8.6 \times 10^{-3}$	
	10000		$3.2 \times 10^{-3}$	
	100000		$3.9 \times 10^{-4}$	
D <sup>+</sup>	100			$5.1 \times 10^{-3}$
	1000			$1.7 \times 10^{-2}$
	10000			$6.4 \times 10^{-3}$
	100000			$7.8 \times 10^{-4}$
T <sup>+</sup>	100			$7.6 \times 10^{-3}$
	1000			$2.5 \times 10^{-2}$
	10000			$9.6 \times 10^{-3}$
	100000			$1.2 \times 10^{-3}$
He <sup>+</sup>	100			$1.1 \times 10^{-2}$
	1000			$5.8 \times 10^{-2}$
	10000			$4.2 \times 10^{-2}$
	100000			$6.1 \times 10^{-3}$
V <sup>+</sup>	100		$1.5 \times 10^{-1}$	
	1000		1.4	
	10000		8.1	
	100000		6.7	

See Figure ( 3 )

Figure ( 3 )



Plot of Calculated Energy-Dependent Sputtering Yield Curves for V-20Ti



## Sputtering of Nb-1Zr

Using Equation ( 5 ), Equation ( 6 ), and Table ( 1 )

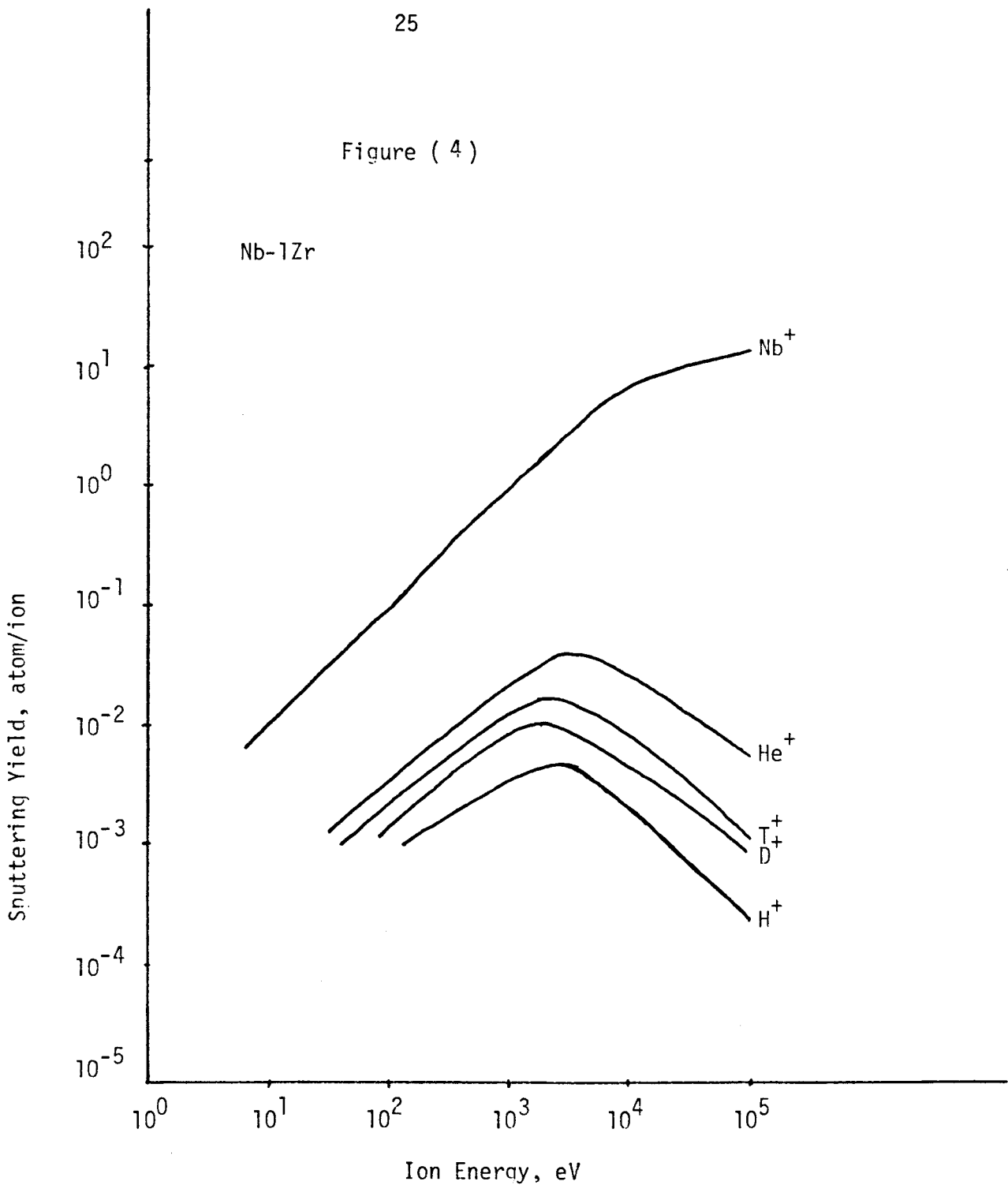
Incident Particle	Material	Terminated Energy ( $E_t$ ) (eV)
H <sup>+</sup>	Nb-1Zr ↓	180.3
D <sup>+</sup>		90.9
T <sup>+</sup>		62.7
He <sup>+</sup>		48
Nb <sup>+</sup>		7.6

## Sputtering of Nb-1Zr (continued)

Incident Particle	Particle Energy (eV)	Material	S(E) atoms/ion	
H <sup>+</sup>	1000	Nb-1Zr ↓	$5.1 \times 10^{-3}$	
	10000		$3.3 \times 10^{-3}$	
	100000		$4.6 \times 10^{-4}$	
D <sup>+</sup>	100			$2.1 \times 10^{-3}$
	1000			$1.0 \times 10^{-2}$
	10000			$6.6 \times 10^{-3}$
	100000			$9.1 \times 10^{-4}$
T <sup>+</sup>	100			$3.1 \times 10^{-3}$
	1000			$1.5 \times 10^{-2}$
	10000			$9.8 \times 10^{-3}$
	100000			$1.4 \times 10^{-3}$
He <sup>+</sup>	100			$4.3 \times 10^{-3}$
	1000			$2.9 \times 10^{-2}$
	10000			$3.8 \times 10^{-2}$
	100000			$7.0 \times 10^{-3}$
Nb <sup>+</sup>	100			$1.1 \times 10^{-1}$
	1000		1.0	
	10000		8.4	
	100000	▼	22	

See Figure ( 4 )

Figure ( 4 )



Plot of Calculated Energy-Dependent Sputtering Yield Curves for Nb-1Zr

From the sputtering yield calculated values and plotted curves, we can see that the sputtering yield increases steeply with energy and reaches a broad maximum in the keV region. The decrease after the maximum is due to increased penetration of the ions into the solid. The yields are lowest for hydrogen and increase with the mass of the bombarding ions. In the threshold energy region, the yield of different ions can differ by several orders of magnitude.

One important thing to notice is that, given the same ions with equal energies, the sputtering yield decreases as the surface binding energy increases. This may explain the better performance of Nb-1Zr compared to the other two materials (316SS and V-20Ti). Nb-1Zr has the lowest sputtering yields out of the three materials in question.

Self-sputtering yields are given in this calculation to make the study of sputtering more complete. In order to have self-sputtering, atoms from the first-wall have to be sputtered first and then these atoms will have to get into the plasma and have enough energy to penetrate the magnetic field to hit the first-wall and cause self-sputtering. These atoms also have to go through a charge exchange at the edge of the plasma to become neutral atoms and then penetrate the magnetic field and cause the self-sputtering. From this we see that the self-sputtering is a very complicated process and the number of atoms of the same mass as the first-wall material will be very small compared to  $H^+$ ,  $D^+$ ,  $T^+$ , and  $He^+$ . 316SS will have the biggest problem with self-sputtering because it is made of more than three different elements

and each one will intend to cause self-sputtering of its own. [316SS is made of Fe, Cr, Mn, and some other elements. In self-sputtering, ions of  $\text{Fe}^+$ ,  $\text{Cr}^+$ , and  $\text{Mn}^+$  will tend to cause higher sputtering yields compared to that of  $\text{He}^+$ ,  $\text{H}^+$ ,  $\text{T}^+$ , and  $\text{D}^+$  due to the higher mass numbers of  $\text{Fe}^+$ ,  $\text{Cr}^+$ , and  $\text{Mn}^+$ . This explains why 316SS has the greatest problem with self-sputtering. Nb-1Zr is made of Nb and 1Zr. In sputtering processes only  $\text{Nb}^+$  will tend to cause self-sputtering because the amount of Zr present in the material is only 1% and that will hardly cause any self-sputtering in Nb-1Zr. V-20Ti will have self-sputtering due to  $\text{V}^+$  and  $\text{Ti}^+$ .]

## 2. Blistering

Irradiation of metal (alloy) surfaces with energetic charged particles not only causes atoms to be sputtered from the first-wall, but it can cause severe surface roughening and blistering. Qualitatively, the energetic ions (helium, hydrogen, and hydrogen isotopes) displace atoms as they penetrate the solid. When they lose most of their energy, they slow down and become trapped because of their low diffusivity. Since the solubility of some of the gases in metals and alloys (e.g. helium) is extremely small, most of the gas precipitates into small bubbles. These small bubbles are formed near the end of the penetrative range for the gas atom and this region also corresponds with that for maximum vacancy production. The bubbles can capture these vacancies, grow and eventually coalesce with other bubbles to form lenticular bubbles below the surface of the metal or alloy. If enough atoms are injected at an elevated temperature, the pressure in these bubbles will be high enough to deform the metal surface causing it to protrude above the original surface. Eventually the blister can rupture causing a large flake of the wall material to be spalled off.

Blister formation has been found with helium ions in all the three materials (Nb-1Zr, V-20Ti and 316SS). The size, density, and shape, and critical fluence for the formation of blisters is known to be a function of at least nine parameters:<sup>12</sup>

1. Energy of ions (i.e. their range)
2. Diffusivity of injected ions
3. Solubility of gas atoms in matrix

4. Yield strength of the material
5. Temperature of metal during the bombardment
6. The dose rate of bombarding ions
7. Total dose
8. The orientation of the crystal structure to the ion beam
9. The metallurgical state of the sample prior to irradiation

Target temperature, ion energy, type of ion, total dose and dose rate are the most important ones out of all the nine parameters.

There are two obvious conditions to be fulfilled for blister formation.<sup>13</sup>

1. The range (R) of the ions must be larger than the thickness sputtered by the critical ion dose ( $n_c$ ) needed for blister formation. If S is the sputtering yield and N the atomic density of the material this means:

$$R > S n_c / N \quad (1)$$

As S decreases and R increases with ion energy for energies above 10 to 50 keV, blistering can occur for all ion of gases at sufficiently high energy. If the covers of the blisters are removed, condition (1) implies that surface erosion by blistering is larger than by sputtering.

2. The diffusivity and solubility of the injected gas ions in the solid must be small in order for the over-saturation leading to bubble and blister formation to develop. As diffusivity and solubility of gases in solids depend on temperature, damage, and impurity concentration in the solid, the appearance of blisters is sensitive to these parameters.

The most important parameters of blistering are:

1. Type of ion

In a D-T fusion reactor, the energetic ions such as deuterium, tritium and helium will strike structural components of the first-wall. Since the permeability of the hydrogen isotopes in most metals (alloys) is quite different from that of the inert gas atom such as helium, the blister formation process will be different. Niobium (from the experimental work of Das and Kaminsky) irradiated at 700°C with  $^4\text{He}^+$  and  $\text{D}^+$ . The blisters formed by  $^4\text{He}^+$  are much larger than those formed by  $\text{D}^+$ , and also some of the  $^4\text{He}^+$  blisters have ruptured in many places. Even though the  $\text{D}^+$  dose was twice that of  $^4\text{He}^+$ , the  $\text{D}^+$  have not ruptured in any place.<sup>13</sup> This observation that blister size for deuteron irradiation is smaller than for helium ion irradiation can be related to the fact that the gas buildup is greatly reduced for deuterium in niobium (representative of Nb-1Zr) since the deuterium permeability (determined by the solubility and diffusivity) is many orders of magnitude larger than that of helium.



For example, the diffusion coefficient of deuterium in niobium is  $D_D = 1.3 \times 10^{-4}$  cm/sec at 800°C, while that of helium in niobium ranges from  $10^{-19}$  to  $10^{-14}$  cm<sup>2</sup>/sec between the temperatures of 600°C and 1200°C. Therefore the hydrogen isotopes blistering will be much less of a problem in the structural materials of the first-wall compared to that of helium.

## 2. Ion Energy, Dose and Dose Rate

In all three of the materials (316SS, V-20Ti, and Nb-1Zr), the erosion rate increases with both the increase of energy or dose to some maximum and then falls down. This is due to the reemission of the helium out of the surface. The erosion is due to the increase in the exfoliation of blisters and to the subsequent loss of blister skin with increasing dose.

The increase in blister size with increase in ion energy can be understood if one considers the gas pressure (P) inside a blister.<sup>13</sup> The pressure (P) is directly proportional to the skin thickness (t) and inversely proportional to the square of the radius (a) of the blister. Hence for a given blister height (h) and pressure (P) (which is roughly proportional to the total dose), a higher ion energy (and corresponding higher skin thickness (t)) will require a larger blister radius (a). This argument is shown graphically for the case of niobium (from the experimental work of J. Roth) in Figure (5) and (9). The critical dose, energy, and temperature interaction is shown in Figure (6) and Figure (9).

Figure (5)

Ref. (13)

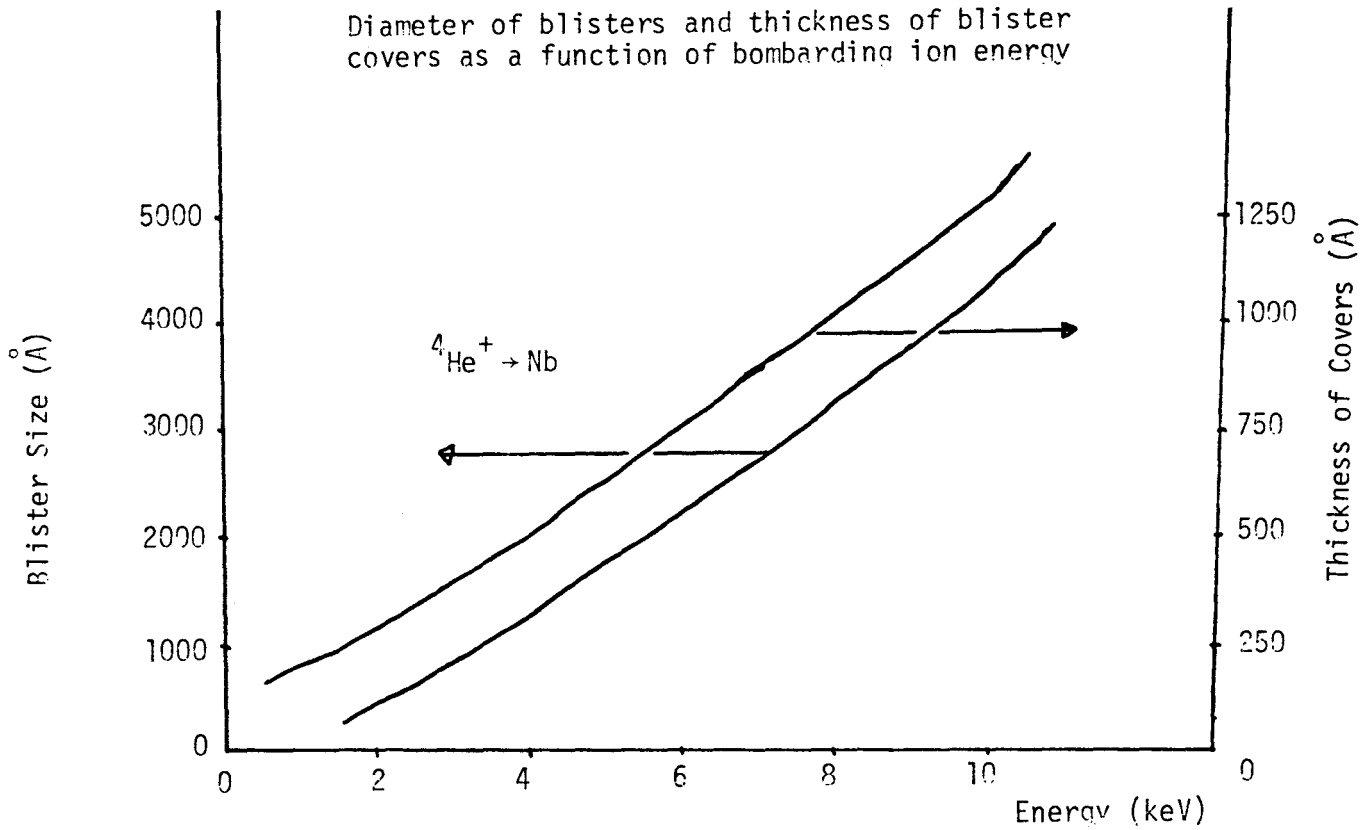
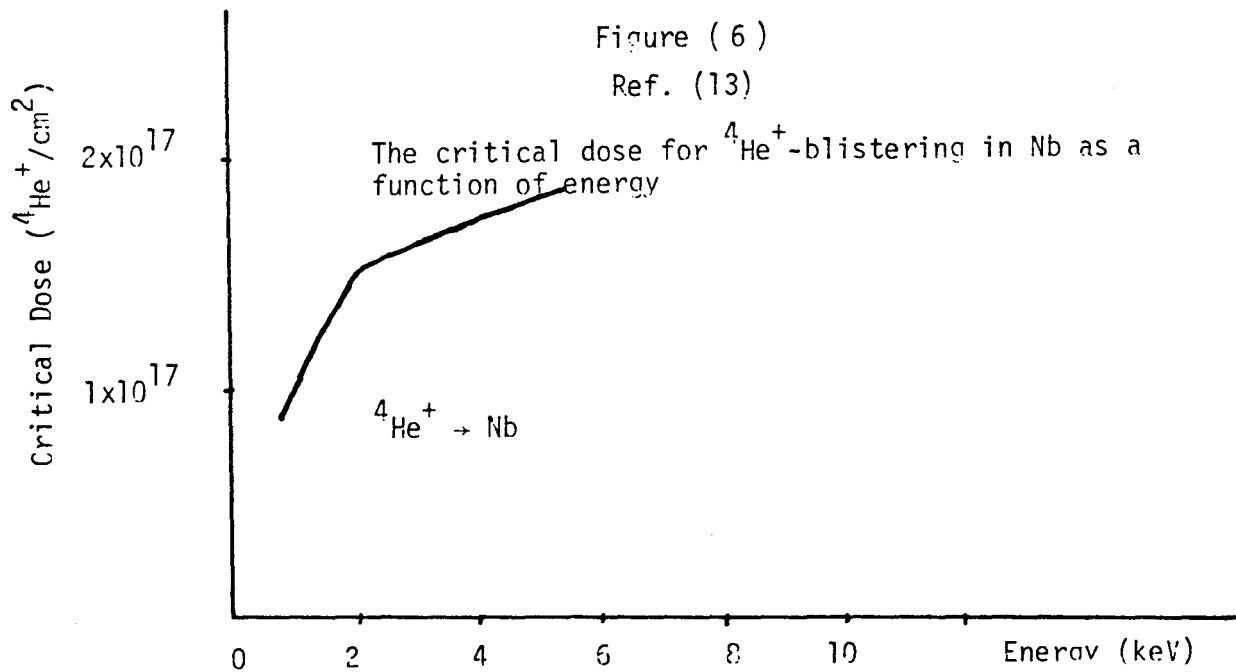


Figure (6)

Ref. (13)



### 3. Target Temperature

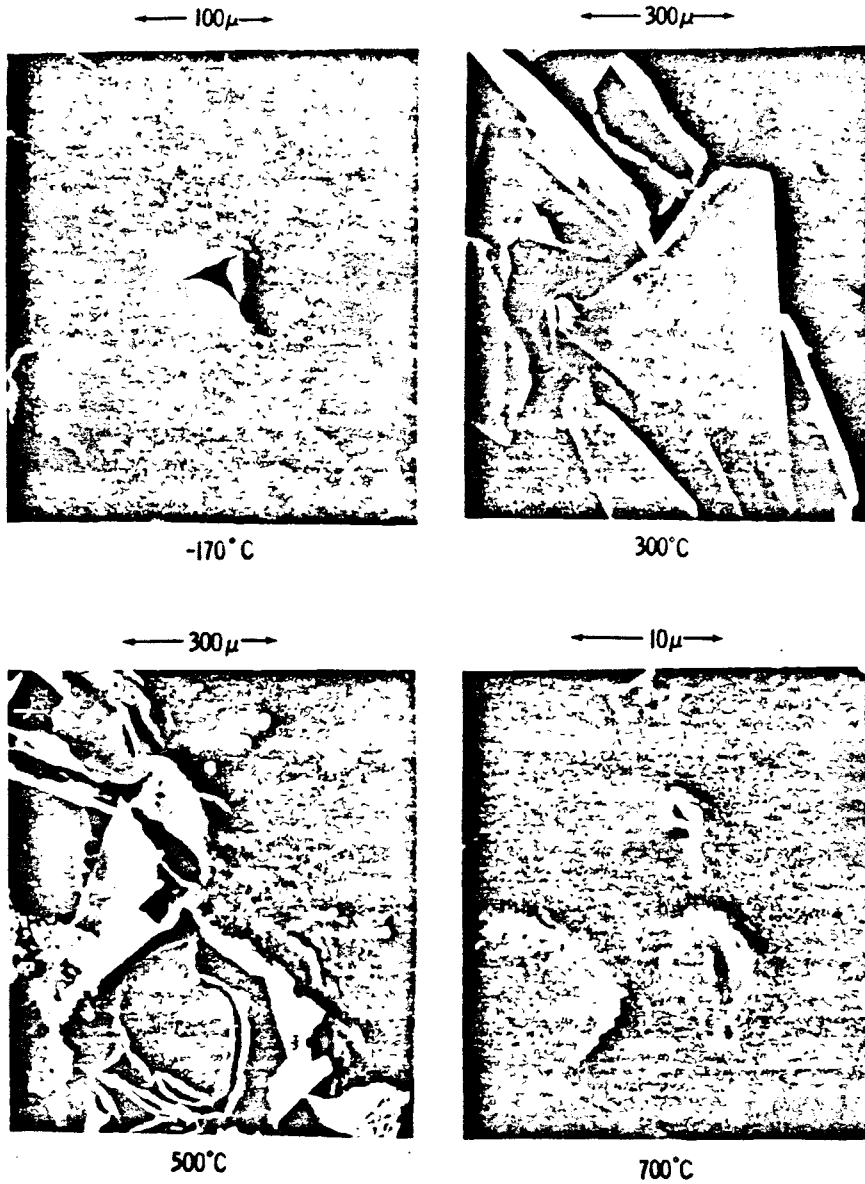
The target temperature is one of the most important parameters affecting blister formation. The degree of blistering is maximized if the temperature is high enough (lower yield strength) so the surface can be deformed easily, but low enough so that the helium release from the surface is still very small.

Data from the literature for a number of different metals and alloys, as shown in Figures (7), (8) and (9), suggest that the maximum erosion rate due to blistering occurs at about 0.40 to 0.45  $T_m$  ( $T_m$  = melting temperature) which, for Nb-1Zr, corresponds to temperatures in the range 1100°C to 1250°C. Therefore, erosion rates for a Nb-1Zr first-wall operating in the range 500°C to 650°C should be lower than for 316SS, since the maximum erosion rate for the latter coincides with these operating temperatures.

Figure (10) shows a plot of the erosion rates versus target temperature for helium blistering of Type 304 stainless steel. It can be seen in Figure (10) that the maximum erosion rate occurs at an irradiation temperature of 450°C. A qualitatively similar temperature dependence has been observed for Type 316SS in Figure (7). Figure (8) shows the effect of temperature on the blister formation in V-20Ti.

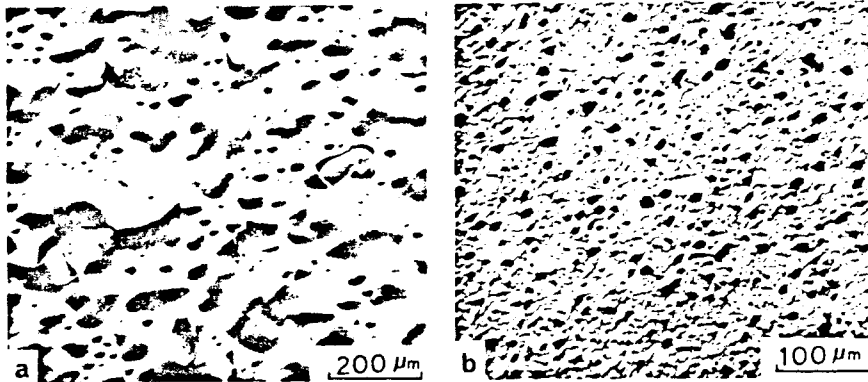
At room temperature, the blisters are bigger in size and some of them have ruptured, whereas at 900°C the blisters are very small and hardly any rupturing occurs.

Figure ( 7 )  
Ref. (15)



Scanning electron micrographs of 316SS implanted with  $^4\text{He}^+$  at four different temperatures to a dose of  $4 \times 10^{18}$  He atom/cm<sup>2</sup>

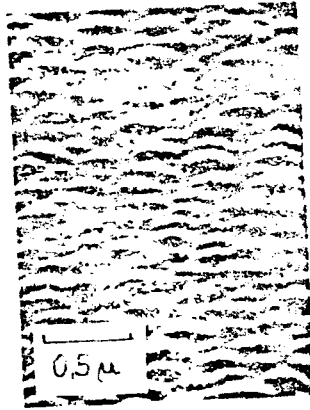
Figure ( 8 )  
Ref. (14)



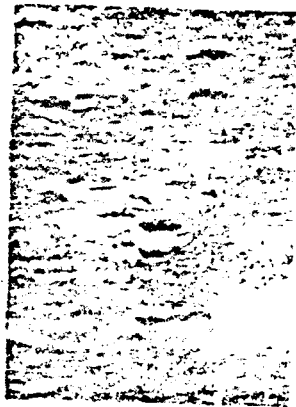
Scanning electron micrographs of V-20Ti alloy after irradiation with 0.5 - meV  $^4\text{He}^+$  ions for a total dose of 1.0 coulomb/cm<sup>2</sup> (a) at room temperature and (b) at 900°C

Figure (9)

Ref. (13)



At Room Temperature

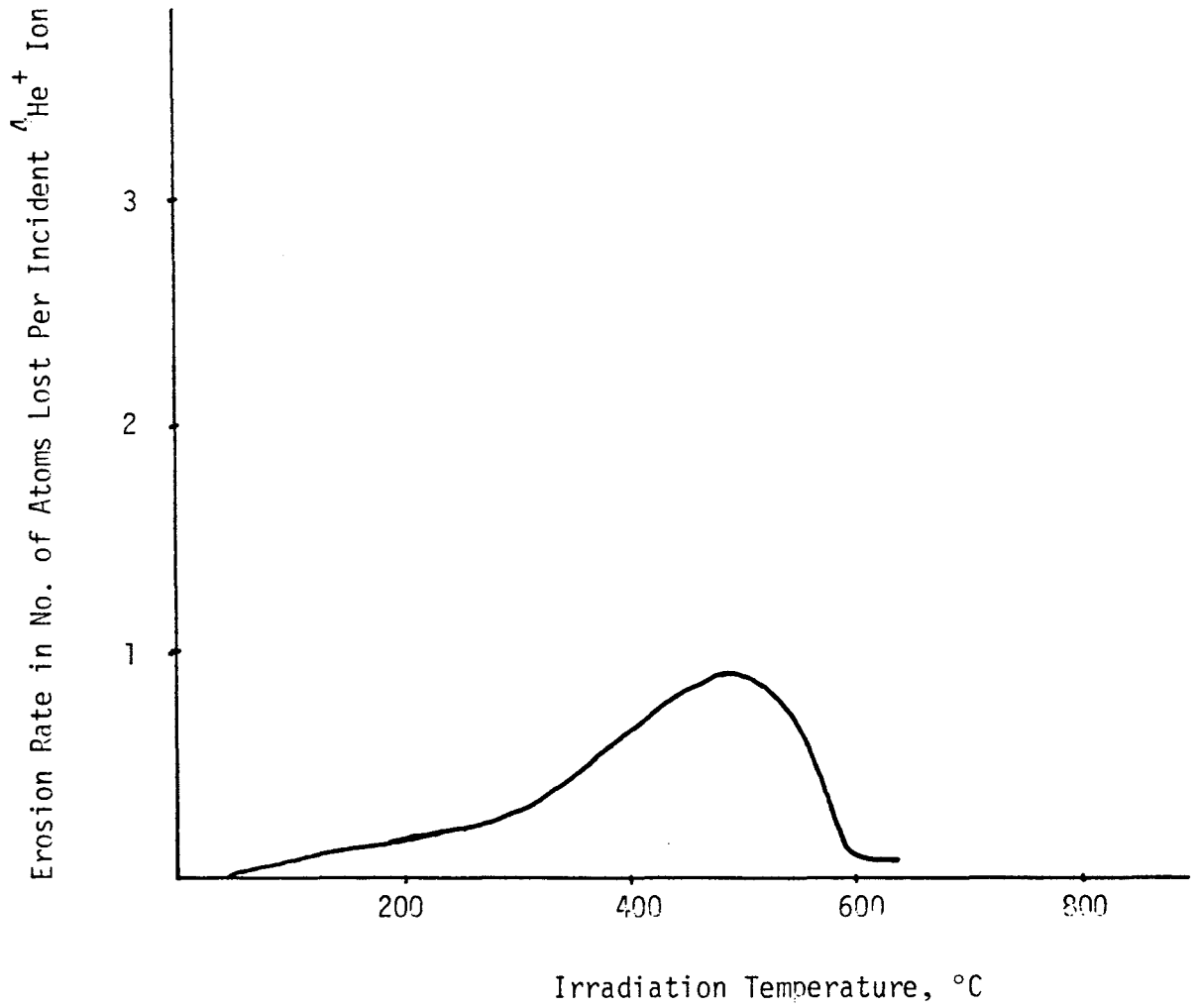


At 650°C

Blistering of Nb after bombardment with  $\approx 6 \times 10^{17}/\text{cm}^2$   $^4\text{He}^+$  ions

Figure (10)

Ref. (16)



Erosion rate of 304 stainless steel as a function of irradiation temperature for ion energy of 0.5 MeV  ${}^4\text{He}^+$  and dose of 0.1 coulomb/cm<sup>2</sup>.

Therefore, for actual design of a fusion reactor, a higher operating wall temperature is preferred, to keep the erosion due to blistering at a minimum. For walls made of Nb-1Zr or V-20Ti, operating temperatures near 900°C or above in the case of Nb-1Zr would be very helpful in reducing erosion due to blistering.

The dependence of blistering on target temperature in Nb-1Zr is shown in Figure (11) from the experimental work of J. Roth.<sup>13</sup> The increase in temperature causes an increase in the blister size but a decrease in its cover thickness. Also the increase in temperature tends to decrease the number of blisters in a given surface area as shown in the following Table (2). Figure (12) shows the critical dose dependence on temperature.

Table (2), Ref. (14)

Ratio of Blister Area to Total  $^4\text{He}^+$  Irradiated Area

Irradiation Temperature, °C	Nb	V-20Ti
Room Temperature	87%	47.2%
600	47.2%	-
900	9.0%	7.4%

The rapid decrease in the blistered area is due to the increase of permeability of helium in Nb at higher temperatures. See Figure (9) for a photographic picture of temperature effect in Nb.



Figure (11)

Ref. (13)

Diameter of blisters and thickness of blister covers  
as a function of irradiation temperature

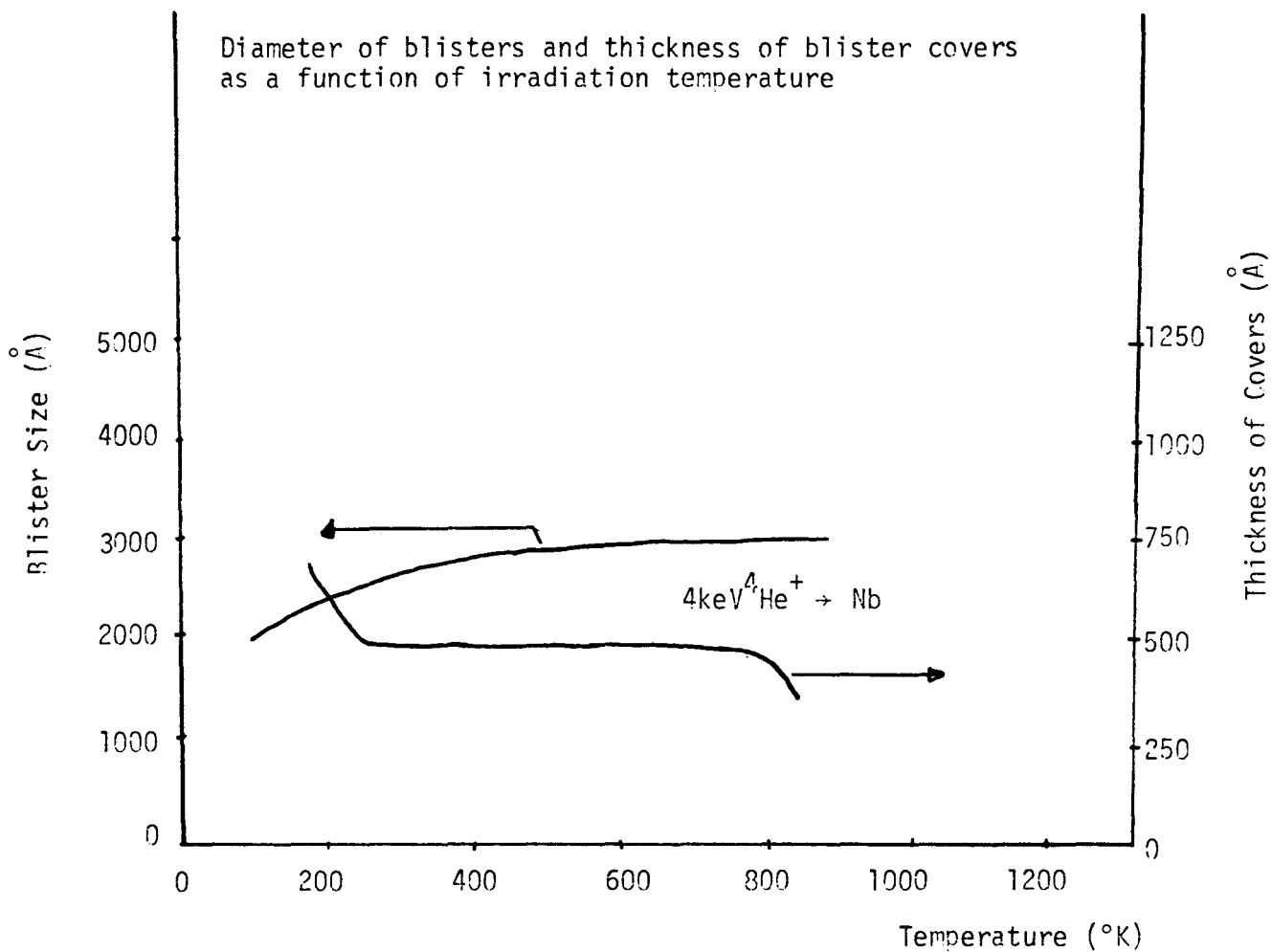
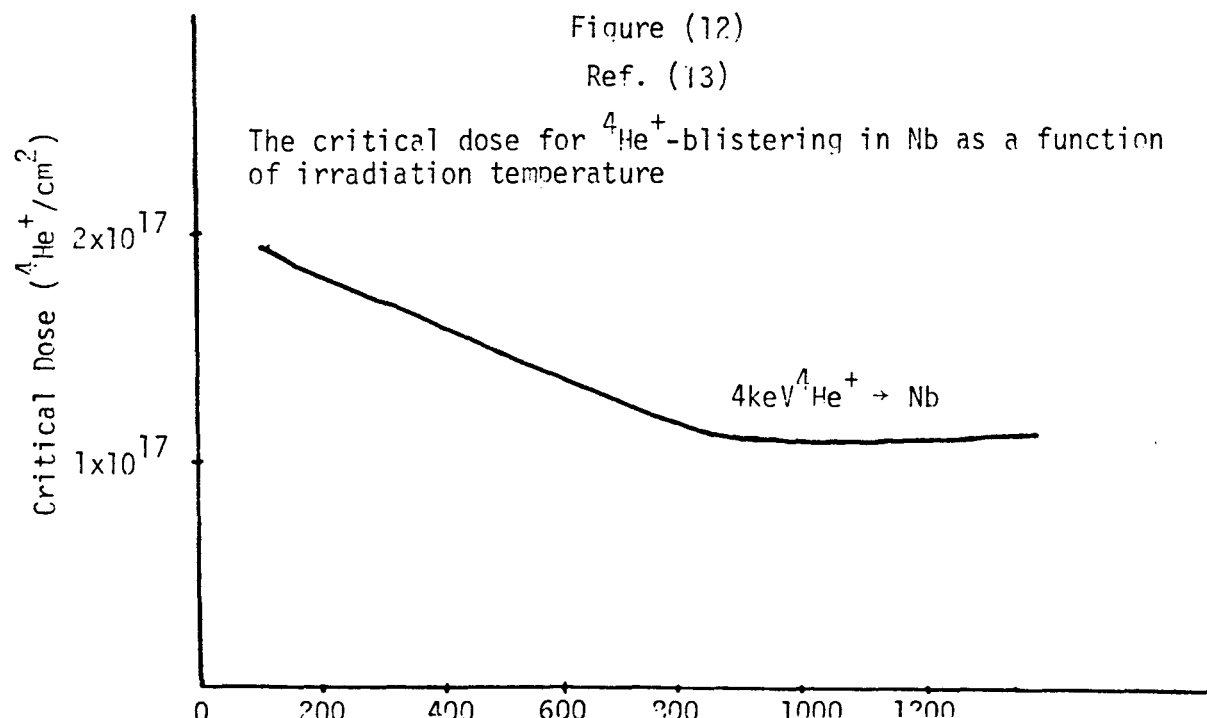


Figure (12)

Ref. (13)

The critical dose for  $^4\text{He}^+$ -blistering in Nb as a function  
of irradiation temperature



From all the information given here and in the literature, one can see how serious the problem of blistering is, especially in the case of 316SS and Nb-1Zr. Out of the two, 316SS seems to have the greater problem because its operating temperature coincides with that of maximum blistering. Also, at higher temperatures, 316SS yield strength becomes very small, which helps the blisters to form easily on the surface. After irradiation in a fusion environment, the yield strength of Nb-1Zr increases to very high values over a wide range of temperatures (see mechanical properties), while the yield strength of 316SS increases to small values up to 300°C - it then starts to decrease very rapidly. Therefore, in a fusion environment, Nb-1Zr will be more resistant to helium blistering than 316SS. Hydrogen and hydrogen isotopes blistering might cause more blistering in the case of 316SS due to the low permeability coefficient of hydrogen in 316SS at the operating temperatures (see Table (1-1)). This is not the case in Nb-1Zr where hydrogen has a high permeability coefficient at operating temperatures (see Table (1-1)).

V-20Ti seems to have the least problem with respect to blistering<sup>14</sup> at temperatures up to 600°C, but at higher temperatures it becomes comparable with that of Nb-1Zr.

COMPARATIVE STUDY IN THE USE OF 316SS, V-20Ti, AND Nb-1Zr AS A STRUCTURAL MATERIAL IN THE FIRST-WALL OF A TOKAMAK REACTOR	العنوان:
Al Morished, Mutlaq Hamad	المؤلف الرئيسي:
Johnson, Ernest F.(Super.)	مؤلفين آخرين:
1981	التاريخ الميلادي:
Princeton	موقع:
1 - 161	الصفحات:
617900	رقم MD:
رسائل جامعية	نوع المحتوى:
English	اللغة:
رسالة ماجستير	الدرجة العلمية:
Princeton University	الجامعة:
School of Engineering and Applied Science	الكلية:
الولايات المتحدة الأمريكية	الدولة:
Dissertations	قواعد المعلومات:
الهندسة النووية، فيزياء البلازما، المفاعلات النووية	مواضيع:
<a href="https://search.mandumah.com/Record/617900">https://search.mandumah.com/Record/617900</a>	رابط:

## Chapter Three

### Bulk Radiation Damage

1. Swelling
2. Embrittlement (Loss of Ductility)
3. Transmutation
4. Effect of Radiation in General on a Power Producing Tokamak

## BULK RADIATION EFFECTS

- a) Void formation leading to swelling and dimensional instability. High stresses are often generated due to uneven expansion as a result of temperature and thermal flux gradients.<sup>17</sup>
- b) Helium embrittlement due to helium accumulated in metals from  $\alpha$  bombardment,  $(n,\alpha)$  reactions and  $\beta$  decay of dissolved tritium. The results are severe embrittlement at elevated temperatures ( $T/T_m > .5$ ). Swelling also takes place as a result of helium agglomeration into bubbles.
- c) Transmutation effects other than helium, e.g. the production of zirconium, yttrium and hydrogen in Nb. These elements may change the properties of the primary metal.
- d) Hardening and loss of ductility at lower temperatures ( $T/T_m < .3$ ) due to displacement damage.<sup>17</sup>
- e) Enhanced in-reactor deformation due to neutron flux resulting in creep rates higher than experienced out of reactor.
- f) Fatigue properties will be affected to some degree.

Swelling, embrittlement, and transmutation will be discussed in detail in this chapter. Creep and fatigue will be discussed in Chapter five (mechanical and thermal properties).

## 1. Swelling

The swelling or volume change in metal (alloy) can be caused by void formation, the presence of insoluble gas (He), or a combination of the two. Applied stresses may also affect swelling. Void swelling is essentially due to displacement damage which promotes the clustering of vacancies (the unoccupied position in the lattice is called a vacancy) to form voids and the precipitation of interstitials along dislocation loops.<sup>5</sup> (The struck atom moves through the lattice and gradually loses energy until it comes to rest between equilibrium sites in the lattice - this atom is now referred to as an interstitial.)

Significant swelling occurs during irradiation when vacancies survive annihilation (no recombination of vacancies and interstitials) and precipitate as cavities; the corresponding interstitials create new lattice sites by precipitation at dislocations. Transmutation-produced gases may accelerate the nucleation and growth of the cavities, and in extreme cases the pressure of the gas within the cavities may equal or exceed the surface tension restraint. Gas production rates will be high enough in fusion reactors that some cavity formation is inevitable. If the cavities contain excess vacancies, swelling may pose a serious problem. Stresses and distortion of components from non-uniform swelling, changes in strength and ductility that accompany the swelling, and the formation of paths for easy propagation of cracks are other consequences of swelling.<sup>10</sup>

Helium tends to enhance swelling by promoting the nucleation of both voids and dislocation loops. Because helium may drive cavity

growth at higher temperatures, the temperature dependence of swelling for the fusion reactor case where helium contents are high may differ significantly from the fast reactor case where they are relatively low. Hydrogen is expected to be less important as a cause of swelling because of its high solubility and diffusivity at temperatures of interest in the fusion reactors. It may, however, undergo chemical reactions that produce species that influence swelling (e.g., with carbon to form methane). Its behavior in the presence of structural imperfections is unknown.

Swelling due to Voids: There is one major dimensional instability associated with metals when they are irradiated at temperatures approximately 25-55% of their melting point. The generation of vacancies at temperatures above which they are mobile and the preferential absorption of the associated interstitials at dislocations produce a situation where the vacancies become highly supersaturated and tend to precipitate into voids. The metals (alloys) then decrease in density with the net result that significant swelling can occur. Values up to 50% have been reported for 316SS. This phenomenon is rather general. Some smaller values have been reported for Nb-1Zr, but there has not been any report about swelling in V-20Ti.<sup>24</sup>

Swelling due to Gas Bubbles: The generation of insoluble gas (in this particular case, He) inside of metals (alloys) at high temperatures ( $> 0.5 T_m$ ) has been known to promote bubble formation and dimensional changes associated with that phenomenon. This is not too serious in most metals and alloys (except for perhaps 316SS) because the amount of gas generated is relatively low (see Table ( 2 ) or Figure ( 4 )).

The effect of such high helium contents on the dimensional instability can be estimated as a function of bubble size and temperature from the following expression.<sup>19</sup>

$$\frac{\Delta V}{V_0} \% = 100 N \left[ \frac{nkT}{2\gamma} + b \right] \quad (1)$$

where

$N$  = number of gas atoms per  $\text{cm}^3$

$n$  = bubble radius

$T$  = temperature

$k$  = Boltzmann constant

$\gamma$  = surface energy

$b$  = Van der Waals constant

Beside swelling due to voids and gas bubbles, swelling in the first wall components at typical operating conditions can come from at least two different sources:

1. Distortion of the lattice due to the generation of isolated points defects. This effect is negligible in metallic components but may, at high temperatures, be of considerable importance in SiC and graphite, which might be used as a coating or neutron thermalizing material in fusion reactors.<sup>19</sup>



2. Transmutation reactions which produce atoms which are larger than the original atoms. One example of this effect is the production of Zr in Nb, but these transmutation reactions will occur in practically all the first-wall materials.

Swelling Mechanism: Void formation is responsible for a swelling of the material. The swelling starts at a threshold temperature increase with higher temperatures and decreases at  $0.5 T_m$  after reaching a maximum. Unfortunately, it is impossible to consider the use of materials at temperatures higher than  $0.5 T_m$  because the mechanical properties required for the construction of the first wall/blanket are marginal for temperatures close to  $0.5 T_m$ . It is desirable to operate the first wall/blanket at higher temperatures in order to achieve a high efficiency of the power cycle. The operation temperature will therefore most probably coincide with the temperature of a maximum swelling. The average size of the voids becomes rapidly large with increasing temperature, whereas the number of voids per volume unit is decreasing. The total volume of the voids increases as a function of the fluence  $F$  after a certain threshold ( $F_t$ ) has been passed. For  $F < F_t$ , a nucleation of voids occurs, and voids cannot be observed, e.g. by a transmission electron microscope. For  $F > F_t$ , the total void volume increases with a relative large power of  $\phi t$  ( $\phi$  = flux,  $t$  = time), reaching some sort of saturation at large values of  $F$ . Swelling of 316SS has been observed to be higher than that of V alloys and Nb-1Zr, but it is possible to reduce swelling in 316SS by coherent precipitations or high displacement densities<sup>19</sup> (cold work, PE 16).

Besides the swelling due to void formation, it may be expected that swelling will also be produced by the precipitation of helium gas bubbles due to  $(n,\alpha)$  processes. These gas bubbles are different from the voids because their size is determined by the balance between the inside gas pressure and the surface tension of the material in question. Their influence on swelling can be neglected, compared to the voids, if it is possible to keep the bubbles small.

From a practical point of view, there is a connection between voids and  $(n,\alpha)$  processes: the voids are partially filled by helium, obstructing the annihilation of voids if the temperature is raised. For example, at temperatures far below  $0.5 T_m$  swelling is determined by the formed voids, and at temperatures close to or far above  $0.5 T_m$ , the helium inside the voids keeps the swelling elevated.

The general features of void swelling of niobium have been studied since 1971, and the results are summarized in Table (1). The data indicate that for pure niobium, swelling reaches a maximum at  $585^\circ\text{C}$ , which is roughly equal to  $0.32 T_m$ . Exposure to higher temperatures tends to increase the void size while decreasing the void density. Studies into the neutron-induced void swelling of niobium indicate that annealing out of the voids occurs at  $T > 0.5 T_m$ . The addition of reactive gettering elements such as zirconium appears to suppress the incubation period for void formation. However, once the voids are formed they appear to rapidly grow in size and are larger than those found in pure niobium at the same temperature and fluence<sup>21</sup> (see Table (1)).

Table (1)  
Ref. (5) and (34)

Material	Irradiation		Void Parameters		
	Temperature (°C)	Fluence (n/cm <sup>2</sup> ) E>0.1 MeV	Concentration (voids/cm <sup>3</sup> )	Average Diameter (Å)	Volume Fraction (%)
Niobium	425	2.5x10 <sup>22</sup>	1.6x10 <sup>17</sup>	70	3.1
	585	2.5x10 <sup>22</sup>	2.1x10 <sup>17</sup>	71	4.8
	790	2.5x10 <sup>22</sup>	2.8x10 <sup>15</sup>	186	1.04
Nb-Zr	425	2.5x10 <sup>22</sup>	0		
	585	2.5x10 <sup>22</sup>	0		
	790	2.5x10 <sup>22</sup>	1.8x10 <sup>14</sup>	575	2.2
Vanadium (comm)	450	3.6x10 <sup>22</sup>	1.06x10 <sup>16</sup>	110	0.7
	550	3.6x10 <sup>22</sup>	1.6x10 <sup>15</sup>	224	0.9
	600	3.6x10 <sup>22</sup>	3.2x10 <sup>14</sup>	281	0.4
Vanadium (pure)	475	0.97x10 <sup>22</sup>	10.6x10 <sup>15</sup>	82	0.34
	550	1.4x10 <sup>22</sup>	5.9x10 <sup>15</sup>	170	1.77
	600	1.4x10 <sup>22</sup>	2.0x10 <sup>15</sup>	230	1.47
V-20Ti	475	0.97	0		
	525	2.0	0		
	470 to 780	6x10 <sup>22</sup>	0		

Swelling Data of Refractory Metals and Alloys

Table (1) continued  
Ref. (20)

Irradiation Temperature, °C	Fluence 0.1 MeV (n/cm <sup>2</sup> )	Displacement (dpa)	Helium Concentration ppm	Swelling %
379	7.05 x 10 <sup>22</sup>	97	4020	6.7
456	7.69 x 10 <sup>22</sup>	107	4820	8.7
528	8.27 x 10 <sup>22</sup>	114	5450	8.3
535	3.79 x 10 <sup>22</sup>	52	1930	3.5
574	4.21 x 10 <sup>22</sup>	58	1791	3.3
602	8.71 x 10 <sup>22</sup>	121	6090	14.1

Helium Effect on Swelling of 316SS

The equation for void swelling for Nb-1Zr is given by Brailsford and Bullough.<sup>22</sup>

$$\frac{\Delta V}{V} \% = Sk (t - t_0) F(\eta) \quad (2)$$

where

$kt$  = dose in displacement per atom (dpa)

$kt_0$  = incubation dose in dpa ( $\sim 1$  to 10 dpa)

$$F(\eta) = \frac{2}{\eta} \left[ (1+\eta)^{1/2} - 1 - \frac{1}{2} \eta \exp \left( -\frac{Q}{k} \left( \frac{1}{T} - \frac{1}{T_f} \right) \right) \right]$$

$$\eta = 400 \exp \left[ -\frac{E_m^v}{k} \left( \frac{1}{T_s} - \frac{1}{T} \right) \right]$$

$$S = p_d \frac{4\pi r_s c_s}{[(P_d + 4\pi r_s c_s)(P_d + 4\pi r_s c_s + 4\pi r_p c_p)]}$$

$E_m^v$  and  $Q$  are the activation energies for vacancy motion and self-diffusion by the vacancy mechanism respectively.  $T_s$  and  $T_f$  are respectively the start and finish temperatures for the void-swelling.

$P_d$  = total dislocation density

$r_s$  = radius of the neutral sinks at a concentration of  $c_s$

$r_p$  = radius of the coherent sinks at a concentration of  $c_p$

$k$  = Boltzmann constant

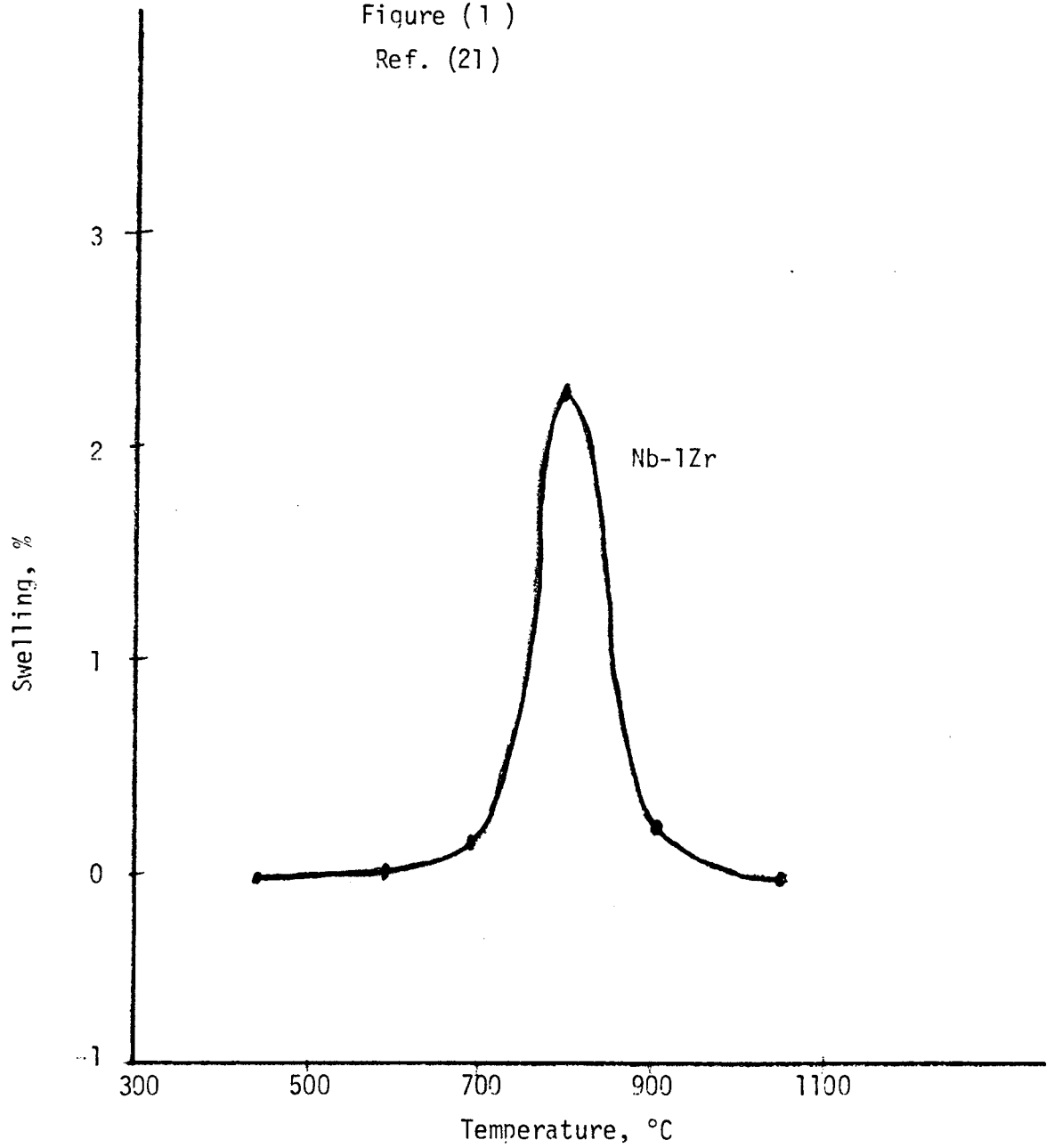
$T$  = temperature

$F(n)$  was calculated for Nb-1Zr using  $Q = 4.06$  eV and  $E_m^V = 0.68$  eV (these values for  $Q$  and  $E_m^V$  are taken from the work of Kothe,<sup>23</sup> A). Based on the experimental data in the literature, the values of  $T_s$  and  $T_f$  were estimated to be 400 and 1400°C, respectively. From the work of Brailsford and Bullough<sup>22</sup>  $S$  is taken to be 0.17.

The graph of the swelling in Nb-1Zr using the above values and the given equation is shown in Figure (1).

The discussions of swelling in Nb-1Zr so far have not included the presence of the solid or gaseous transmutation elements that will be produced. With respect to solid transmutation products in a Nb-1Zr first wall, it has been calculated that for one year of operation with a neutron wall loading of  $1 \text{ MW/m}^2$ , a 0.3% volume change would result from the transmutation of 0.18 atomic percent niobium to zirconium.<sup>5</sup> The gaseous transmutation products will have a similar effect. Of the two gaseous elements, helium and hydrogen, hydrogen is not expected to affect swelling in Nb-1Zr primarily because of its low solubility and its higher permeability and diffusivity at elevated temperatures. It is likely that hydrogen produced in this way will diffuse to either wall surface (i.e., the plasma cavity or the blanket coolant) and will end up in the tritium-deuterium handling system a short time after it is created. However, the effects of helium are much more damaging. Because of its low solubility in metals and its relatively low diffusion rate, helium precipitates in the form of gas bubbles. A rough estimate

Figure (1 )  
Ref. (21)



Temperature Dependence of Radiation Swelling for Nb-1Zr

has been made on the amount of swelling caused by helium in Nb-1Zr. At 600°C, an equilibrium helium bubble concentration of  $1.1 \times 10^{18}$  bubbles/cm<sup>3</sup> would result in a volume change of 0.6%. Comparing this to the void swelling shown in Table (1), it appears that the swelling produced by void formation alone will be at least an order of magnitude greater than the swelling produced by helium alone.<sup>5</sup> However, the combination of displacement damage plus helium transmutation has the potential for creating more swelling than either operating separately. This synergistic effect can be seen by comparing the stainless steel swelling data in Table (2) produced from EBR-II irradiation with HFIR swelling data. At approximately the same temperature (500°C) and displacements (37-42 dpa), stainless steel with roughly 3000 appm helium has about 9 times more volume change than material with 15 appm helium.<sup>20</sup>

In the case of V-20Ti, void swelling is primarily a high fluence effect. Neutron irradiation data for vanadium and its alloys extend to about  $6 \times 10^{22}$  n/cm<sup>2</sup> ( $E_n > 0.1$  MeV); this is only a fraction of the  $1-3 \times 10^{23}$  n/cm<sup>2</sup> fluences which a fusion reactor first wall will experience. The neutron spectra are also obviously mismatched. This latter factor may be important to void formation phenomena in that only extremely low values of helium have been attained.<sup>23</sup>

Experimental data have been reported for unalloyed vanadium irradiated to fast fluences up to about  $3 \times 10^{22}$  n/cm<sup>2</sup>. Irradiation temperatures have covered the range from about 385° to 700°C. Maximum



swelling values have generally been 1.5 to 2% and occur, depending somewhat on purity, for irradiations at 500° - 600°C. The trends are the same as those observed in other pure metals, with void concentrations and sizes dependent on both dose and irradiation temperature (see Table (1)). Voids are cubic in shape with cube perfection increasing with an increase in irradiation temperature. Void ordering on a superlattice, which has been reported in other bcc metals such as Nb, has not been observed in vanadium.

High fluence irradiations have been carried out on several vanadium-base alloys. The V-Ti binary compositions, in particular, have been the subject of more experimental observations on the effects of neutron irradiations than any other class of vanadium-base alloys. At least part of the reason for this interest is due to the early observations of the lack of void formation in V-20Ti.<sup>24</sup>

Additions of as little as 3% Ti have been found to essentially eliminate void swelling in V-Ti binaries for fluences up to  $6 \times 10^{22}$  n/cm<sup>2</sup> ( $E_n > 0.1$  MeV) and temperatures from about 470° to 780°C. The mechanism by which this void suppression takes place is not obvious. Researchers at both the Argonne and Oak Ridge National Laboratories suggest the following possibilities.<sup>24</sup>

1. Titanium acts as a gettering agent for interstitial impurities which had been serving as void nucleation sites.
2. The formation of a high number density of coherent precipitates accommodates the excess vacancies.

3. Enhanced recombination of vacancy - interstitial defects occur due to the presence of substitutional solute atoms.

316SS has the most serious problem of the three candidates because of the high displacement damage and its very high helium production rate. The effect of the high helium concentrations is to increase cavity nucleation and overall swelling in the temperature range 380 to 680°C. This can be seen from Table (2), where the sample with large helium concentrations has the highest swelling. The general swelling equation for 316SS is given below from the Nuclear Systems Material Handbook.<sup>27</sup>

$$\frac{\Delta V}{V_0} = R \left[ \phi t + \frac{1}{\alpha} \ln \left( \frac{1 + \exp[\alpha(\tau - \phi t)]}{1 + \exp(\alpha\tau)} \right) \right] \quad (3)$$

where

$$\frac{\Delta V}{V_0} = \text{fractional volume change}$$

$$\phi t = \text{fluence, 1 unit} = 10^{22} \text{ n/cm}^2 \quad (E_n > 0.1 \text{ MeV})$$

$$R = 0.01 \exp(-49.8592 + 0.195283T - 1.87409 \times 10^{-4} T^2)$$

$$\alpha = -1.117 + 6.889 \times 10^{-3} T$$

$$\tau = 1.0 / (7.98769 - 2.98448 \times 10^{-2} T + 2.87279 \times 10^{-5} T^2)$$

$$T = \text{temperature, } ^\circ\text{C}$$

R,  $\alpha$ , and  $\tau$  = material constants that vary with temperature. The values which are given here are for 316SS.

The swelling curves for 316SS using the above equation are shown in Figures (2) and (3) as functions of temperature and displacement damage.

The importance of swelling in choosing the structural materials comes from the fact that swelling can interfere with dimensional tolerance, closing cooling channels or misaligning components, for example, or can impose buckling and bending stresses in components of the first wall and some other part of the nuclear reactor structure close to the first wall.

Figure ( ? )  
Ref. (29)

Temperature  
Dependence of  
Radiation Swelling  
for 316SS

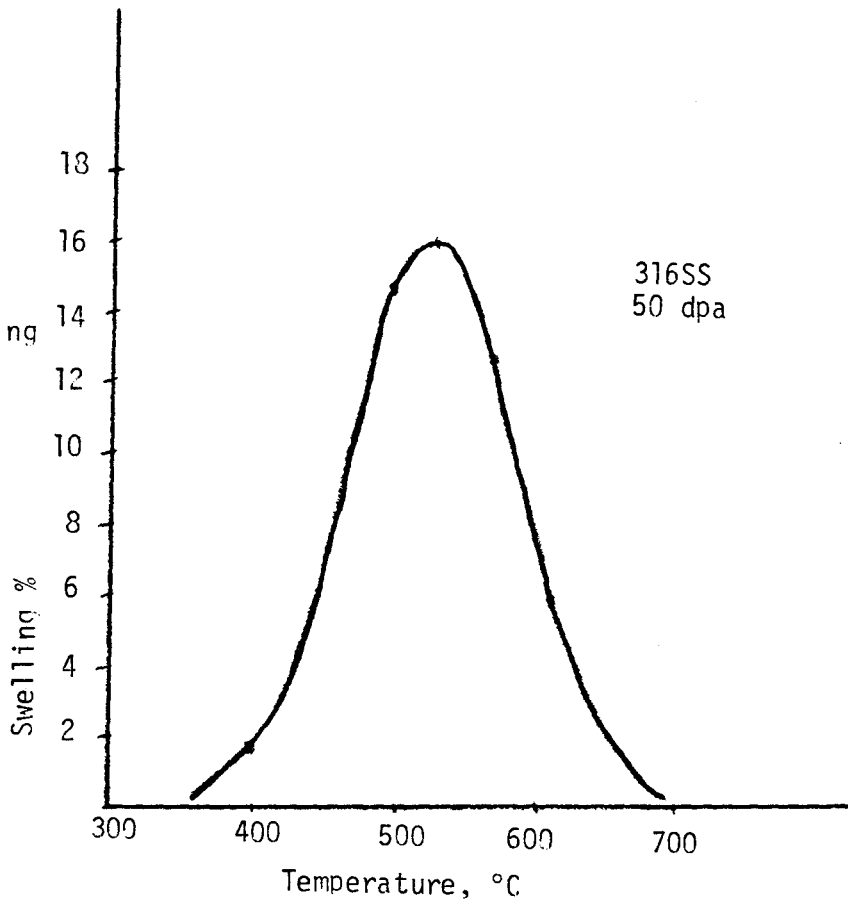
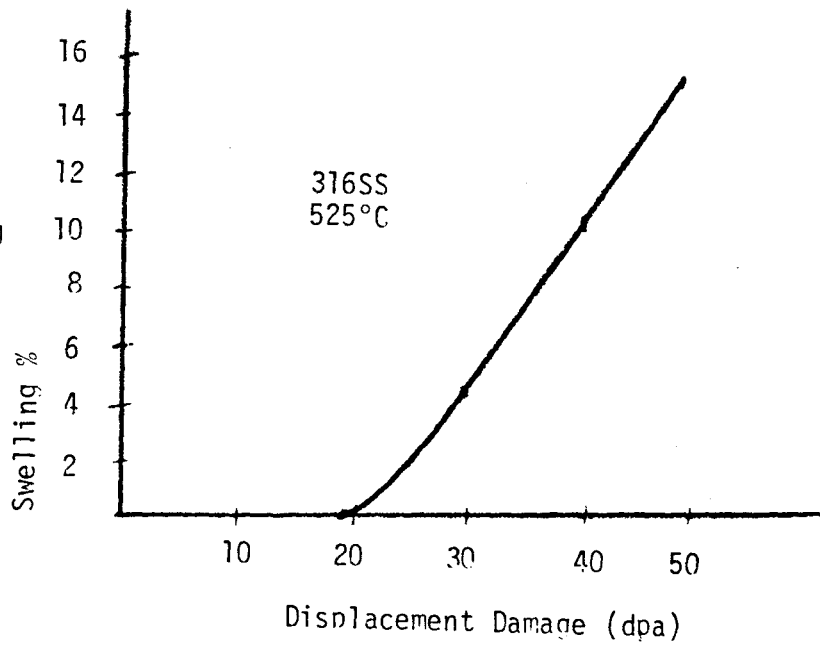


Figure ( ? )  
Ref. (24)

Radiation  
Fluence Depend-  
ence of Swelling  
Curve for 316SS



## 2. Embrittlement (Loss of Ductility)

It is absolutely essential that any massive structure such as fusion reactors have the ability to absorb a certain amount of strain energy without plastic yielding or fracturing. This will be required to offset thermal expansion between burn cycles, finite amounts of non-uniform swelling, or simple fabrication defects. The fact that the first wall will be extremely radioactive and therefore inaccessible except for remote techniques, coupled with the high cost of having an entire power plant off the line because of a single component failure, means that the designers will need as big a safety margin as possible to keep the plant running. It is not easy to establish what that margin will be until a very detailed reactor design with respect to the material is available. However, we can take some lessons from the LMFBR (liquid-metal fast breeder reactor) program: there it was determined that the component must be changed when the properties of the fuel cladding are degraded such that a strain of more than 0.4 percent exceeds the uniform elongation limit. It would be naive to simply assume that the same limit applied to the first wall of a Tokamak fusion reactor, which must maintain absolute vacuum tightness over a large surface area in the order of  $1000 \text{ m}^2$  or more in the face of changing magnetic fields, temperatures, flow rates, damage rates, and environments. The probabilities for failure are greater, and the time required to correct the fault will be longer in Tokamak fusion reactors than those required to pull out a defected fuel element in a fission reactor.<sup>19</sup>

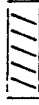

The presence of helium in the first wall is due to  $(n,\alpha)$ -reactions. The high helium generation rate will decrease the ductility of the materials and probably place an upper temperature limit (maximum operating temperature) on the first wall (the higher the temperature, the higher the embrittlement due to helium). The displacement damage and helium concentration in the three materials in question are shown in Figure (4), where it can be seen that Nb-1Zr has the least of He appm and displacement damage<sup>28</sup> (dpa).

Loss of ductility (embrittlement) is measured by the decrease in the uniform elongation of the material in question. Figure (5) shows the uniform elongation of irradiated V-20Ti and Nb-1Zr, up to a dose of  $3.7 \times 10^{22}$  n/cm<sup>2</sup> ( $> 0.1$  MeV), and for comparison the unirradiated curves are sketched in the same graph. Figure (6) shows the total elongation of the same material.

From Figure (5), we see that Nb-1Zr suffer severe loss of ductility, but its curve stays consistent over a wide range of temperatures, while V-20Ti has a good ductility, but its curve goes down very rapidly (losing ductility) when the temperature approaches 600°C.

In the case of 316SS, we have more information about its ductility behavior from the literature (see Nuclear Systems Material Handbook<sup>27</sup>). The uniform elongation is given by the equation:

Comparison of Current Radiation Effects Data Base With Target  
 316SS, Nb-1Zr, and V-20Ti Levels Equivalent to 40 MW·Years/m<sup>2</sup>

 Damage Achieved by Experiment  
 Possible Damage Region

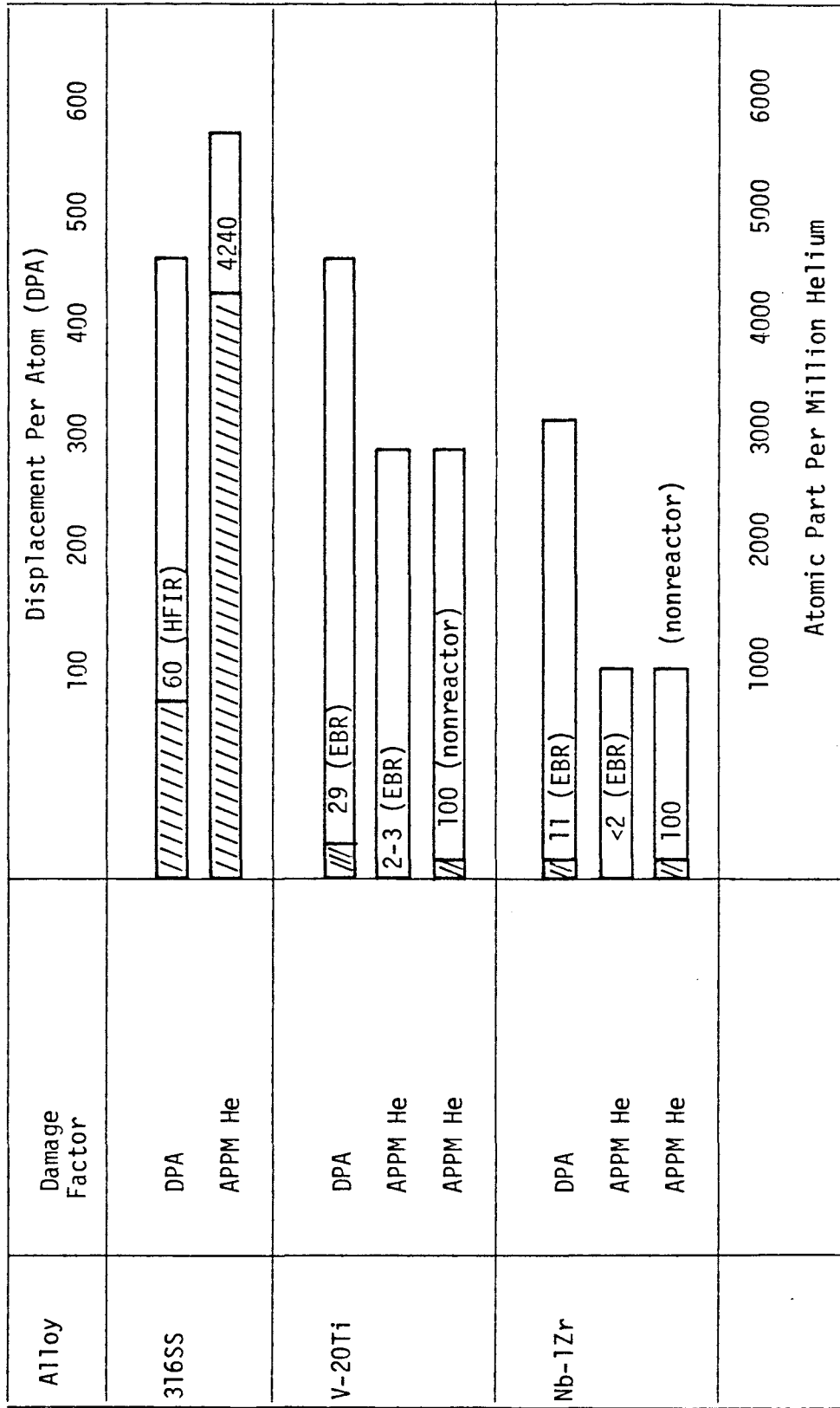
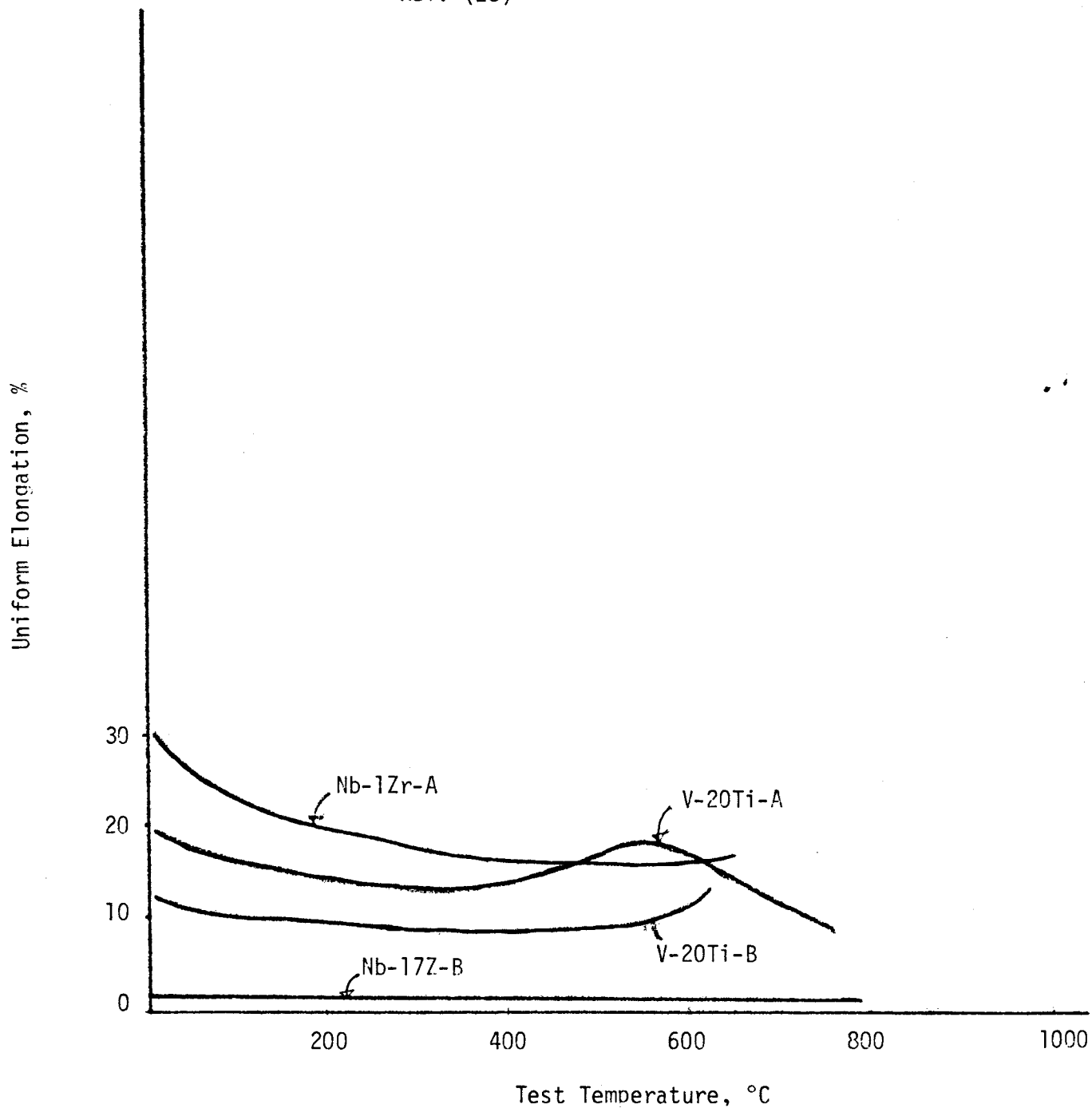


Figure (4)  
 Ref. (28)

Figure (5 )  
Ref. (28)



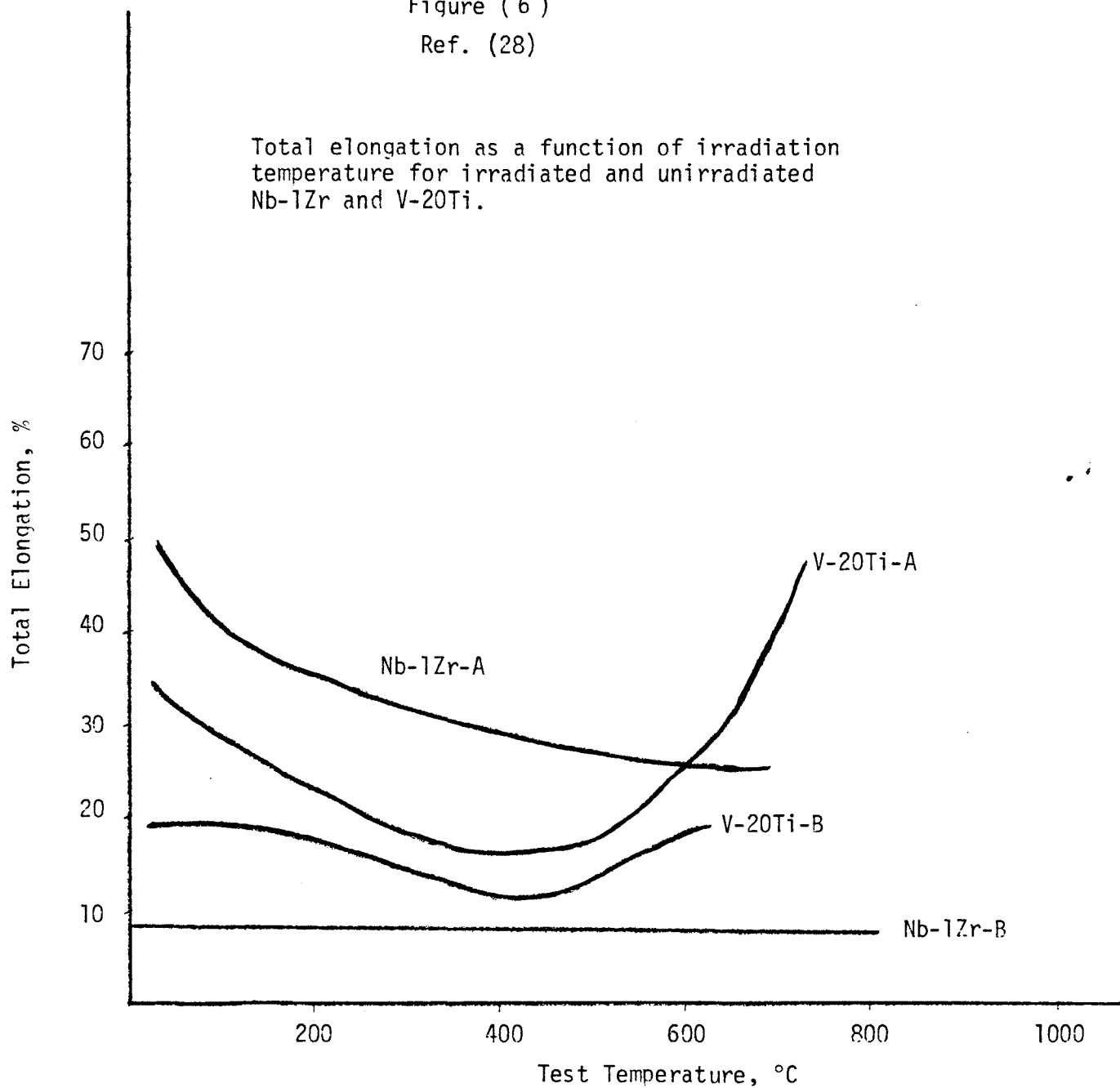
Tensile ductility as a function of irradiation temperature for irradiated and unirradiated Nb-1Zr and V-20Ti



Figure (6)

Ref. (28)

Total elongation as a function of irradiation temperature for irradiated and unirradiated Nb-1Zr and V-20Ti.



Nb-1Zr A - Unirradiated  
 B -  $3.7 \times 10^{22}$  n/cm<sup>2</sup> (> 0.1 MeV)

V-20Ti A - Unirradiated  
 B -  $2.6 \times 10^{22}$  n/cm<sup>2</sup> (> 0.1 MeV)

$$\epsilon_u(\phi t) = \epsilon_f + (\epsilon_i - \epsilon_f) \exp(-D\phi t) \quad (4)$$

$\epsilon_u(\epsilon t)$  = uniform elongation as function of displacement damage

$\epsilon_i$  = unirradiated value of uniform elongation

$\epsilon_f$  = asymptotic value of uniform elongation approached at high fluences

D = material constant

$\phi t$  = integrated radiation damage

The temperature dependence of the uniform elongation for 316SS

$$\epsilon_u(\phi t, T) = \epsilon_u(\phi t) \left[ B \exp(-CT) + \frac{1}{\exp[(T-T_{emb})/2\Delta T] + 1} \right] \quad (5)$$

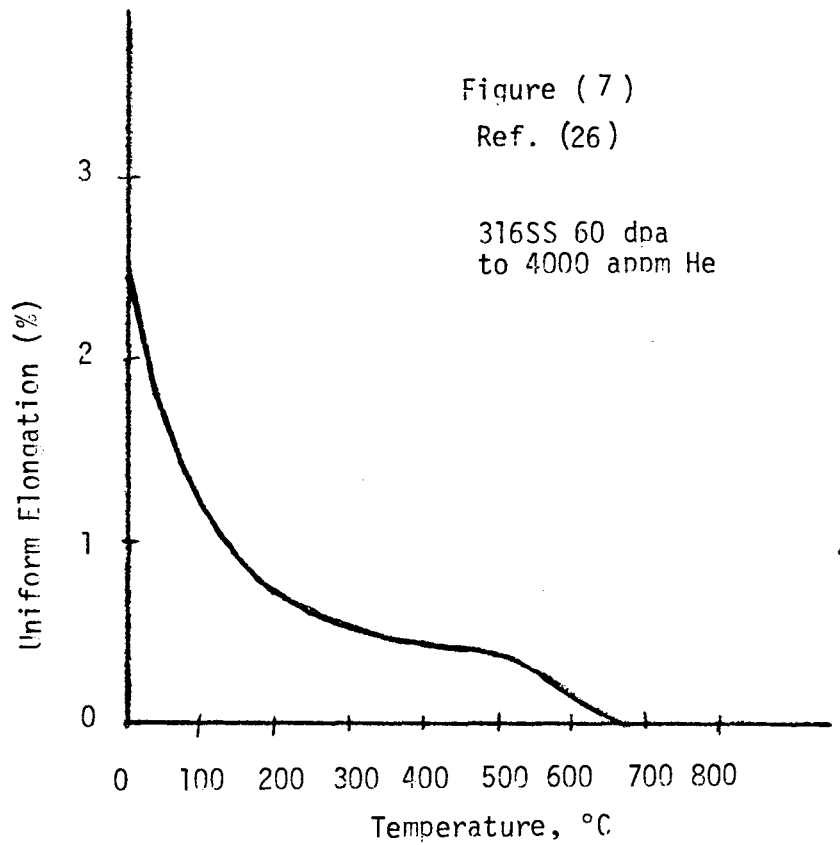
B and C = materials constant

$\Delta T$  = temperature range over which helium embrittlement becomes important

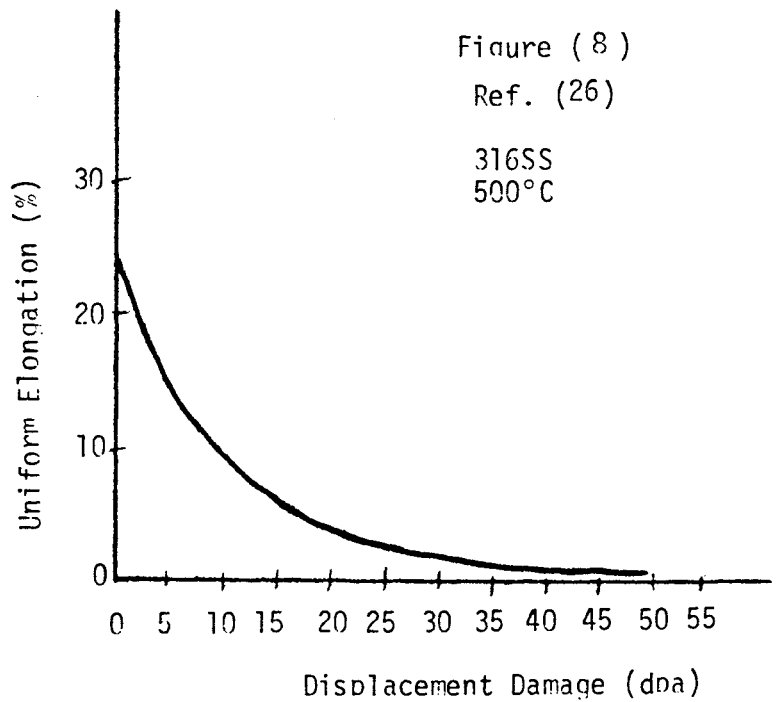
T = operating temperature

Figure (7) and Figure (8) show the curves of uniform elongation for 316SS using the above equation.<sup>5</sup> From the curves we see that 316SS has a severe loss of ductility at elevated temperatures.

Temperature Dependence of  
Uniform Elongation for  
Highly Irradiated 316SS



Uniform Elongation as  
a Function of Radiation  
Damage for 316SS



### 3. Transmutation of the First Wall Materials

Due to  $(n,\gamma)$ ,  $(n, 2n)$ , and  $(n,\alpha)$  processes, a considerable percentage of the first wall material undergoes radioactive transmutation. The transmutation chains of Nb (niobium) are shown in Fig. (9). The end products of the Nb chains are always Zr, Mo, helium, and hydrogen. The composition of originally 100% pure Nb first wall after 20 years of irradiation is calculated to have 9.5% Mo and 13.4% Ar. This figure shows that the subject is far from trivial because the transmuted alloy may have properties quite different from the original material. This problem of transmutation is also found in 316SS and V-20Ti (see Table (2)).

Helium produced in  $(n,\alpha)$  reaction is believed to be the most important of the transmutation products of the 14-MeV irradiation. Helium has two important effects on structural materials. First, it affects the failure mode during elevated-temperature loading and results in reduced ductility. The second major effect of helium is the irradiation produced swelling that results from cavity formation. The agglomeration of helium into equilibrium bubbles can lead to swelling. The higher concentration of void-capture sites that form in irradiated bcc metals (alloys) should not allow the formation of the fewer, larger helium bubbles that are required for appreciable swelling due to helium. The latter process will occur if the pressure in the bubble exceeds that balanced by the surface tension. For example, in stainless steel, the helium from  $(n,\alpha)$  reaction during Tokamak reactor service will probably cause the nucleation of more cavities than would be produced during irradiation in a fission reactor. To give some kind of feeling for helium production in all the three materials, see Table (2).



Table ( 2 )  
 Ref. (30)  
Transmutation Reactions in Potential CTR First-Wall Materials

	Net Production Rate atomic ppm/MW/m <sup>2</sup> /yr.	After 20 Years	
		at % change	% change of original comp.
316SS	Fe	-1.2	-2.0
	Cr	+0.024	+0.13
	Ni	-0.18	-1.3
	Mn	+1.2	+58
	V	+0.18	+80
	Ti	+0.045	+390
	H	6370 <sup>a</sup>	NA
	He	2790 <sup>a</sup>	NA
Nb-1Zr	Nb	-1.5	-1.5
	Zr	+1.5	+1.5
	Y	+0.012	NA
	H	1140 <sup>a</sup>	NA
	He	362 <sup>a</sup>	NA
V-20Ti	V	-0.16	-0.2
	Cr	+0.099	+260
	Ti	+0.053	+0.27
	Sc	+0.0091	NA
	H	2190 <sup>a</sup>	NA
	He	718 <sup>a</sup>	NA

a = at ppm

NA = not applicable

#### 4. Effect of Radiation in General on a Power-Producing Tokamak

The effect of radiation on the structural materials of a power-producing Tokamak is important to any power company operating such a machine. The economics of the plant will be greatly influenced by the performance of the materials in the plant with respect to radiation damage. This performance of the materials could be the deciding factor in the use of the Tokamak as a power producer. Therefore, the degradation of material properties by radiation results in at least six major effects.

1. Reduced efficiency. The generation of helium gas tends to reduce the maximum temperature at which structural materials of Tokamak fusion reactors can operate for long periods of time. This, in turn, reduces allowable coolant temperature which, in turn, will lower the overall plant efficiency.<sup>19</sup>

2. Reduced plant factors. The fact that certain components of the reactor (especially the first wall) will have to be replaced before the full lifetime of the plant is reached, means that costly shut-down must occur. The exact downtime is a function of many complex considerations, but some perspective on the costs can be obtained if one knows that the revenue from a 2000 MW(e) plant is approximately \$1,000,000 per day at 20 mill/KWh(e). Estimates for some reactor designs predict that approximately 30 days per year may be lost due to radiation damage, and changing the first wall costs approximately 30 million dollars per year per 2000 MW(e) plant in downtime alone.<sup>19</sup>

3. Increased capital costs. Spare modules must be purchased at the start of the plant to replace those involved in the first change-out (thereafter, the costs are included in operating costs). Increased remote-handling equipment will be necessary to minimize the time involved in plant shut-down. Added hot-cell facilities may also be required. Shielding requirements for gamma rays emitted from damaged components will also increase the overall plant costs. Waste storage facilities will have to be expanded beyond those required for components which fail for "conventional" reasons such as corrosion, machining faults, etc.

4. Increased operating costs. Items (1), (2), and (3) combine with other costs to raise the unit cost of electricity. Clearly, the longer the lifetime of the wall, the cheaper the electricity, and vice versa.

5. Increases in the volume of radioactive waste which must be processed and stored. Most of the major reactor studies to date have made some assumptions about the first-wall lifetime. These are listed in Table (3), along with the alloy system and the amount of material to be replaced per MW(e).yr. If we ever do get into a large-scale fusion reactor economy, such as  $10^6$  MW(e) perhaps by 2040, then this means that approximately 400,000 t (ton) of radioactive waste would be generated per year. Clearly such a number represents a potential problem in waste management.<sup>19</sup>



6. Demand on scarce elements. When components become defective and radioactive at the same time, it is usually more economical to compact, process, and store them until the radioactivity decays to safe levels, then try to refabricate them. However, all the structural materials (I had chosen (316SS, Nb-1Zr, and V-20Ti) except the V-20Ti), will stay radioactive for long periods of time. V-20Ti could be re-fabricated after 50 years approximately. Therefore, the replacement of any defected, radioactive component will have to come from new elements.

TABLE ( 3 ), Ref. (19)

Summary of Radioactive Waste Amounts for Various CTR Reactor Designs

Reactor	First-Wall	Predicted Wall Life (MW·yr/m <sup>2</sup> )	Material Replacement (t/MW(e)·yr)
UWMAK-I	316SS	2.5	0.69
UWMAK-II	316SS	2.3	0.49
UWMAK-III	TZM	3.4	0.31
BNL	AL	3.8	0.27
ORNL	Nb-1Zr	>10	0.41
LASL-ANL	Nb-1Zr	10	0.33

UWMAKI,II,III University of Wisconsin Conceptual Design of Commerical Tokamak Reactors

BNL Brookhaven National Laboratory

ORNL Oak Ridge National Laboratory

LASL-ANL Los Alamos Scientific Laboratory and Argonne National Laboratory

COMPARATIVE STUDY IN THE USE OF 316SS, V-20Ti, AND Nb-1Zr AS A STRUCTURAL MATERIAL IN THE FIRST-WALL OF A TOKAMAK REACTOR	العنوان:
Al Morished, Mutlaq Hamad	المؤلف الرئيسي:
Johnson, Ernest F.(Super.)	مؤلفين آخرين:
1981	التاريخ الميلادي:
Princeton	موقع:
1 - 161	الصفحات:
617900	رقم MD:
رسائل جامعية	نوع المحتوى:
English	اللغة:
رسالة ماجستير	الدرجة العلمية:
Princeton University	الجامعة:
School of Engineering and Applied Science	الكلية:
الولايات المتحدة الأمريكية	الدولة:
Dissertations	قواعد المعلومات:
الهندسة النووية، فيزياء البلازما، المفاعلات النووية	مواضيع:
<a href="https://search.mandumah.com/Record/617900">https://search.mandumah.com/Record/617900</a>	رابط:

## Chapter Four

### Compatibility of the First-Wall Materials with Coolants

1. Liquid Lithium
2. Helium
3. Molten Salt
4. Water ( $H_2O$ )

### Compatibility of the First-Wall Materials with Breeders

1. Liquid Lithium
2. Molten Salt
3. Solid Breeder

## COMPATIBILITY OF THE FIRST WALL MATERIALS WITH COOLANT

The compatibility of 316SS, Nb-1Zr and V-alloys with coolant materials has been judged almost exclusively in terms of the thinning of the first wall. On this basis, a corrosion rate of approximately 25  $\mu\text{m}/\text{year}$  is usually taken as the upper bound for acceptable coolant compatibility.

Because the other face of the first wall, that facing the plasma, will have a thinning problem coming from sputtering and blistering by energetic ions and neutral atoms, a lower limit set for the thinning by the coolants.<sup>31</sup>

Other corrosion effects may argue for even lower corrosion limits on coolant. Among these effects are the selective leaching of certain elements contained in the first wall, interstitial impurity transfer to or from the first wall, and accumulation of corrosion products in heat exchanger tubes. Another important corrosion consideration is the degree of mass transport of radioactive first-wall elements to piping and heat exchanger surfaces outside the reactor radiation shield. This transport is particularly significant if it requires remote maintenance for regions outside the nuclear island.

### 1. Liquid Lithium

Lithium has been considered a serious choice as a coolant in the Tokamak reactor, especially if the refractory metal alloys are used as a first-wall structural material. The lithium is very compatible with

Nb-1Zr up to 1000°C and V-20Ti up to 850°C; it is not a practical coolant with 316SS above 500°C because of the corrosion problem.

Liquid lithium has a problem in the present of a strong magnetic field where a force will be generated by the magnetic field to oppose the flow and this will require the use of more pumping power. But this problem can be solved by the design of the coolant flow patterns in the magnetic field.

The use of lithium as a coolant as well as blanket eliminates the need for an intermediate heat exchanger between the blanket and coolant circuits. The intermediate heat exchanger will still be used in the steam generators.<sup>31</sup>

The refractory metal alloys (Nb-1Zr and V-20Ti) all show very good compatibility with liquid lithium at temperatures well above those of interest for the first-wall. This generalization is true, however, only as long as the purity, particularly with regard to the interstitial level, of both the liquid lithium and refractory metal alloys remain quite high. Of special concern is the possibility of interstitial transport from one part of the coolant system, where non-refractory metal alloys might be use, to the refractory metal alloy first wall structure.<sup>28</sup>

In liquid lithium, oxygen transport will be from the metal into the lithium for virtually any Li-metal combination. Therefore, carbon and nitrogen effects may be of more concern than oxygen transport in Nb-1Zr and V-alloys since these materials will preferentially remove carbon and

nitrogen from liquid lithium. With regard to the use of refractory metal alloys in liquid lithium cooled reactors, the hot trapping of nitrogen and carbon might ultimately be required for systems using Nb-1Zr and V-alloys. Both offer clear advantages over 316 stainless steel for temperatures above about 500°C.

The refractory metal alloys (Nb-1Zr and V-20Ti) are compatible only with liquid lithium coolant at temperatures sufficiently high enough to provide attractive power conversion efficiency. Therefore, the choice of coolant in the case of Nb-1Zr and V-20Ti might be limited to that of liquid lithium.<sup>31</sup>

## 2. Helium

The physical and chemical properties of pressurized helium make it an attractive coolant for magnetically confined fusion reactors. Helium is compatible with many structural alloys, is not subjected to MHD effects, does not present a significant radiation hazard, and affords favorable chemical characteristics for tritium containment and processing. In addition, a well-developed technology base exists for helium from its use as a coolant for fission reactors. Although helium itself is chemically inert, impurity gases carried by the helium tend to be chemically reactive with the first wall materials. The impurity content of the helium will be determined by inleakage, desorption from loop components, diffusion through the helium containment from the plasma and power conversion system, transmutation, chemical reaction of

impurities with each other or other materials in the loop, and the efficiency of the coolant purification system. The more probable impurities include hydrogen isotopes, water, Co,  $\text{Co}_2$ ,  $\text{CH}_4$ , and  $\text{N}_2$ .

316 stainless steel effectively resists carburization and oxidation by normal impurities in helium up to about  $750^\circ\text{C}$ , but Nb-1Zr and V-alloys can react with impurities in the very low concentration range with unfavorable consequences. Thermodynamic calculations indicate the partial pressure of all (active impurities) in the gas must be maintained below about  $1.3 \times 10^{-3}$  Pa ( $10^{-6}$  torr) in order to avoid serious contamination of Nb-1Zr and V-alloys at  $600^\circ\text{C}$  in times less than a year. This partial pressure is equivalent to an impurity concentration of about 1 part per billion; for helium pressures which are likely to be in the 5MP (about 50 atm) range, the impurity concentration would have to be kept in parts per trillion range. By comparison, typical active impurity levels in helium for gas-cooled fast reactors are in 1-5 ppm range. The only possible relief from these potential problems appear to be operational at lower temperatures where both the surface reaction rates and bulk diffusion rates are low. For Nb-1Zr and V-alloys this temperature might have to be as low as  $400^\circ\text{C}$  and almost certainly no higher than  $500^\circ\text{C}$ , which is completely uneconomical for a fusion reactor with Nb-1Zr or V-alloys as a first wall structural material.<sup>31</sup>

### 3. Molten Salts

Molten salts as a class afford relatively high boiling points and, hence, can be contained at relatively low static pressures. Their electrical resistivities are higher than those of liquid metal coolants (liquid lithium), so that they can be moved across strong magnetic fields without incurring the strong breaking action induced in liquid lithium. However, those molten salts systems that are known to provide acceptable chemical and radiation stability have characteristically high melting points ( $> 300^{\circ}\text{C}$ ). Also, the electrical potential induced by the movement of molten salts through magnetic fields poses an important unknown in assessing their corrosivity.<sup>28</sup>

The most commonly considered coolants of the molten salts for fusion reactor first-wall are LiF-BeF<sub>2</sub> mixtures. Only molybdenum or Ni-Mo alloys have demonstrated any capability for long term operation in active molten salts at elevated temperatures V and Nb alloys are generally much too reactive for such service.<sup>31</sup>

### 4. Water (H<sub>2</sub>O)

The experience and data available on the use of water as a coolant and working fluid far exceed those of any other material. The compatibility of structural materials such as 316SS is very well understood and documented for pressurized water or water-steam mixtures.<sup>31</sup>

The most serious corrosion problems in water circuits are associated with evaporation since the expulsion of steam during boiling can produce high concentrations of nonvolatile corrosive impurities in water phase.



Thus the control of water chemistry, principally through the removal of undesirable impurities and the addition of chemical inhibitors, is fundamental to the operation of water circuits, irrespective of the containment material. In the presence of high-level radiation fields, the dissociation of water into hydrogen and oxygen further complicates the water chemistry problem. Because there are no presently accepted techniques for effecting oxygen recombination in boiling water circuits, fission reactors cooled by conversion of water to steam (BWRs, Boiling Water Reactors) typically operate with dissolved oxygen concentrations as high as 0.2 wt ppm. Such oxygen concentrations have produced stress-corrosion cracking of weldsensitized 316SS under cyclic or steady-state loading. In the case of fission reactors cooled by pressurized water (PWRs), a hydrogen overpressure is maintained to effect oxygen recombination. The efficiency of this approach in the case of fusion reactors will depend on the degree to which hydrogen from the water phase would tend to degrade the D-T plasma reactions.

In the case of refractory metal alloys (Nb-1Zr and V-20Ti), the presence of oxygen in the water phase plus all kinds of impurities that will be carried by the water will tend to react with the alloys resulting in unfavorable consequences. This will limit the use of water as a coolant in a fusion reactor with a first-wall made of Nb-1Zr or V-20Ti to 400°C and possibly only to 300°C.

## THE EFFECT OF COOLANT TEMPERATURE

Power conversion efficiency increases with increasing temperature. For a typical Rankine cycle, the efficiency goes from  $\sim 26\%$  for a  $320^\circ\text{C}$  turbine inlet temperature, to  $\sim 43\%$  for a  $540^\circ\text{C}$  turbine inlet temperature. Therefore, there is an obvious advantage in extracting heat from the blanket at as high a temperature as possible, within the constraints of a steam cycle. The coolant temperature for 316SS will not exceed  $500^\circ\text{C}$ , therefore the efficiency will be some where around  $40\%$ . In the case of V-20Ti, the coolant temperature will be  $650^\circ\text{C}$  with efficiency of  $\sim 52\%$ . Nb-1Zr can operate at temperatures as high as  $1000^\circ\text{C}$  or more. The coolant temperature, therefore, in the case of Nb-1Zr first wall will be much higher than that of 316SS and V-20Ti, and the efficiency will be higher also.

Figure ( 1 ) summarizes the compatibility of the structural materials (316SS, Nb-1Zr, and V-20Ti) with the coolants. In this figure we can see what problem each coolant will have with every one of the three structural materials. Corrosion and impurity contamination are the most common problems.

Compatibility of 316SS, V-20Ti, and Nb-1Zr with Coolants

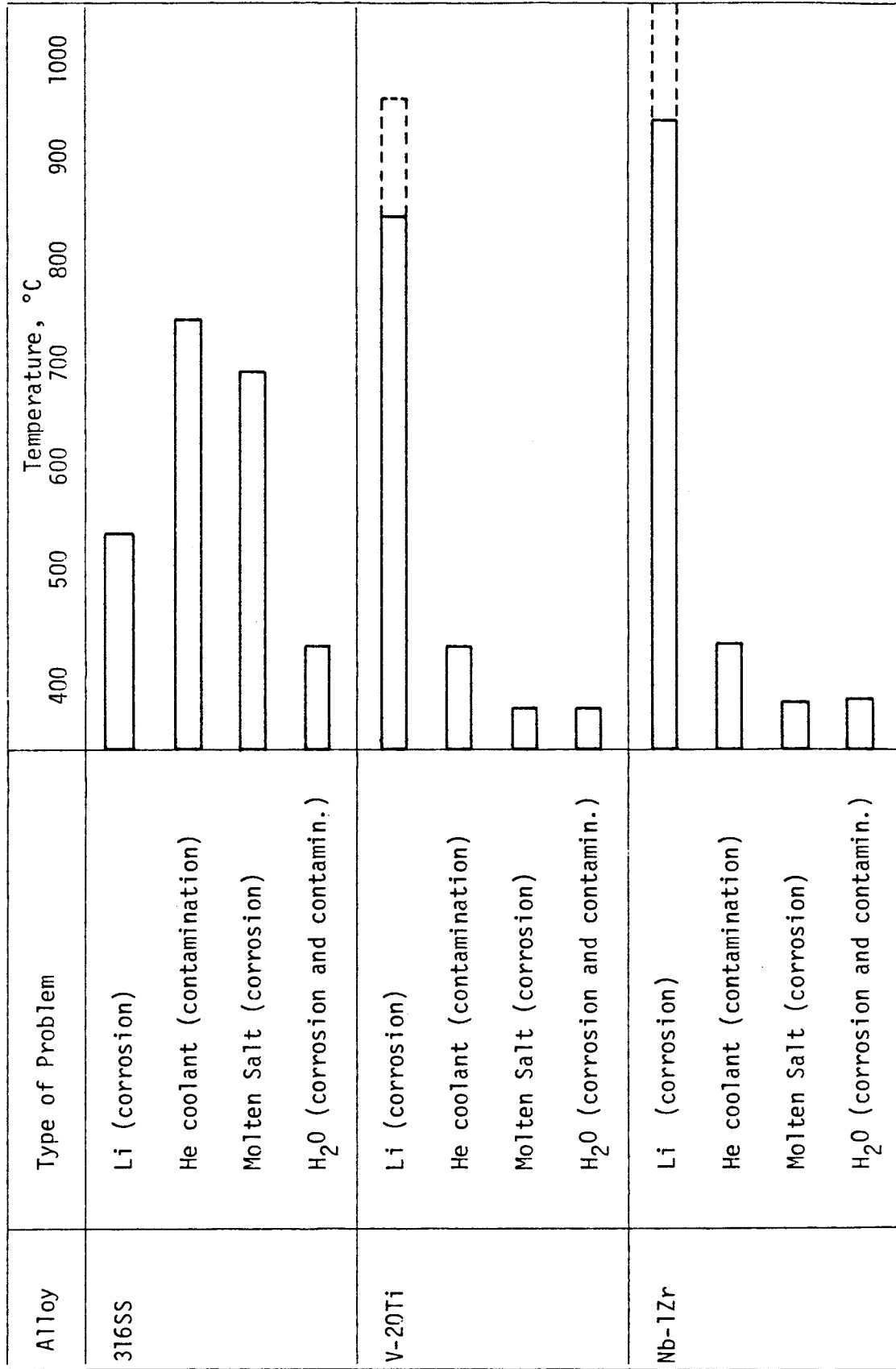


Figure ( 1 )

## COMPATABILITY OF THE FIRST-WALL MATERIALS WITH BREEDERS

1. Liquid Lithium

Among the prospective breeding materials for fusion reactors, liquid lithium is the most seriously considered one. The MHD problem associated with the use of lithium in magnetically confined machines is its major drawback.

Table (1) sets the lithium compatibility question in context. Several candidate first-wall materials are listed (316SS, V-20Ti, and Nb-1Zr), together with estimates of the highest temperatures at which these materials could be used in contact with lithium. The upper value is an estimate of highest operating temperature that we are likely to achieve given the 25  $\mu\text{m}/\text{year}$  wastage rate as a limiting criterion. The lower value is a more pessimistic estimate, which disallows any reduction in currently measured corrosion rates and set up criteria other than wastage rates as more constraining. The latter criteria include the deposition of corrosion products, interstitial impurity mass transport, preferential grain boundary attack, and radioactive isotope mass transport.<sup>31</sup>

Table (1)

Candidate Structural Material	Temperature Limit	
	Lower	Upper
316SS	500	600
V-20Ti	650	800
Nb-1Zr	700	1100

## 2. Molten Salts (LiF-BeF<sub>2</sub>)

Among the lithium-containing molten salts of potential interest as breeding material, only the fluorides offer the high chemical binding energies necessary for radiation stability along with reasonable tritium breeding ratios and the potential for tritium recovery. Extensive testing in support of fission reactor programs has provided a detailed data base on the chemical and physical properties of molten Li<sub>2</sub>BeF<sub>4</sub>. The chemical stability of this salt makes it particularly attractive for blanket applications, where chemical compatibility with structural and moderator materials is essential. Also, the limited solubility of tritium in the salt greatly facilitates tritium removal. The primary disadvantages of the salt are: (1) its relatively high melting point (364°C) and (2) its breeding properties, which may require the use of a neutron multiplier in concert with the salt blanket.<sup>31</sup>

The corrosion properties of LiF-BeF<sub>2</sub> mixtures have been studied over a wide range of temperature and flow conditions. The mixtures are relatively unreactive toward such metals as Ni and Fe. However, more reactive alloying elements or metals such as Cr and Ti or Nb and V are oxidized by LiF-BeF<sub>2</sub> melts unless highly reducing conditions can be maintained in the melt. Acceptable corrosion rates of type 316SS at 650°C have been attained in LiF-BeF<sub>2</sub> systems where the redox potential of the salt was buffered by a beryllium reduction. The redox potentials required to accommodate alloys based on niobium and vanadium (Nb-1Zr and V-20Ti) appear impractical, given the unique operating features of fusion reactors.

### 3. Solid Breeder

Of the solid lithium, containing compounds suggested as breeding materials, only  $\text{Li}_2\text{O}$  has been studied experimentally with respect to chemical compatibility. In compatibility tests of  $\text{Li}_2\text{O}$  with 316SS between 800 and 1100°C,  $\text{LiCrO}_4$  and  $\text{Li}_5\text{FeO}_4$  has been found as a reaction product, but there have not been any report on the structural integrity of the container material. There is no doubt about the poor compatibility of  $\text{Li}_2\text{O}$  with the refractory metal alloys because of the presence of the oxygen.<sup>31</sup> The use of solid breeder will require the use of a neutron multiplier such as Be.

COMPARATIVE STUDY IN THE USE OF 316SS, V-20Ti, AND Nb-1Zr AS A STRUCTURAL MATERIAL IN THE FIRST-WALL OF A TOKAMAK REACTOR	العنوان:
Al Morished, Mutlaq Hamad	المؤلف الرئيسي:
Johnson, Ernest F.(Super.)	مؤلفين آخرين:
1981	التاريخ الميلادي:
Princeton	موقع:
1 - 161	الصفحات:
617900	رقم MD:
رسائل جامعية	نوع المحتوى:
English	اللغة:
رسالة ماجستير	الدرجة العلمية:
Princeton University	الجامعة:
School of Engineering and Applied Science	الكلية:
الولايات المتحدة الأمريكية	الدولة:
Dissertations	قواعد المعلومات:
الهندسة النووية، فيزياء البلازما، المفاعلات النووية	مواضيع:
<a href="https://search.mandumah.com/Record/617900">https://search.mandumah.com/Record/617900</a>	رابط:

## Chapter Five

### Mechanical and Thermal Properties (Irradiated)

1. Yield Strength
2. Creep Strength
3. Fatigue
4. Thermal Stress Parameter



## MECHANICAL AND THERMAL PROPERTIES

Mechanical properties of the first wall structural materials are important in determining the reliability and economics of the fusion power plant. Furthermore, these properties are significantly affected by the high neutron flux experienced by components in the regions near the plasma of the fusion reactor. In general, irradiation hardens the material and leads to a reduction in ductility. An exception to this is some complex engineering alloys where either hardening or softening can be observed depending on the alloy and the irradiation conditions. Regardless of this restriction, irradiation leads to a reduction in ductility.

Thermal properties of the first wall structural materials are more important than mechanical properties in determining the economics of the fusion power plant and the environmental impact. The higher the operating temperature, the higher the efficiency of the power cycle of the plant and the less waste heat dumped into the environment.

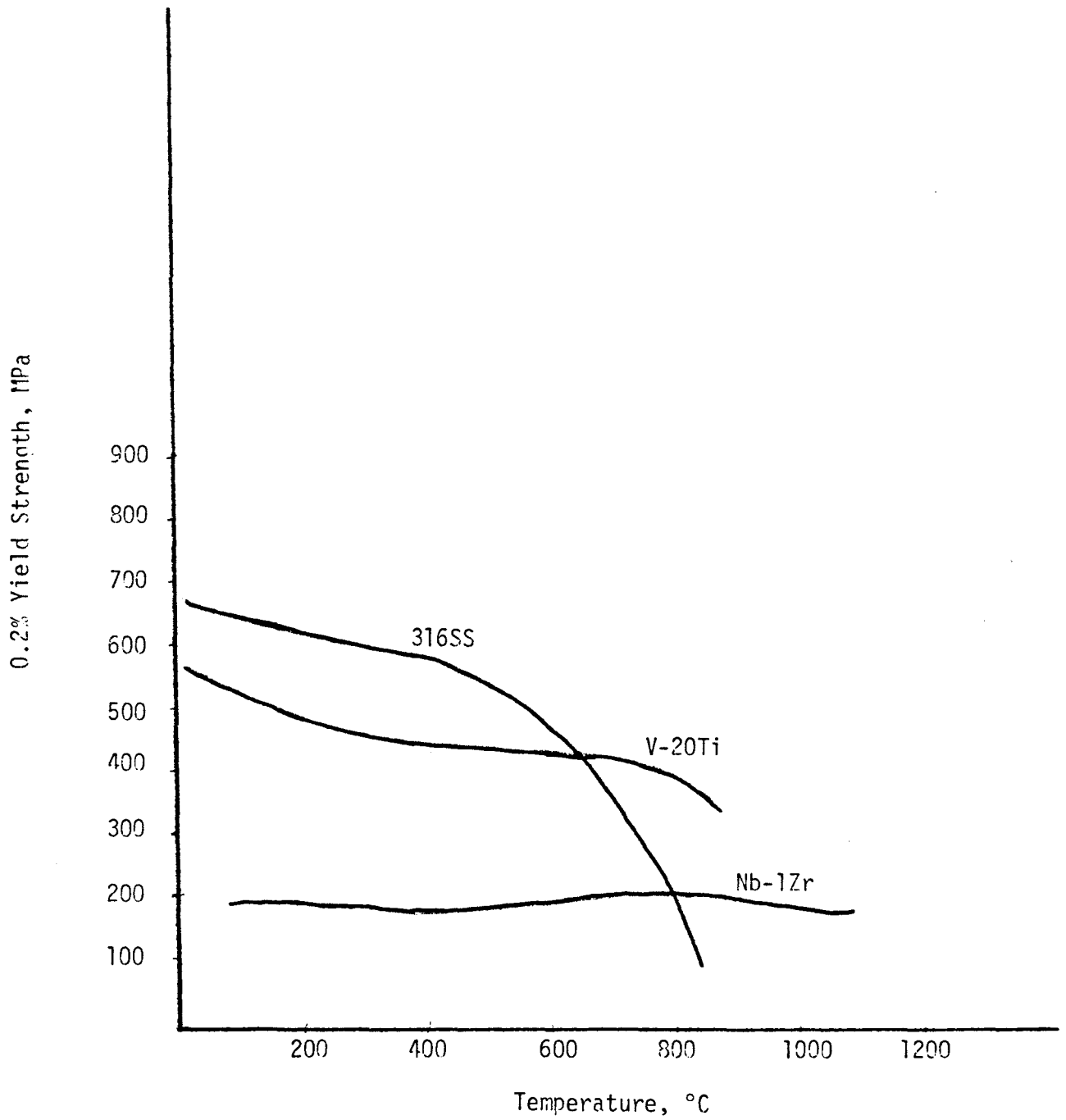
The most important mechanical and thermal properties (yield strength, creep strength, fatigue, and thermal stress parameter) will be discussed throughout this chapter.

## 1. Yield Strength

The yield strength is the stress at which a material under strain is deformed some definite amount<sup>32</sup> (as 0.1 or 0.2 percent). The yield strength is an important factor in deciding what material should be used in the first wall of the Tokamak. It influences the material ability to resist blistering; the higher the yield strength, the less chances that a blister will deform the surface of the material. Also, the yield strength influences the creep and the fatigue behavior of a given material. The elevated temperature yield strength of 316SS, V-20Ti and Nb-1Zr is shown in Figure (1). 316SS has the highest yield strength, but it goes down very rapidly when the temperature approaches 500°C. V-20Ti has a yield strength in the middle between 316SS and Nb-1Zr, and also its curve goes down when the temperature approaches 600°C, while Nb-1Zr has a yield strength lower than that of 316SS and V-20Ti, but its yield strength continues almost in a straight line to temperatures of 1000°C or over.

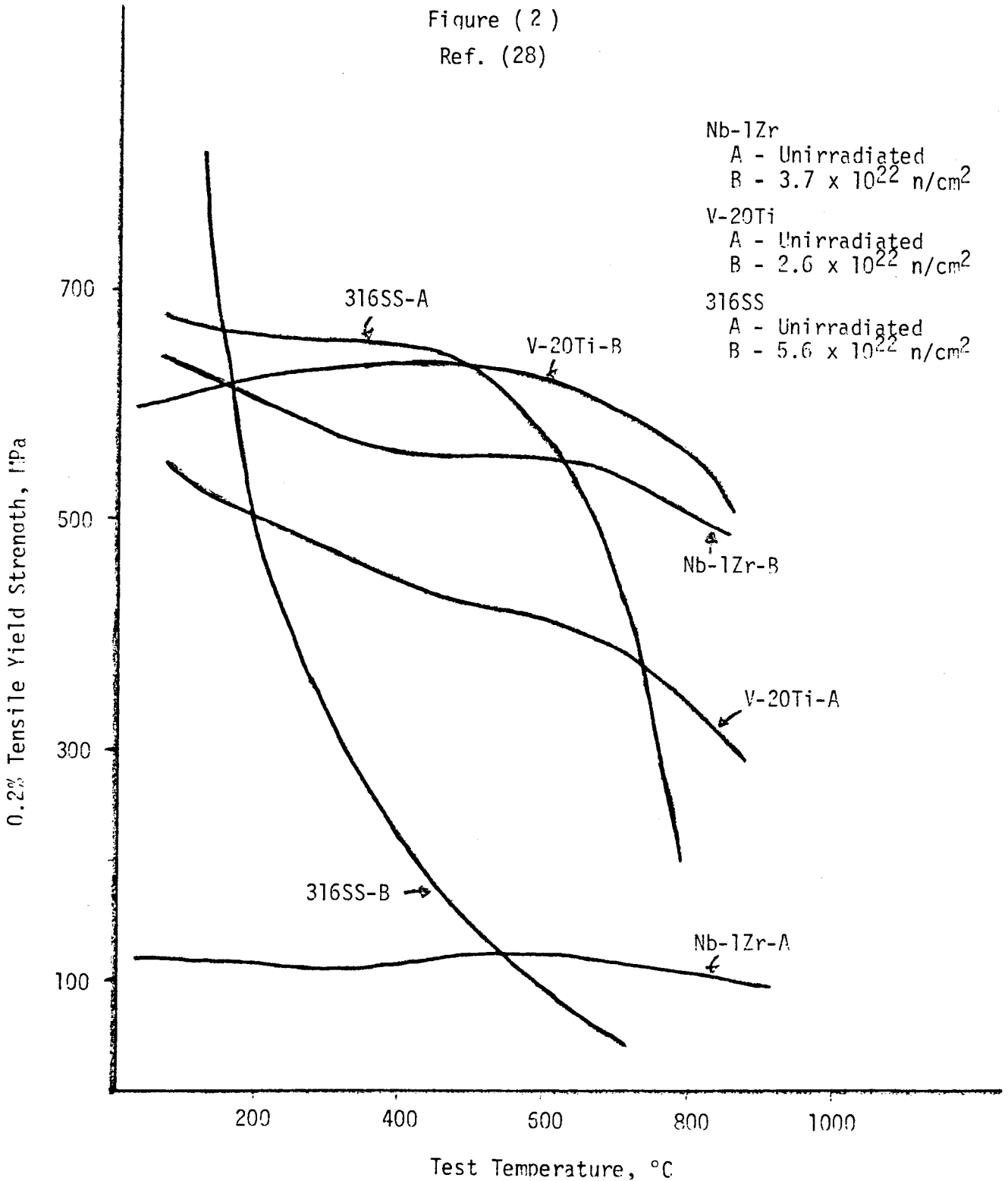
Irradiation will influence the mechanical properties of the material including the tensile yield strength. From Figure (2), the yield strength of Nb-1Zr has been increased by a factor of nearly six and also that of V-20Ti has been increased but not as much as Nb-1Zr. The yield strength of 316SS has been increased in the lower temperature region but then decreased at the higher temperature.

Figure (1)  
Ref. (28)



Elevated temperature yield strength of 316SS, V-20Ti, and Nb-1Zr

Figure (2)  
Ref. (28)



Tensile yield strength as a function of temperature for irradiated and unirradiated, 316SS, V-20Ti, and Nb-1Zr

## 2. Creep Strength

The desire for high efficiency normally means high temperatures, and each new design of a fusion Tokamak reactor pushes its structural material to the stress limit. It is well known that the combination of high temperatures (close to half the melting point) and high stresses over long periods of time will cause materials to plastically deform. It has been demonstrated that a superposition of neutron irradiation can increase the deformation (creep) rate over the thermal values. All three ingredients (high stress, high temperature, and neutrons with high energy and hard spectrum) required for gross deformation are present in a Tokamak fusion reactor first wall. We should expect that creep-rupture lives of 316SS, Nb-1Zr and V-20Ti, will have to be further lowered over their unirradiated values.

From the Nuclear Systems Materials Handbook<sup>27</sup>, the thermal creep equation for 316SS is:

$$\epsilon = \epsilon_L + \epsilon_x [1 - \exp(-St)] + \epsilon_t [1 - \exp(-rt)] + \dot{\epsilon}_m t \quad (1)$$

where

$\epsilon$  = total thermal creep strain

$\epsilon_L$  = loading strain

$\epsilon_x$  and  $\epsilon_t$  = primary creep strain

S and r = time constants

t = time

$\dot{\epsilon}_m$  = steady state creep rate

All of these parameters are functions of both stress and temperature.

The equation of irradiation creep for 316SS is:

$$\bar{\epsilon}/\bar{\sigma} = A [1 - \exp(-\phi t/B)] + C\phi t \quad (2)$$

where

$\bar{\epsilon}/\bar{\sigma}$  = effective strain-to-effective stress ratio

A = transient creep parameter

C = steady-state creep parameter

B = time constant

$\phi t$  = integrated radiation damage

Graphs of this equation are shown in NSMH.<sup>27</sup>

From the work of Mattas and Smith,<sup>29</sup> the general equation that describes the steady-state thermal creep in vanadium is given by:

$$\dot{\epsilon} = k \sigma^n \exp[-Q/RT] \quad (3)$$

where

$\dot{\epsilon}$  = steady-state creep rate

k = materials constant

$\sigma$  = applied stress

n = stress exponent

Q = creep activation energy

R = gas constant

T = temperature

which could be used in the case of vanadium-alloys.

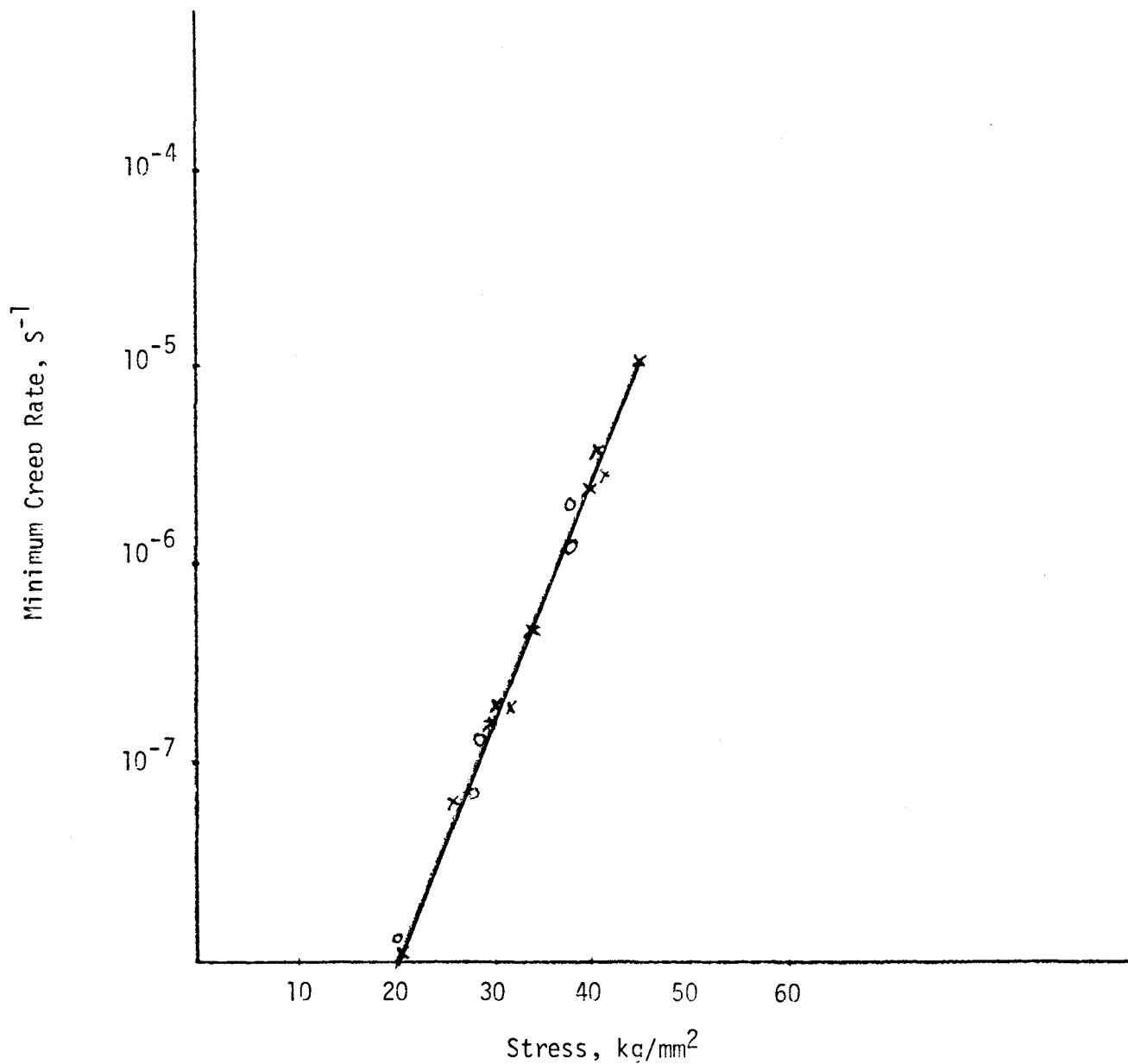
The radiation creep in vanadium alloys has not been considered because of the lack of data in literature, but from the experimental work given in Radiation Effect Design Handbook for V-20Ti, it seems that there are little changes in the creep rate of vanadium-alloy after irradiation. Figure (3) shows this.

Figure (4) shows an experimental creep curve for the V-15% Cr-5% Ti alloy at 650°C under a stress of 145 MPa and the steady-state creep curve derived from Equation (3) for similar conditions.<sup>26</sup>

The available data for niobium and its alloys bear the imprint of past investigations whose motivation was the development of alloys for nuclear and aerospace applications. These programs were primarily interested in alloys capable of operating in high stress environments for relatively short times (100 - 1000 hours) and at temperatures  $> 0.5 T_m$  ( $\sim 1200^\circ\text{C}$ ). As a result, little creep data have been developed for the lower temperatures and longer times ( $> 10,000$  hours) proposed for fusion reactor structures.<sup>5</sup>

From the work of F.W. Wiffen,<sup>33</sup> at Oak Ridge National Laboratories, it was shown by experimentation that helium contents up to at least 18 appm do not reduce the ductility of Nb-1Zr for test temperatures in the range 1000 to 1400°C. Tensile tests showed only differences that are expected from normal data scatter. Creep-rupture ductility values at first seemed to indicate helium embrittlement. However, lack of dependence

Figure (3)  
Ref. (34)



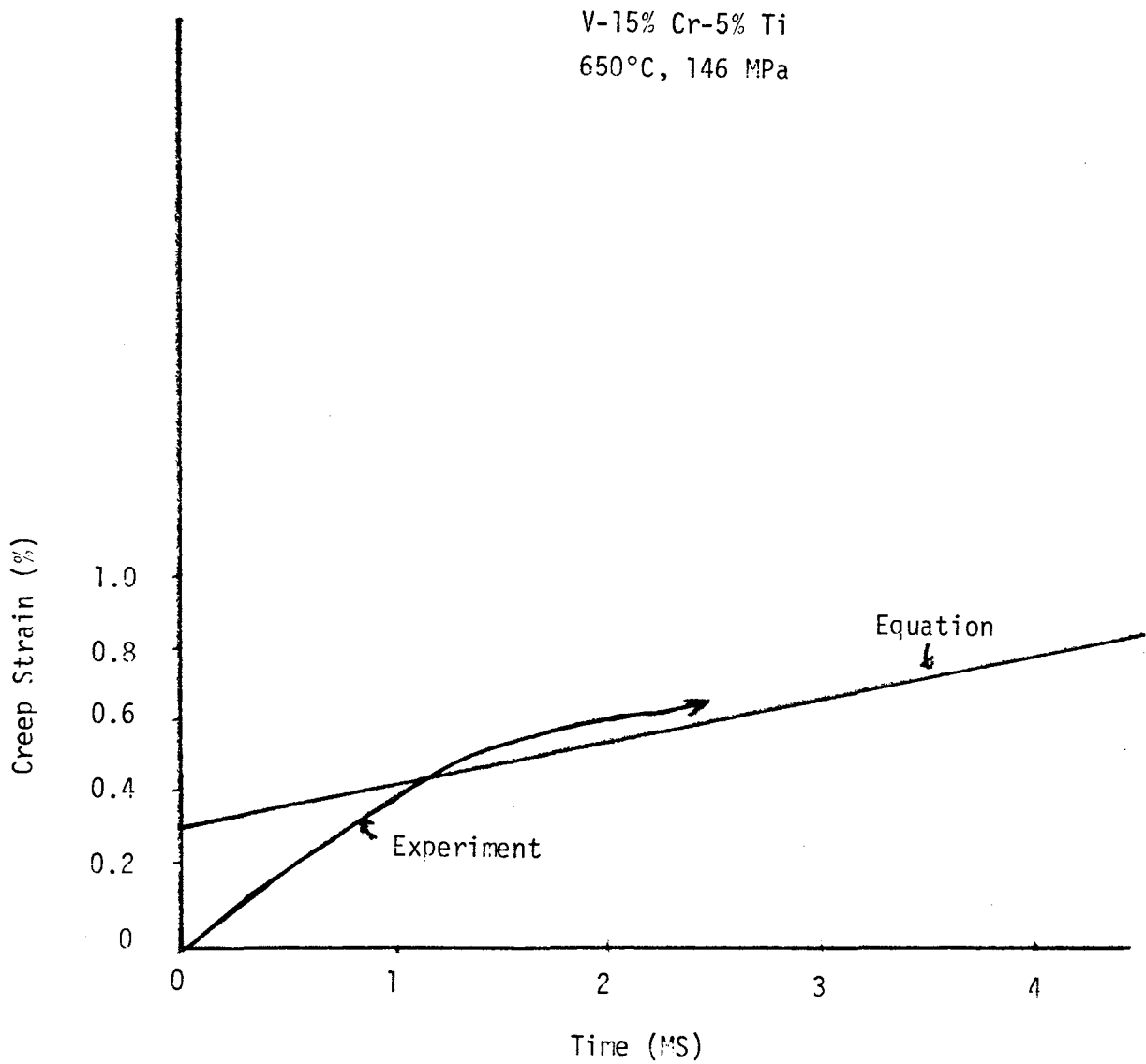
Minimum creep rate of unirradiated and irradiated ( $2 \times 10^{22}$   $n/cm^2$ )  
V-20Ti at 650°C

x, Unirradiated  
o, Irradiated



Figure ( 4 )

Ref. (26)



Creep strain curves for V-15% Cr-5% Ti alloy under a 145-MPa stress at 650°C

on the helium content, an apparently smaller effect at 1200°C than at 100°C, and absence of the classical features of helium embrittlement in fractography, metallography, and microscopy examination all suggest that the creep ductility reduction is not due to helium. The observed precipitate phase suggests that the embrittlement in the creep tests is probably due to interstitial impurity pickup in the Nb-1Zr during the helium injection. Precipitation of this impurity, possibly as  $ZrO_2$ , occurred during elevated-temperature testing and was especially effective in reducing creep rupture ductility.

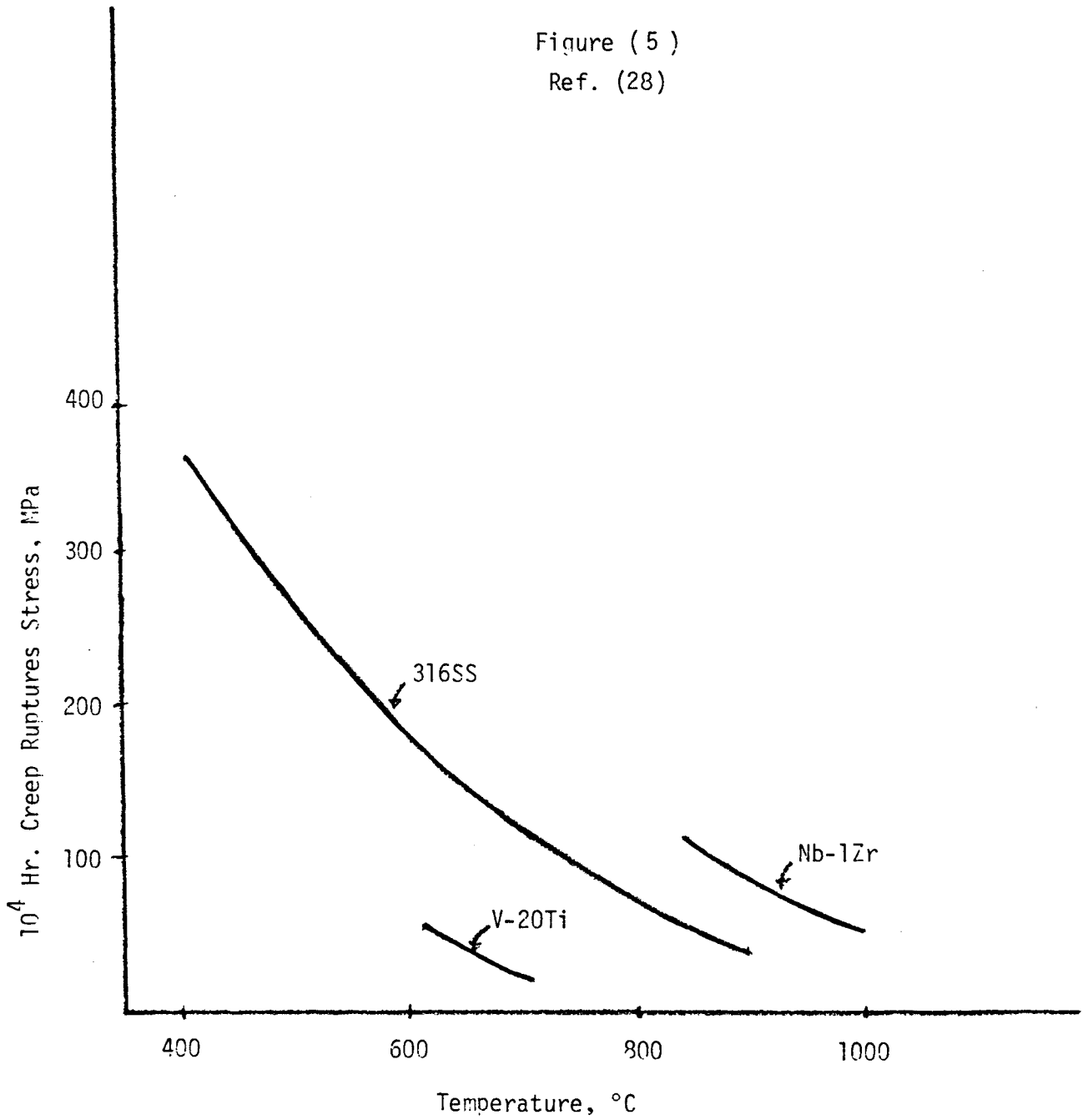
In a Tokamak reactor with Nb-1Zr first wall structural material and liquid lithium as a coolant, the oxygen interstitial pickup will be from the Nb-1Zr to the liquid lithium. This will reduce the creep problem if not eliminate it in the Nb-1Zr first wall structure.

Of great interest in irradiation creep, the deformation rate of a stressed material can be controlled by the biased flow of point defects to dislocations.<sup>35</sup> Complete measurements of irradiation creep rates require sophisticated experiments, with measurements performed during irradiation. As a result of this difficulty, the amount of data available is severely limited, especially in the case of the refractory metal alloys (V-20Ti and Nb-1Zr). Some of the considerations that relate to irradiation creep are given in Table (1).

Table (1)  
Irradiation Creep

1. Cause:
  - 1) Biased flow of point defects control deformation
  - 2) Deformation rates exceed out of reactor rates
  
2. Critical Parameters:
  - 1) Flux - dpa generation rate
  
3. Modifying Parameters:
  - 1) Fluence
  - 2) Stress
  - 3) Temperature
  - 4) Composition and metallographic state
  
4. Measurements:
  - 1) Stress or yield strength
  - 2) Temperature
  - 3) Strain with high precision

Because of a lack of data in the case of irradiation creep strength, no firm conclusions can be derived. But, by showing the creep strength for unirradiated 316SS, V-20Ti, and Nb-1Zr, some overall idea could be realized. The creep strength of refractory metal alloys (unirradiated V-20Ti and Nb-1Zr) and unirradiated 316SS are compared in Figure ( 5 ). Though V-20Ti shows reasonable short time tensile strength at 600°-700°C, its creep strength is poor. The other refractory metal alloy (Nb-1Zr) was developed for service at temperatures generally above the temperature range of interest in fusion Tokamak reactors; hence, data below about 900°C are extremely limited. From Figure ( 5 ), Nb-1Zr has reasonable creep strength at 900°-1000°C and, therefore, it should have a good creep strength at lower temperatures. The 316SS has a very good creep strength but loses it very rapidly when the temperature starts to increase. The displacement per atom is also very high in 316SS compared to Nb-1Zr. This will influence the creep strength of 316SS more than that of Nb-1Zr (dpa is a critical factor in the creep strength of irradiated materials).



10,000 Hour Creep-Rupture Stress for 316SS, V-20Ti, and Nb-1Zr at Elevated Temperatures

### 3. Fatigue

While it is desirable to have the fusion reactors operate in steady state modes, some will be pulsed (Tokamak), which means that the first wall could receive on the order of  $10^5$  cycles per year.<sup>28</sup>

In general, the term "fatigue" relates to the special behavior pattern exhibited by materials in response to cyclic loading. Such loadings have been found to be particularly detrimental under certain conditions, resulting in fatigue damage in limited exposures and eventual fatigue failure (i.e., fracture) in continued exposures. The important aspect of such failures is that they occur in cyclic exposures when the peak stress is much lower than that which would be completely safe if imposed in an unidirectional (static) application.<sup>36</sup>

Cyclic or repeated loading is particularly detrimental because this type of exposure gives rise to the formation of internal or surface microcracks that are propagated in continued exposures to reach, eventually, critical size such that the remaining cross-sectional area is reduced to the point where it can no longer support the applied load. The mechanism of fatigue is "individual crystals of the metal are seen as yielding first at some point of localized weakness. This first yielding is considered to be a slipping action in which bonds between the atoms are broken and then frequently new and stronger bonds are formed. Along with this slipping action, and perhaps caused by it, there seems to develop actual fractures, that is, the breaking of atomic bonds with no formation of new bonds. These fractures start minute cracks in the metal.

At the ends of each minute crack the stress concentration is very high so that under successive loading the cracks tend to spread like minute hacksaw cuts until insufficient sound metal is left to carry the load; at this point, sudden fracture occurs."

Fatigue life expresses the ability of a material to withstand a given cyclic exposure and is generally measured in terms of the number of cycles to produce fracture. Exposure conditions are characterized by:<sup>36</sup>

1. Stress or strain amplitude
2. Mean stress or strain
3. Cyclic frequency
4. Wave form of the stress or strain cycle
5. Temperature
6. Test environment

Clearly, fatigue life at a given temperature and in a certain environment has significance only when associated with a specific description of the exposure cycle.

Another important facet of fatigue life is the differentiation that has evolved between high-cycle and low-cycle fatigue. The dividing line is important, although not well defined. Some definitions of the low-cycle-fatigue regime include cycles to failure below 100,000 cycles, whereas others set the limit at 10,000 cycles. A distinguishing feature of the low-cycle-fatigue regime is that the peak stresses are above the tensile yield strength, and hence the strains induced usually have a noticeable plastic component. In high-cycle fatigue the strains are

confined, at least from a macroscopic point of view, to the elastic region. The differentiation between high- and low-cycle fatigue is most logical when based on elastic- and plastic-strain differences, even though it is really no great obstacle to have no clear and distinct dividing line between the two regimes.

Data concerning the fatigue behavior of niobium and its alloys (Nb-1Zr) at room and elevated temperature are meager primarily because past applications have not been fatigue limited. The data that have been developed cover a wide variety of material conditions, compositions, and types of tests, making correlations difficult. For example, pure niobium with 100 wppm oxygen was studied using fully reversed bending in a rotating cantilever machine. The test frequency was 3450 cycles per minute and the test temperature varied from 25 to 600°C. The test results indicate that for annealed niobium, an endurance limit for  $10^7$  cycles would be between 103 to 124 MPa for temperatures ranging from 25 to 500°C.<sup>5</sup> Using the same number of cycles ( $10^7$  cycles) the endurance for powder metallurgy Nb-1Zr was determined using flexural tests. This material was evaluated in both the cold work and fully annealed condition. The annealed room temperature tensile strength was 367 MPa which is higher than normally produced today (280 MPa) using electron beam melting or arc casting techniques. The strength difference is essentially due to a finer grain size and higher interstitial content. Room temperature flexural fatigue tests revealed that an endurance limit at  $10^7$  cycles would be between 172 and 200 MPa for annealed and between 193 and 214 MPa for the cold worked material.

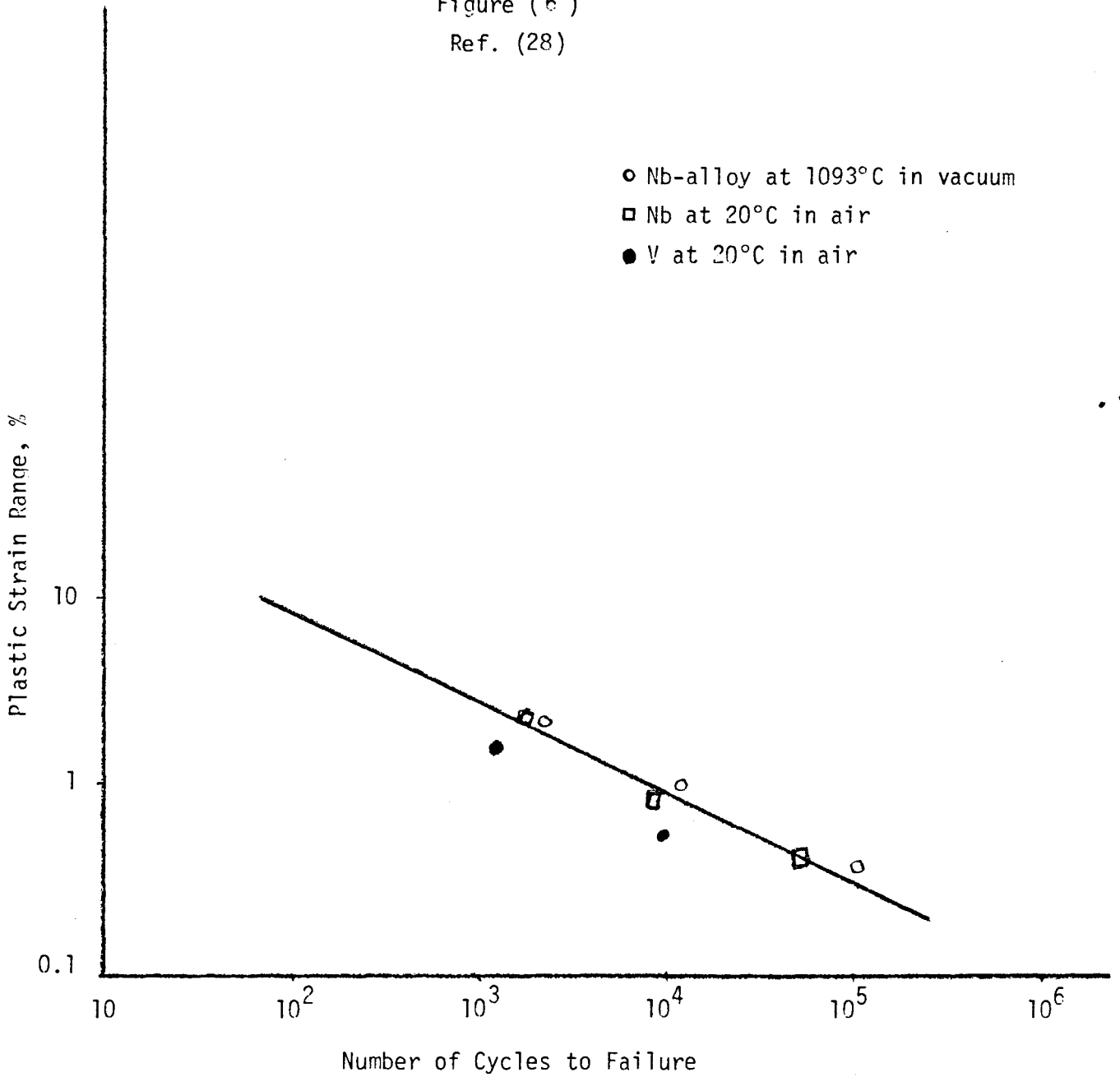


The fatigue properties of the refractory metals (V and Nb) are shown in Figure (6) (strain-life data) and Figure (7) (stress-life data). The strain-controlled or low-cycle fatigue behavior of vanadium is seen to be a little inferior to that of niobium. From this, one can conclude that Nb-1Zr must be superior to that of V-20Ti.<sup>28</sup>

High-cycle fatigue curves are shown in Figure (7). In some cases, the stress is the saturation stress from strain controlled tests. Clearly there is a very large difference in fatigue strength among the various metals. The refractory metals (V and Nb) tend to show an endurance limit. Because of dynamic strain aging effects, the endurance limit might be higher at some elevated temperature than at room temperature. Since the endurance limit of the refractory metals appears to be about 60% to 80% of the ultimate tensile strength, large variations in high-cycle fatigue strength are to be expected.

No fatigue tests have been conducted on Nb-1Zr and V-20Ti irradiated to high dpa levels and high helium content. The most important parameter in determining low cycle fatigue behavior is ductility. Tensile and creep-rupture tests in this and the proceeding chapter show that ductility is reduced at nearly all temperatures.<sup>28</sup> It is thus expected that the fatigue life will also be adversely affected. Large amounts of helium will also reduce the temperature at which the transition from transgranular to intergranular fracture occurs. This past argument is also true in the case of 316SS and may be more serious due to the high dpa levels and helium productions.

Figure (6)  
Ref. (28)



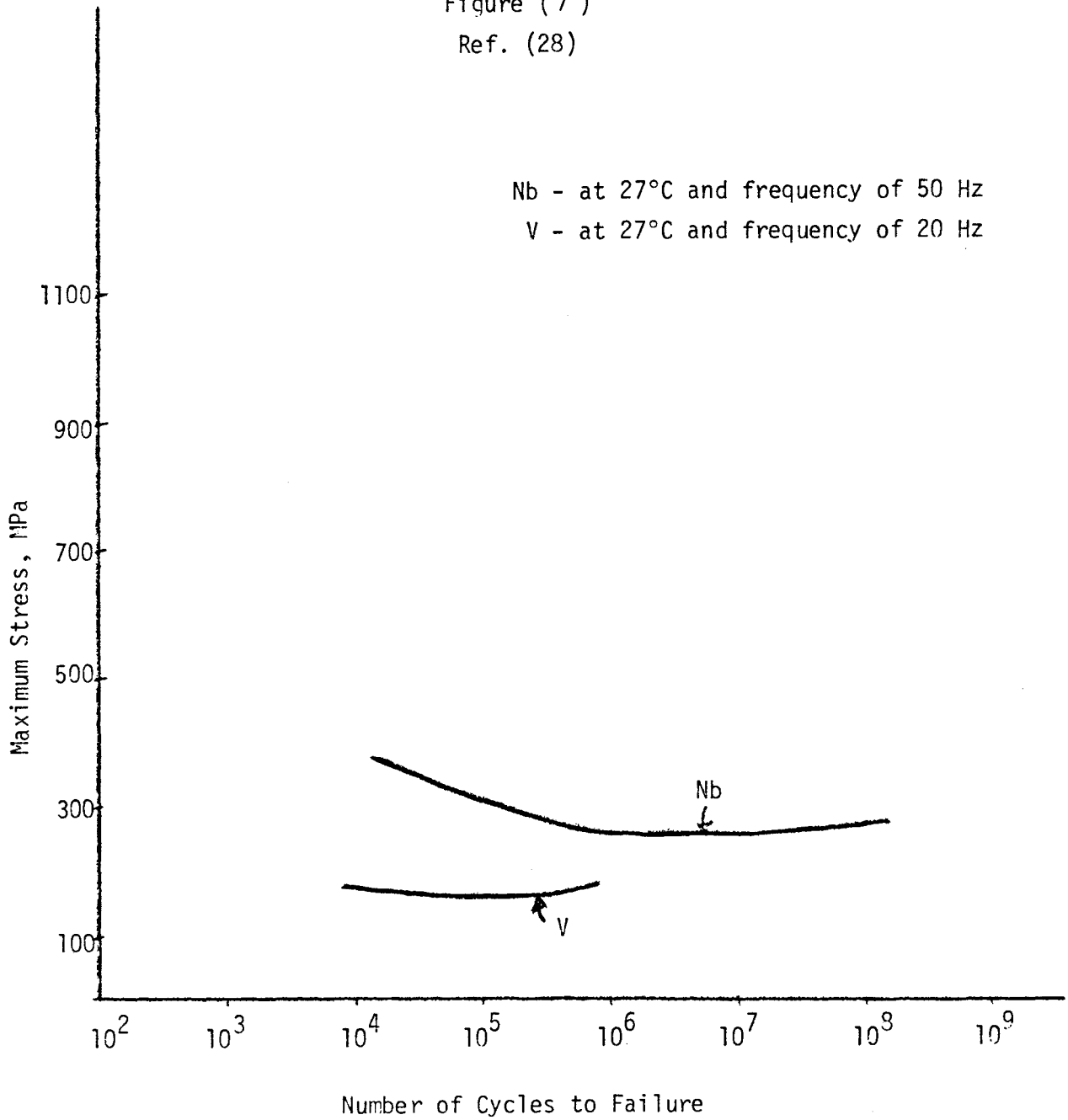
Plastic Strain Range Fatigue Properties of V and Nb

Figure (7)

Ref. (28)

Nb - at 27°C and frequency of 50 Hz

V - at 27°C and frequency of 20 Hz



Number of Cycles to Failure  
High-Cycle Fatigue for Niobium and Vanadium

In the case of 316SS, fatigue life is generally ductility-dependent in the low-cycle range (plastic strain range dominant) and strength-dependent in the high-cycle range (elastic strain range dominant). Several semi-empirical expressions have been developed that incorporate this concept and relate tensile properties to fatigue life. Two of these expressions are as follows:<sup>36</sup>

Universal slopes equation:

$$\Delta\epsilon_t = \frac{3.5\sigma_{UTS}}{E} N_f^{-0.12} + D^{0.6} N_f^{-0.6} \quad (4)$$

Characteristic slopes equation:

$$\Delta\epsilon_t = 2\epsilon_{ef} \left[ \frac{N_f}{10} \right]^{-m/2} + \frac{D^2}{\dot{\epsilon}} \left[ \frac{N_f}{f} \right]^{-1} \quad (5)$$

where

$\Delta\epsilon_t$  = total strain range

$\sigma_{UTS}$  = ultimate strength

$E$  = Young's modulus

$D$  = fracture ductility =  $\ln(100/(100-RA))$

$RA$  = reduction in area, %

$N_f$  = cycles to failure

$\epsilon_{ef}$  = elastic strain at fracture = True fracture stress divided by Young's modulus

$\dot{\epsilon}$  = strain rate =  $2f\Delta\epsilon_t$

$f$  = cyclic frequency

Both of the foregoing expressions reflect the importance of ductility and strength in the plastic and elastic components of the total strain range.

A method has been proposed for estimating irradiated fatigue properties of 316SS from a knowledge of the unirradiated strain-controlled properties and the irradiated and unirradiated tensile properties. This method is based on a fraction modification of the unirradiated fatigue data defined by the equation:

$$\Delta\varepsilon_t = \Delta\varepsilon_e + \Delta\varepsilon_p = AN_f^a + BN_f^b \quad (6)$$

where  $\Delta\varepsilon_e$  and  $\Delta\varepsilon_p$  are the elastic and plastic strain ranges and A, B, a, and b are the coefficients and exponents defined by the unirradiated fatigue data. In the absence of pertinent irradiated fatigue data, this equation is then modified by making a fractional correction as follows:

$$(\Delta\varepsilon_t)_{\text{irrad}} = \phi_u AN_f^a + \phi_t BN_f^b \quad (7)$$

where

$$\phi_u = \frac{(\sigma_{\text{UTS}})_{\text{irrad}}}{(\sigma_{\text{UTS}})_{\text{unirrad}}}$$

$$\phi_t = \left( \frac{D_{\text{irrad}}}{D_{\text{unirrad}}} \right)^{0.6}$$

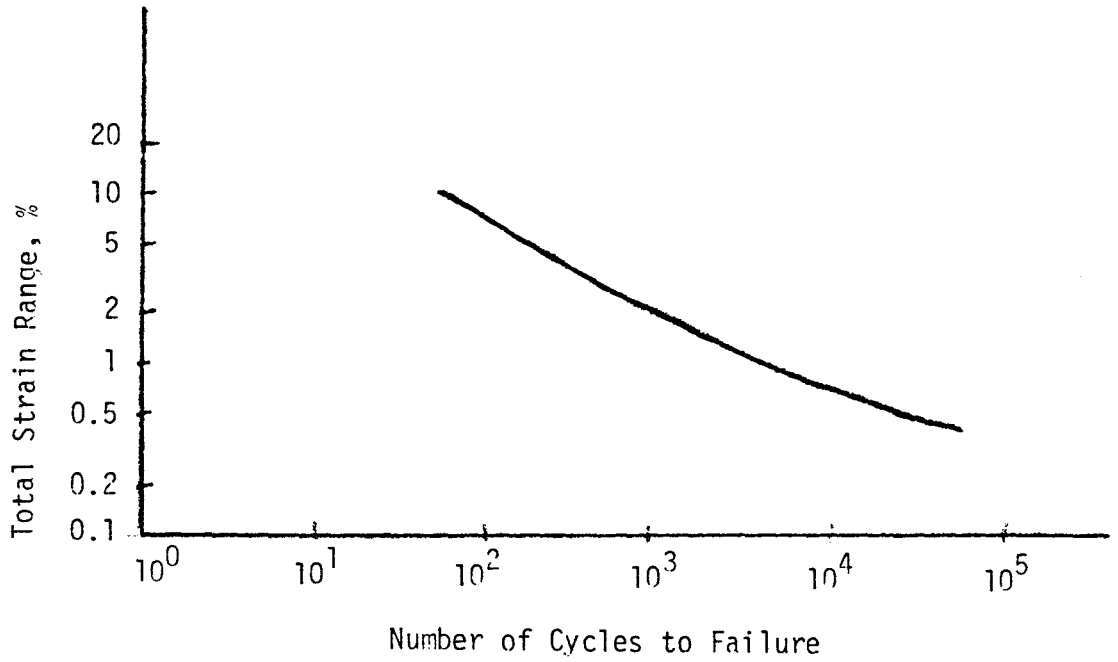
and  $\sigma_{UTS}$  and  $D$ , as defined previously, are determined from irradiated and unirradiated tensile tests at the same strain rate and temperature as the unirradiated fatigue tests.

Predicted fatigue lives based on Equation (4) are shown in Figure (8) and Figure (9) for temperatures of 430°C and 650°C and an axial strain rate of  $4 \times 10^{-3} \text{ sec}^{-1}$ , where we see the reduction of the fatigue life with the increase in temperature. Figure (10) shows the irradiated and unirradiated fatigue behavior of 316SS tested at 700°C, using Equations (4), (5), and (7). The data to construct these figures are taken from the experimental work of J.B. Conway<sup>36</sup>, R.H. Stentz<sup>36</sup>, J.T. Berling,<sup>36</sup> C.R. Brinkman,<sup>37</sup> G.E. Karth,<sup>37</sup> and T.M. Beeston.<sup>37</sup>

To conclude this argument concerning fatigue in 316SS, Nb-1Zr and V-20Ti, I would like to quote Mr. K.C. Liu<sup>38</sup> (Oak Ridge National Laboratory) wherein his conclusion he said, "Results of a cyclic fatigue test at  $\pm 0.25\%$  strain range indicate that Nb-1Zr is more fatigue resistant than 20%-cold worked type 316 stainless steel for low strain range tests."

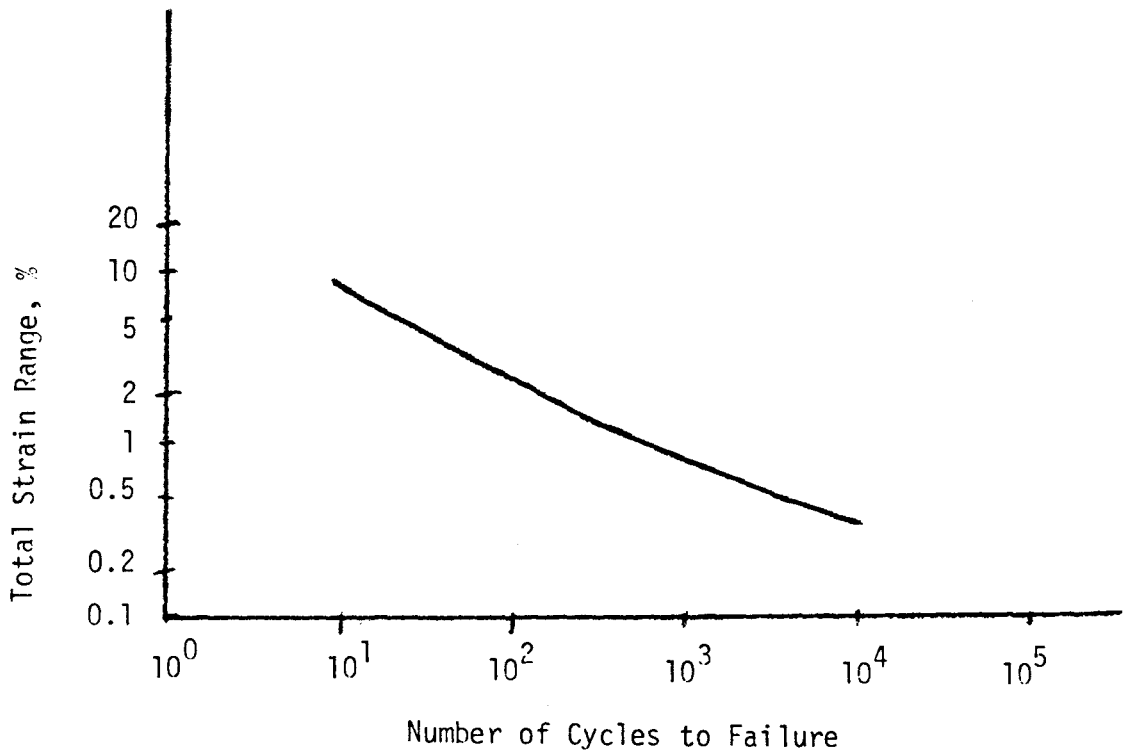
In concluding this chapter regarding the mechanical properties, I add that, compared with 316SS, the refractory metal alloys (Nb-1Zr and V-20Ti) show no advantage in tensile strength up to about 500°C-600°C, but a decisive advantage above that range. In the event that 316SS does not possess adequate creep strength at 600°C, only Nb-1Zr is likely to offer usable creep strength at temperatures much above about 700°C. The low-cycle fatigue properties of V-20Ti and Nb-1Zr appear as good as

Figure ( 8 )  
Ref. (36)

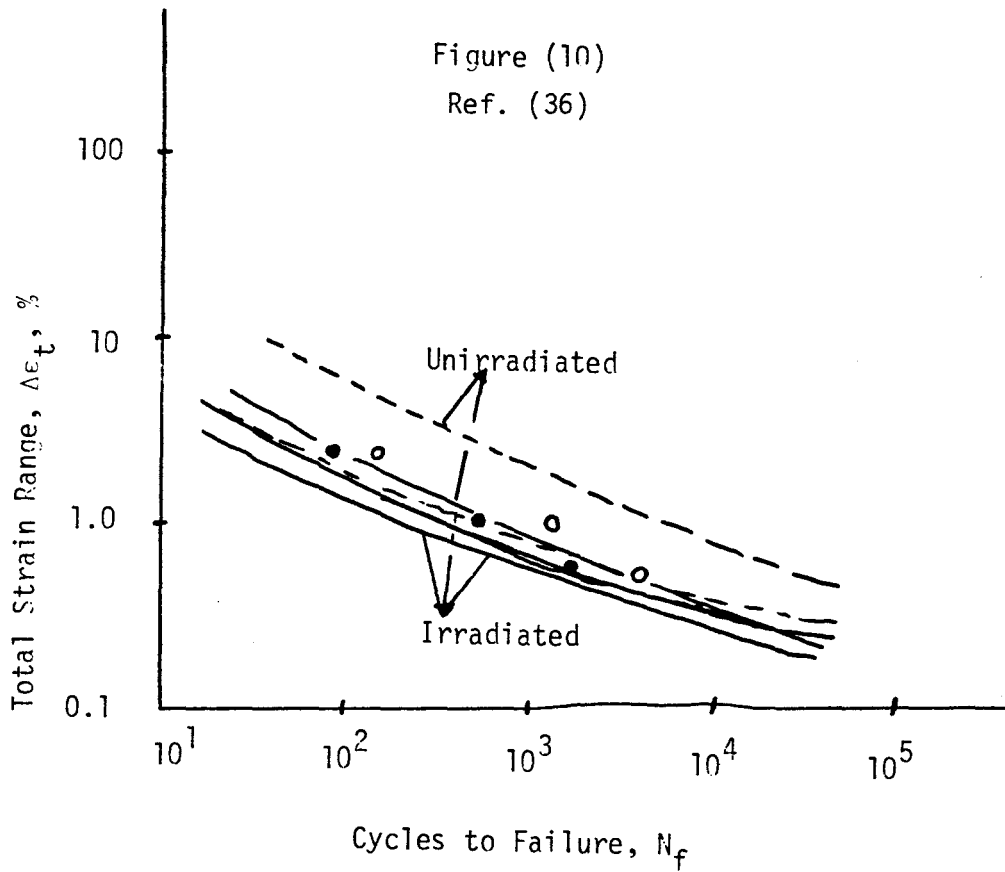


Low-Cycle-Fatigue for 316SS at 430°C and an Axial Strain Rate of  $4 \times 10^{-3} \text{ sec}^{-1}$

Figure ( 9 )  
Ref. (36)



Low-Cycle-Fatigue for 316SS at 650°C and an Axial Strain Rate of  $4 \times 10^{-3} \text{ sec}^{-1}$



Irradiated and Unirradiated Fatigue Behavior of 316SS  
tested at 700°C

● = Irradiated  $1.5 - 4.3 \times 10^{22}$  n/cm<sup>2</sup>,  $E > 0.1$  MeV

○ = Thermal control, 9240 hours at 750°C

Strain rate =  $8 \times 10^{-4}$  sec.<sup>-1</sup>

Tested in air at 700°C

\_\_\_\_\_ = Universal slopes equation

----- = Characteristic slopes equation

----- = Fraction modification



those of 316SS; the high-cycle fatigue properties are superior to those of 316SS.

The thermal properties of the refractory metal alloys (V-20Ti and Nb-1Zr) are much superior to those of 316 stainless steel. This can be seen from the thermal stress parameter (M) where Nb-1Zr has the greatest edge over the other two (316SS and V-20Ti). The higher values of M in the case of Nb-1Zr (see Figure (11)) will make the Nb-1Zr resistant to thermal stress, creep, and fatigue.

#### 4. Thermal Stress Parameter

Thermal stresses are an important source of cyclic fatigue and creep fatigue damage, particularly in pulsed fusion reactors (Tokamak). The comparative resistance to thermal stress can be estimated by a parameter, M, which is a function of thermal conductivity, thermal expansion coefficient, Poisson's ratio, Young's modulus and yield strength. Thermal stress resistance increases with increasing M, and from Figure (11) we see that the curve for Nb-1Zr from M, vs temperature is higher than that of 316SS and V-20Ti.<sup>39</sup> This will give Nb-1Zr an edge in resisting the creep and fatigue damage over the other structural materials.

$$M = \frac{2\sigma_y k(1-\nu)}{\alpha E}$$

M = Thermal stress parameter

$\sigma_y$  = Yield strength

k = Thermal conductivity

$\nu$  = Poisson's ratio

$\alpha$  = Thermal expansion coefficient

E = Young's modulus

## Thermal Stress Parameter vs. Temperature

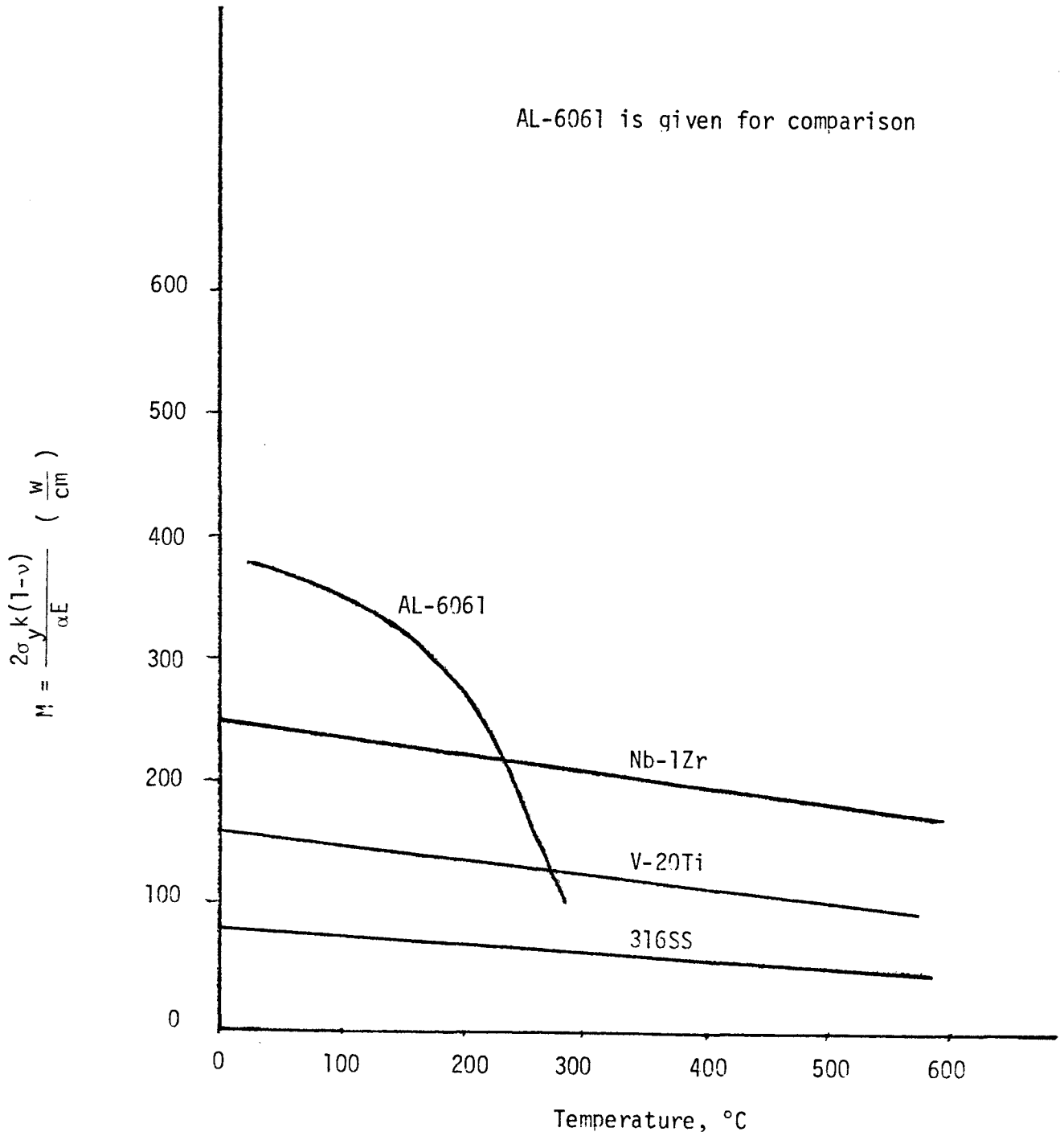


Figure (11)

Ref. (39)

COMPARATIVE STUDY IN THE USE OF 316SS, V-20Ti, AND Nb-1Zr AS A STRUCTURAL MATERIAL IN THE FIRST-WALL OF A TOKAMAK REACTOR	العنوان:
Al Morished, Mutlaq Hamad	المؤلف الرئيسي:
Johnson, Ernest F.(Super.)	مؤلفين آخرين:
1981	التاريخ الميلادي:
Princeton	موقع:
1 - 161	الصفحات:
617900	رقم MD:
رسائل جامعية	نوع المحتوى:
English	اللغة:
رسالة ماجستير	الدرجة العلمية:
Princeton University	الجامعة:
School of Engineering and Applied Science	الكلية:
الولايات المتحدة الأمريكية	الدولة:
Dissertations	قواعد المعلومات:
الهندسة النووية، فيزياء البلازما، المفاعلات النووية	مواضيع:
<a href="https://search.mandumah.com/Record/617900">https://search.mandumah.com/Record/617900</a>	رابط:

## Chapter Six

### Some General Properties of the Structural Materials

1. Fabricability and Joining
2. Induced Radioactivity
3. Cost
4. Resources Availability (U.S.A.)

## 1. Fabricability and Joining

The need to fabricate the large and complex shapes required for fusion reactors must be considered in the choice of the structural materials. Microstructural constraints necessary to produce desirable properties places an added burden on fabrication; the part must have not only a specific size and shape but a uniform and controlled internal structure as well.

There are three areas where fabrication consideration impact the choice of any alloy:<sup>18</sup>

1. Alloys must be fabricable to the desired shapes and sizes.

In many cases it may be necessary that some fabrication operations be performed at the reactor site. Alloys must be weldable, and welds must survive in the fusion reactor irradiation environment.

2. It must be possible to obtain uniform and controlled microstructures or, more likely, microstructures that have uniform and controlled properties. This is an especially difficult problem in welding where the melting action may introduce impurities, residual stresses, and a variable microstructure.

3. The structural material (316SS, V-20Ti, or Nb-1Zr) should be easy to repair by remote control after irradiation.

In comparison with stainless steels, the refractory metal alloys (Nb-1Zr and V-20Ti) are all difficult to fabricate. Moreover, there are wide variations in fabricability among different refractory metals

and even among different alloys of a particular base metal. However, tremendous advances in the forming and joining characteristics of a wide variety of refractory metal alloys were achieved during the last few years, due to the interest of using the refractory metal alloys, especially Nb-1Zr in the space program. A significant number of "sheet" alloys were produced and evaluated; this was particularly true for Nb base alloys. The strong parallels between vanadium and niobium alloys leave little doubt that V-alloys can be developed with suitable combinations of strength and formability. Hence, while fabrication will be more difficult and certainly more expensive for the refractory metal alloys than for more traditional materials (316SS), they are not likely to be ruled out on such considerations.<sup>28</sup>

More difficulty will be encountered in the area of joining of the refractory metal alloys than in basic fabricability. Joinability of the Group V alloys is extremely good; welds with nearly 100% of base metal properties can be routinely made with either gas-tungsten-arc or electron beam welding procedures. Such welding must be done, however, in extremely well controlled welding atmospheres (e.g., less than about 10 ppm interstitial impurities in the cover gas). While this may pose added difficulty or higher costs, it is still quite feasible.<sup>28</sup>

With regard to overall fabricability and joinability, the refractory metal alloys must be considered to rank far below the conventional structural alloys such as stainless steels or titanium base alloys.

There does not appear to be any basic reasons why V and Nb alloys could not be made to work in this regard; the major requirements will probably be the investment of considerable time and money to develop and implement the necessary fabrication and joining procedure.



## 2. Induced Radioactivity in the Structural Materials

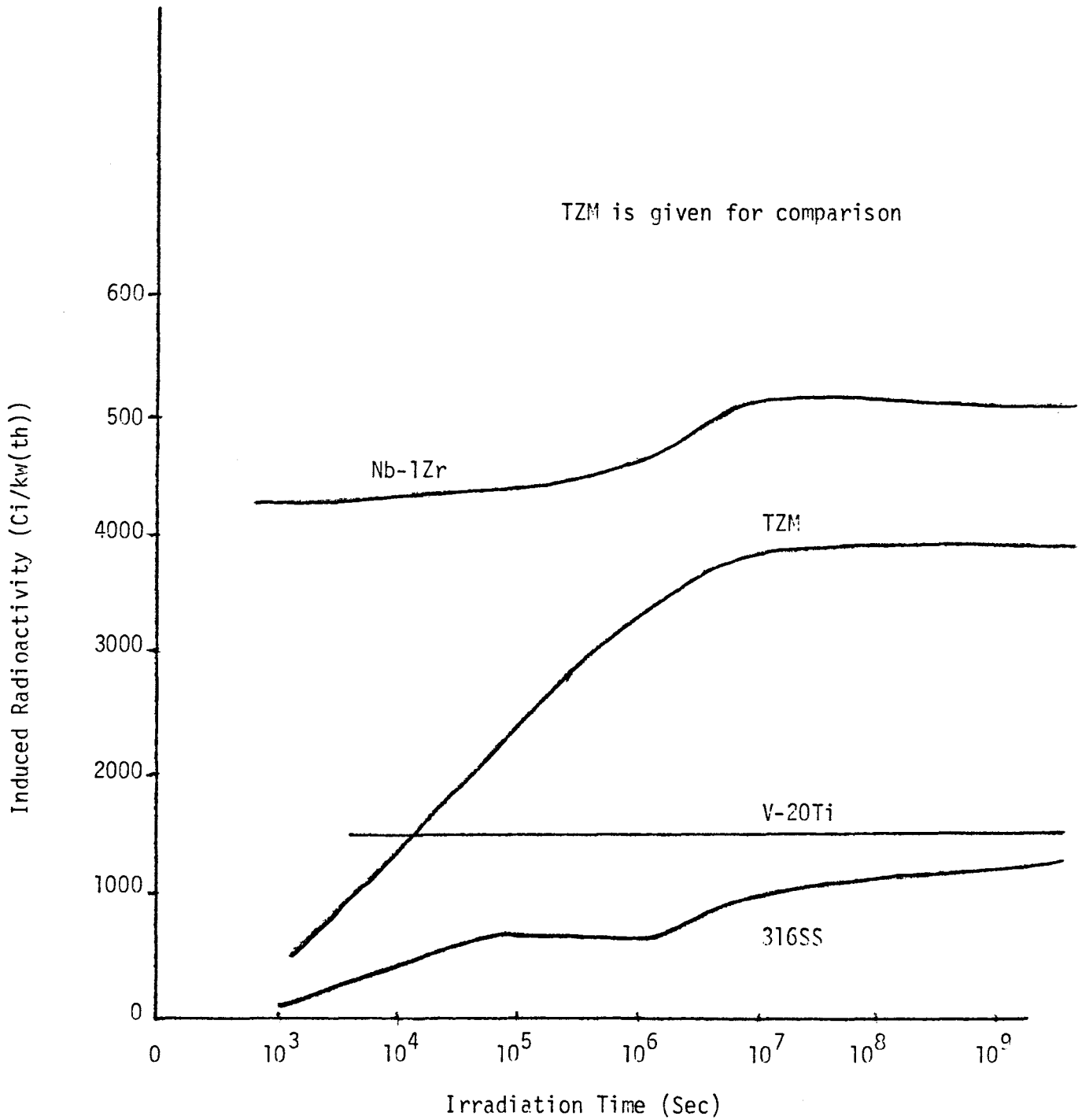
The level of radioactivity in metallic structure will decide what kind of maintenance, contact or remote control maintenance, should be used. It is clear from Figure (1) and Table (1) that all three candidate first wall structural materials become radioactive during reactor operation. They remain radioactive for a time such that there is little hope for contact maintenance of the first wall. Once the maintenance operation proceeds to the point where the shield is removed and the first wall is exposed, remote maintenance will be required, the possibility of contact or hands-on maintenance operations exist only prior to the removal of the shield and opening of the plasma chamber.

First wall components removed from the reactor after they have achieved their design life must be disposed of according to their radioactivity. Figure (2) presents the radioactivity after shutdown for 316SS, Nb-1Zr, and V-20Ti after reactor operation for two years at a neutron wall loading of  $1.25 \text{ MW/m}^2$ . Only V-20Ti exhibits rapid decay, reaching a level of  $10^{-4} \text{ Ci/KW(th)}$  in approximately 10 years.<sup>19</sup> Studies have indicated that V-20Ti could be reprocessed by conventional techniques 30 to 50 years after removal from the reactor. This means a waste disposal for a limited time (30 to 50 years), and a beneficial effect on raw material cost and resources. In the case of 316SS and Nb-1Zr, they will stay radioactive for much longer periods of time. For Nb-1Zr, the Nb94 with half-life of  $2 \times 10^4$  years will keep it radioactive at least to the level of  $6 \times 10^{-4} \text{ Ci/KW(th)}$ , and for 316SS there are many

isotopes that will keep it highly radioactive for much longer periods of time than Nb-1Zr, as shown in Table (1).<sup>19</sup>

Figure (1)

Ref. (19)



Effect of reactor operation time on induced radioactivity of 316SS, V-20Ti, and Nb-1Zr

Comparison of Induced Activity for 316SS, Nb-1Zr and V-20Ti  
(at shut down after 2 years of operation)

$$(Ci/KW(th)), P_W = 1.25 \text{ MW/m}^2$$

Table (1)

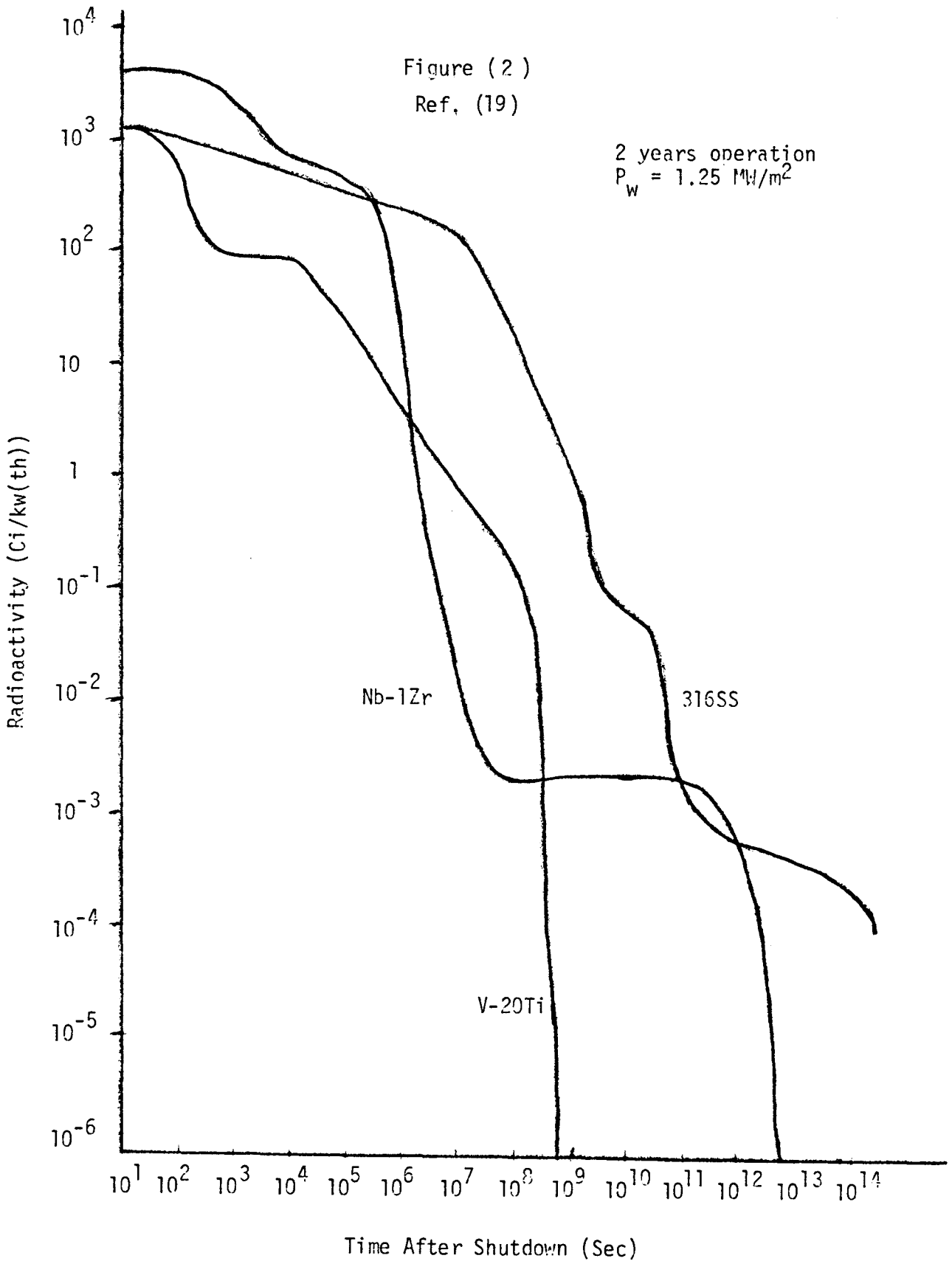
<u>Isotope</u>	<u>Half-Life</u>	<u>316SS</u>	<u>V-20Ti</u>	<u>Nb-1Zr</u>
Mg27	9.46 Min	0.036	-	-
Al28	2.3 Min	13.1	-	-
Ca45	165 Day	0.01	4.8	-
Sc46	83.9 Day	0.01	8.7	-
Sc47	3.43 Day	0.01	8.8	-
Sc48	1.83 Day	0.02	38.4	-
Sc49	58 Min	-	0.91	-
Ti45	3.09 h	-	0.43	-
Ti51	5.8 Min	0.14	79.3	-
V49	330 Day	1.17	1.69	-
V52	3.75 Min	35.4	10267	-
Cr51	27.8 Day	100	-	-
Mn53	$1.9 \times 10^6$ Yr	$5 \times 10^{-6}$	-	-
Mn54	303 Day	53.5	-	-
Mn56	2.58 h	352	-	-
Mn57	7 Day	2.43	-	-
Fe55	2.6 Yr	195	-	-
Fe59	45.6 Day	0.14	-	-
Co57	270 Day	17.4	-	-
Co58	71.3 Day	90	-	-
Co60m	10.5 Min	10.4	-	-
Co60	5.26 Yr	4.8	-	-
Ni57	36 h	3.54	-	-
Ni59	$8 \times 10^4$ Yr	$3 \times 10^{-5}$	-	-

(continued)

<u>Isotope</u>	<u>Half-Life</u>	<u>316SS</u>	<u>V-20Ti</u>	<u>Nb-1Zr</u>
Ni63	92 Yr	0.036	-	-
Sr89	52.7 Day	0.002	-	0.02
Sr90	27.7 Yr	$4 \times 10^{-6}$	-	$4 \times 10^{-5}$
Y90	64 H	-	-	11.6
Y91	58.8 Day	-	-	0.06
Zr84	78.4 h	0.18	-	2.74
Zr95	65.6 Day	0.04	-	-
Nb92m	10.2 Day	0.42	-	717
Nb94m	6.3 Min	-	-	4390
Nb94	$2 \times 10^4$ Yr	-	-	$6 \times 10^{-4}$
Nb95m	90 h	0.07	-	16.2
Nb95	35 day	0.21	-	16.6
Nb96	23.4 h	0.09	-	-
Nb97	72 Min	0.065	-	-
Mo91	15.5 Min	1.28	-	-
Mo93	10000 Yr	$5 \times 10^{-3}$	-	-
Mo99	66.7 h	28.7	-	-
Tc99m	6.87 h	28.7	-	-
Tc99	$2.15 \times 10^5$ Yr	$2 \times 10^{-4}$	-	-
Tc101	14 Min	8.3	-	-
Mo101	14.6 Min	8.3	-	-
<u>TOTAL</u>	-----	<u>1062</u>	<u>1261</u>	<u>5155</u>

Figure (2)  
Ref. (19)

2 years operation  
 $P_w = 1.25 \text{ MW/m}^2$



Radioactivity of the structural materials after shut-down

### 3. Cost

Raw material, fabrication, and completed component costs for three candidate first wall structural materials are given in the next table. Raw material cost is determined by the abundance in the Earth's crust, difficulty of processing, and the demand. Political factors can also control the price. As a class, the refractory metal raw material cost is much greater than for the conventional material, stainless steel. Likewise, the cost of fabricating representative first wall structure is considerably higher for the refractory metals. In 1977, for example, finished part costs ranged from \$29/Kg for stainless steel to \$184/Kg for vanadium alloys. Of these candidate materials, only the niobium resources may be marginal for use in a worldwide fusion power economy. In evaluating niobium resources, the fact that it is a leading constituent in superconducting material must also be considered.<sup>40</sup>

The following table shows the relative prices of Nb-1Zr, V-20Ti, and 316SS in 1977 dollars. Accounting for inflation does not affect the relative costs.

Table ( 2 )

Material	Raw Material Cost \$/Kg (1977\$)	Fabrication Cost \$/Kg	Fabricated Part Cost \$/Kg
Niobium Alloys	77	39	116
Vanadium Alloys	125	59	184
316SS	7	22	29

#### 4. Resources Availability (U.S.A.)

Resources availability is a very important factor in choosing the structural materials for a fusion reactor. If there are not enough resources to supply the materials that are needed for constructing a reasonable number of fusion reactors, then there is no point in spending time and money in studying the use of that material in a fusion reactor first-wall.

In the case of Nb-1Zr, V-20Ti, and 316SS, the most important minerals are Nb, V, Ti, Fe, Mn, and Cr.<sup>41</sup>

##### a) Niobium (Columbium)<sup>41</sup>

The most important mineral source of Nb is a ferrous columbate-tantalate. When niobium (columbium) predominates, the mineral is called columbite, and when tantalum predominates, the mineral is called tantalite.

Niobium is found in the United States in Western Colorado, but since the demand for it is very small, there has been no major established industry. The most important source of niobium has been Nigeria.

##### b) Vanadium<sup>42</sup>

The principal ores of vanadium are patronite, roscoelite, carnotite, and vanadinite. These ores have been found in Colorado, Utah, New Mexico, Arizona, and Nevada.

Again, because of the low demand for vanadium, only a small industry has been established by Vanadium Corporation of America and Union Carbide.



c) Titanium<sup>43</sup>

Titanium is the ninth ranking element in abundance in the earth's crust. It is exceeded by oxygen, silicon, aluminum, iron, calcium, sodium, potassium, and magnesium. Practically all crystalline rocks, sand, clay, and other soils contain titanium. Major sources of titanium in the U.S.A. are located in New York, Virginia, Florida and North Carolina.

The production and concentration of titanium ores have been rather sizable operations in the United States because of the rapid growth in recent years in the use of titanium dioxide pigment.

## d) Iron, Manganese, and Chromium

Iron, manganese, and chromium are the leading constituents in the making of 316SS. Iron is very abundant in the United States. Manganese is found in Arizona, Minnesota and Maine in sizable quantities. Chromium is scarce in this country and might cause a drawback for the use of 316SS in a large scale fusion economy. Chromium is available in sizable quantities from the U.S.S.R.

COMPARATIVE STUDY IN THE USE OF 316SS, V-20Ti, AND Nb-1Zr AS A STRUCTURAL MATERIAL IN THE FIRST-WALL OF A TOKAMAK REACTOR	العنوان:
Al Morished, Mutlaq Hamad	المؤلف الرئيسي:
Johnson, Ernest F.(Super.)	مؤلفين آخرين:
1981	التاريخ الميلادي:
Princeton	موقع:
1 - 161	الصفحات:
617900	رقم MD:
رسائل جامعية	نوع المحتوى:
English	اللغة:
رسالة ماجستير	الدرجة العلمية:
Princeton University	الجامعة:
School of Engineering and Applied Science	الكلية:
الولايات المتحدة الأمريكية	الدولة:
Dissertations	قواعد المعلومات:
الهندسة النووية، فيزياء البلازما، المفاعلات النووية	مواضيع:
<a href="https://search.mandumah.com/Record/617900">https://search.mandumah.com/Record/617900</a>	رابط:

## Chapter Seven

Short Look Into how the Choice and Lifetime of the Structural Material will Influence the Economics of the Tokamak as a Power Producing Plant

STRUCTURAL MATERIALS OF THE FIRST-WALL AND THE ECONOMICS  
OF THE TOKAMAK AS A POWER PRODUCER

The characteristics of the structural material strongly influence the economic potential of fusion power. The cost of energy is affected by:

1. The contribution of the cost of the structural material plus fabrication to the capital cost.<sup>44</sup>
2. The reduction in the plant availability due to the plant downtime to replace the structural material.
3. The cost of replacement which consists of the costs of the new material, maintenance equipment, and labor.<sup>44</sup>

The above effects are determined largely by:

1. The lifetime of the structural material.
2. The downtime for replacement of the first-wall.

The achievable lifetime is a function of intrinsic material properties as well as the operating conditions. The neutron wall load and the operating temperature are two key operating conditions. Higher neutron wall load and operating temperature make it possible to design reactors with higher power density and smaller capital cost; but they also lead to a shorter lifetime and increased frequency of the structural material replacement.

The considerations given above indicate that the impact of the structural material on fusion reactor economics is not determined only

by the material properties but it is also strongly influenced by a host of reactor design parameters and operating conditions. Therefore, comparative evaluations of structural materials for the purposes of making material selection must cover the following parameters:

### 1. The Effect of Fabricated Component Cost

In general, the cost of fabricating a refractory metal structure (Nb-1Zr or V-20Ti) is three to six times higher than for 316SS. This cost delta is primarily due to the higher cost of raw material. The relationship between the cost of electricity and the cost of a fabricated first-wall is shown in Figure (1) for various wall lives. This figure shows that for a life of  $10 \text{ MW}\cdot\text{yr}/\text{m}^2$ , the cost of electricity changes 2 mills/kW-hr for a \$100/kg change in the fabricated component cost. The cost spread between 316SS and the most expensive refractory metal alloy, V-20Ti, is \$155/kg, or in terms of reactor system performance, about 2.5 mills/kW-hr. Therefore, it can be concluded that the fabricated first-wall component cost has a moderate impact upon the commercial fusion reactor performance (cost of electricity). These costs can be offset by either a long component life or higher operating temperature.<sup>40</sup>

### 2. The Effect of Lifetime<sup>44</sup>

One of the major effects on the reactor economics of the lifetime of the structural material being shorter than the plan lifetime is the loss of sale of energy during plant downtime. This affects the cost of

energy only through the change in the plant availability factor,  $F$ , which can be written as<sup>44</sup>

$$F = \frac{365t_w - t_u t_w}{365t_w + t_d} \quad (1)$$

where

$t_w$  = The structural material lifetime in years

$t_d$  = The total plant downtime for replacement of the structural material

$t_u$  = The number of days of downtime per year of operation for other plant maintenance (generally  $\sim 30$  days)

The cost of energy is proportional to  $1/F$ . From these considerations, one can derive a useful relationship between structure lifetime and the increase in the cost of energy due to plant shutdown for replacement of the structure (first-wall or parts of it). This relationship can be expressed as follows. In order to limit the fractional increase in the cost of energy due to the plant downtime for replacement of the structural material to  $\delta$ , the structure lifetime must be sufficiently long to satisfy the following inequality<sup>44</sup>

$$t_w \geq \frac{t_d}{365\delta} \quad (2)$$

where  $t_w$  is in years and  $t_d$  is in days. For example, in order to limit the increase in the cost of energy to 5% (i.e.  $\delta = 0.05$ ) when the downtime

is 90 days, the structure lifetime must be greater than 4.93 years.

The advantage of Equation ( 2 ) is that it is based on simple basic principles independent of any particular system or structural material. Notice that the inequality in Equation ( 2 ) gives a lower limit on the structure lifetime since in addition to the loss of sale of energy during plant downtime, the structure replacement will also increase the cost of energy due to: (1) the cost of replacement material and labor and (2) the cost of the necessary increase in the utility's power generating reserve capacity.

An important conclusion can be deduced from Equation ( 2 ). A target lifetime for structural materials cannot be specified independent of the downtime necessary for structure replacement. The lifetime determines the frequency of replacement but the downtime is a key weighing function that determines the penalty of a replacement. The downtime is a strong function of the reactor complexity; therefore, the desirable lifetime of the structural material can vary from one design concept to another. Figure ( 2 ) shows the lifetime of the first-wall that is made of 316SS as a function of operating temperature and Figure ( 2 ) shows the lifetime of V-20Ti first-wall.

The periodic maintenance of the first-wall components of a fusion reactor will be costly and time consuming. It will be costly in the sense that a large number of connections must be uncoupled, some at least remotely, in order to remove the structure. To reduce maintenance one would like the first-wall to last as long as possible.

Figure (1)

Ref. (40)

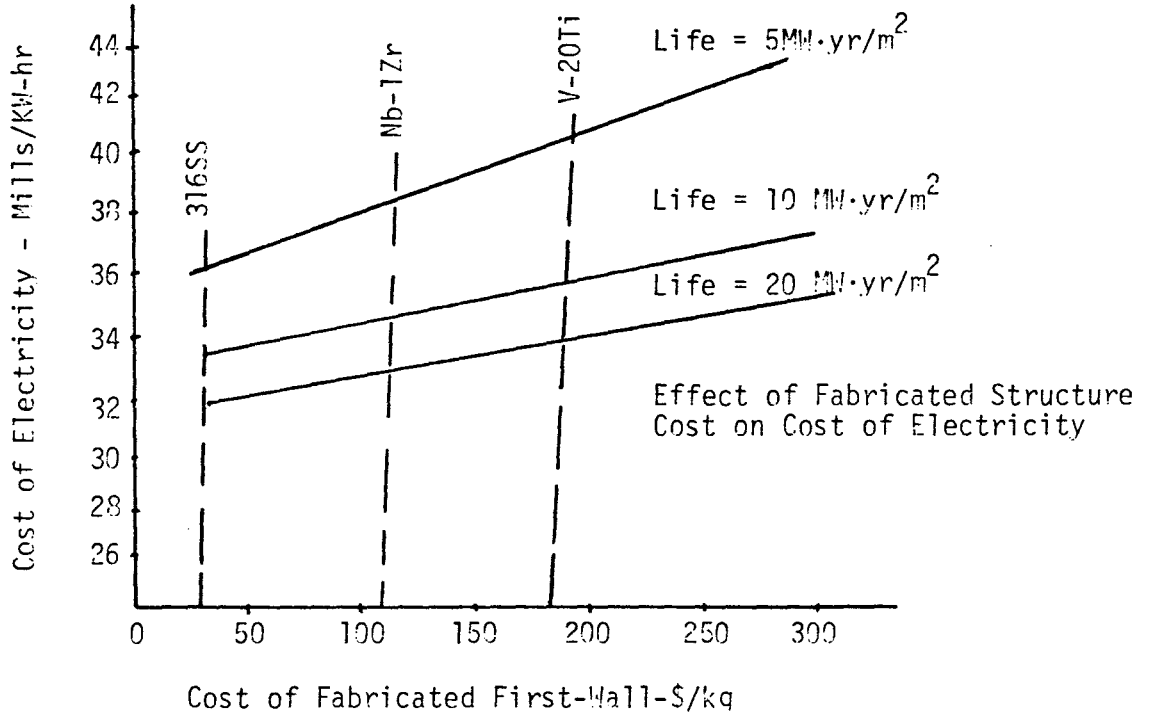
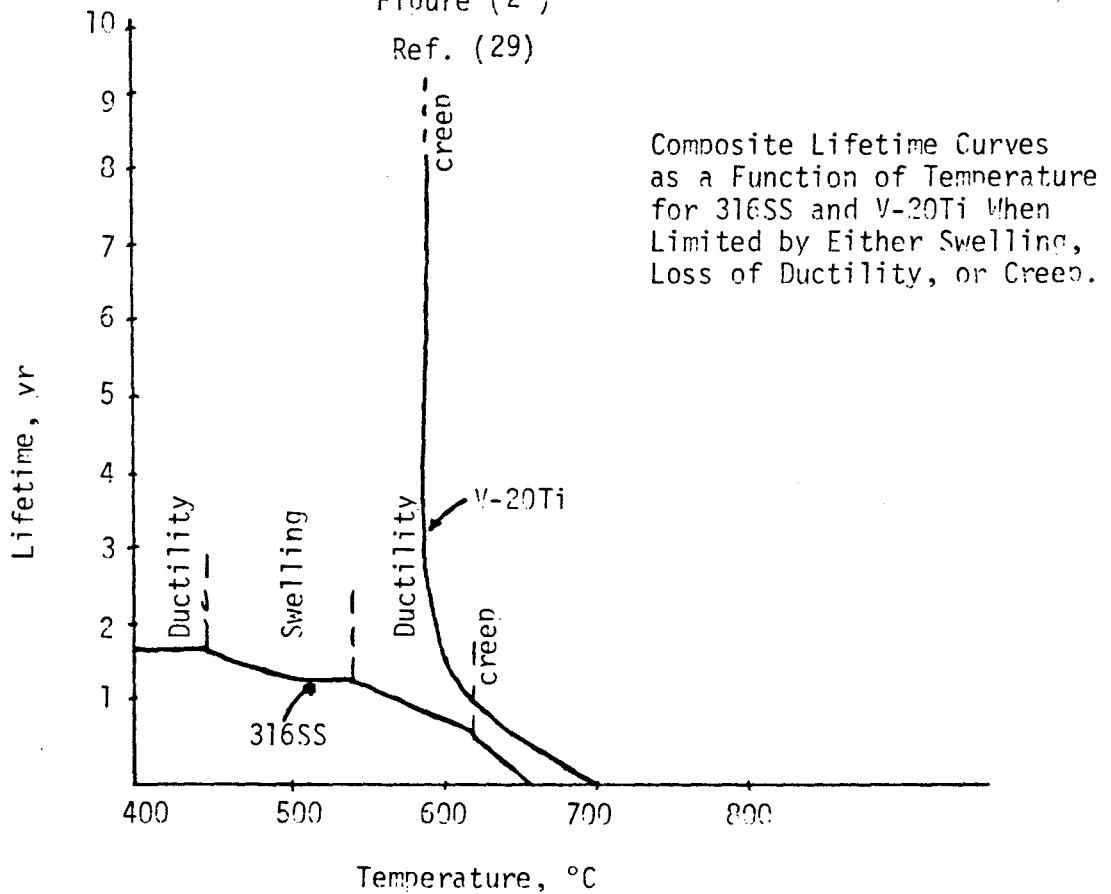


Figure (2)

Ref. (29)





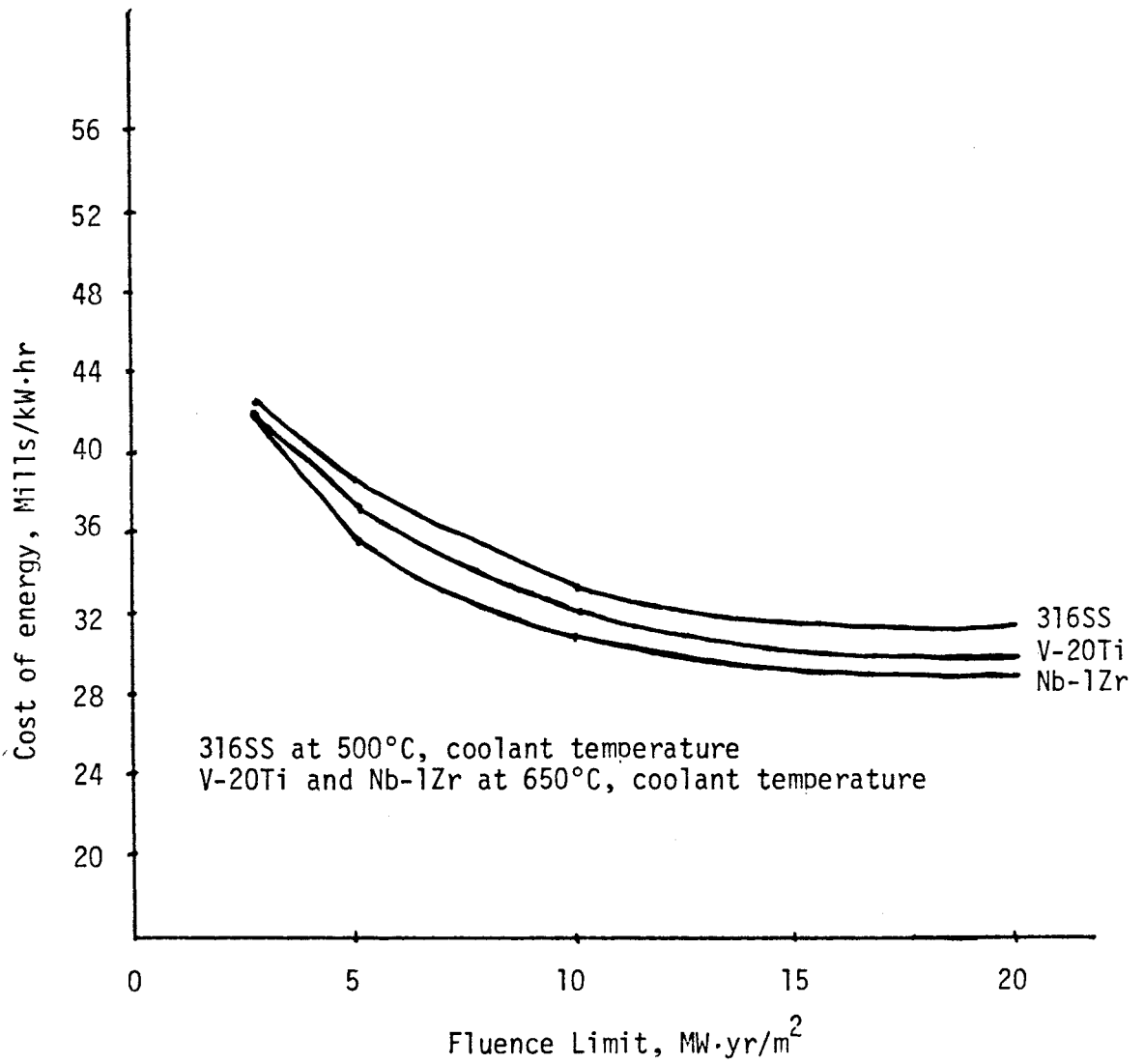
The cost/life relationship associated with using 316SS, V-20Ti, or Nb-1Zr is shown in Figure (3). This figure reveals that there is a strong economic incentive for increased wall life, if life is short. However, after about  $10 - 15 \text{ MW}\cdot\text{yr}/\text{m}^2$ , the benefits of additional life increases are greatly diminished. This cost of electricity to wall life relationship is independent of peak coolant temperature. A potentially economic advantage for the refractory metal alloys (V-20Ti and Nb-1Zr), however, results from the capability of operating with a higher coolant temperature (especially Nb-1Zr) than for 316SS.

### 3. Effect of Operating Temperature

Operating the first-wall at high temperatures results in a significant gain in the thermodynamic efficiency and a reduction in the cost per unit power. On the other hand, higher operating temperatures cause, in general, a reduction in the structural material lifetime and a decrease in the plant availability. Figure (4) shows: a) the thermodynamic efficiency,  $\eta$ , b) the fluence lifetime,  $I_w$ , in  $\text{MW}\cdot\text{yr}/\text{m}^2$ , and c) the cost of energy as a function of the maximum operating temperature for the case of 316SS. The limiting properties for 316SS are shown in Figure (2) where it has a loss of ductility from  $400 - 450^\circ\text{C}$ , swelling from  $400 - 550$  and loss of ductility from  $550 - 650^\circ\text{C}$ . The figure shows that the optimum operating temperature for 316SS is  $485^\circ\text{C}$  with the cost of energy exhibiting a broad minimum in the temperature range of  $475 - 500^\circ\text{C}$ . Figure (4) also shows that the penalty from operating at temperatures<sup>44</sup>

Figure ( 3 )

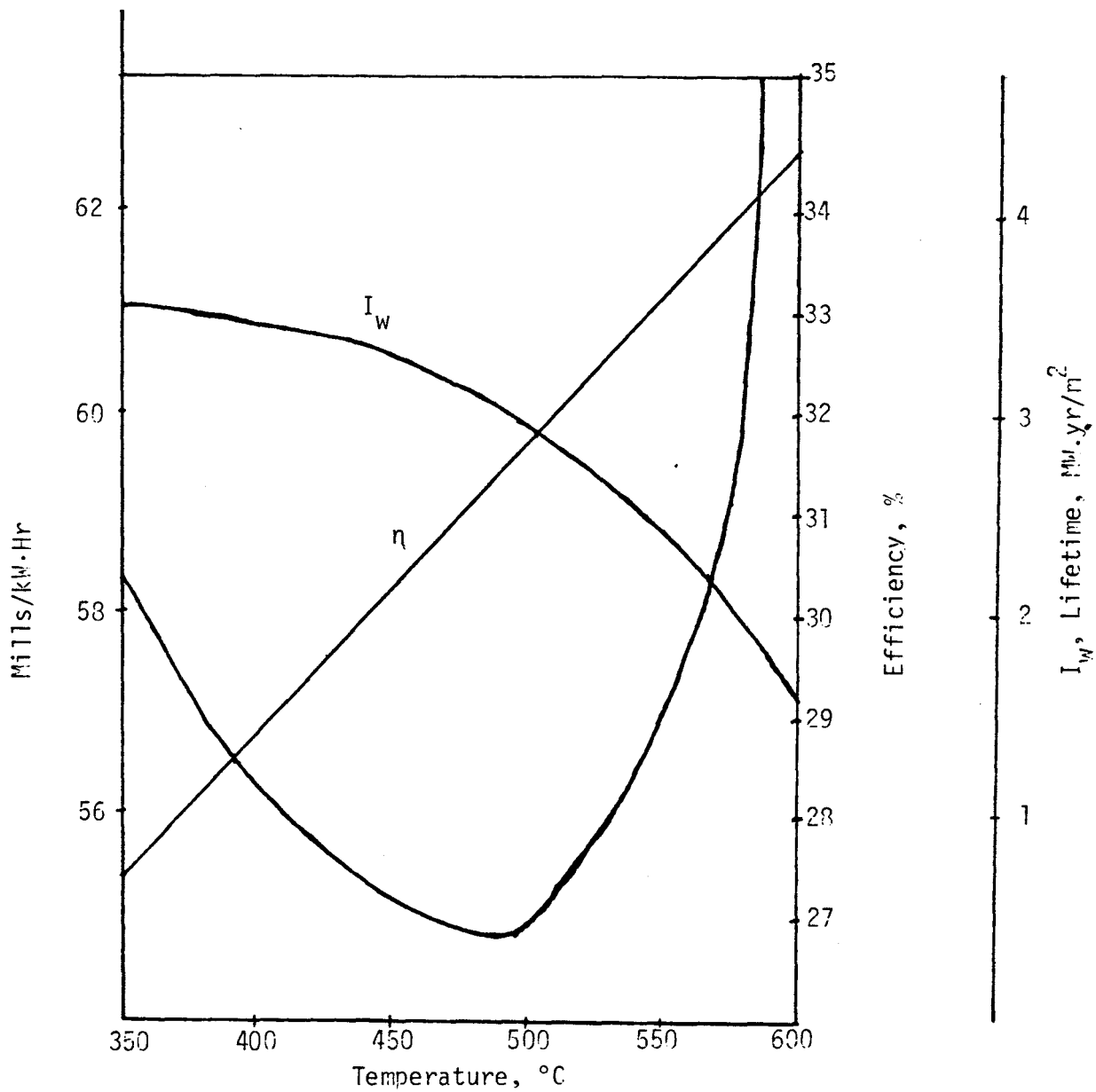
Ref. (40)



Effect of life and coolant temperature on the cost of energy

Figure ( 4 )

Ref. (44)



Efficiency, lifetime and cost of energy as functions of operating temperature for 316SS

lower than the optimum is less than that resulting from operating at temperatures higher than the optimum. This is a consequence of the fact that the relative reduction in the lifetime per unit increase in the temperature is larger at higher temperatures.

Figure (5) is similar to Figure (4) but the structural material is a V-20Ti. The life limiting properties are shown in Figure (2), where creep, with 1% end-of-life and a design stress of 103.425 MPa, is the life limiting property above 600°C. The cost of energy is minimum at 590°C with relatively small variation in the temperature range 620 - 660°C.

#### 4. Effect of Neutron Wall Load

The neutron wall load,  $P_w$ , is related to the reactor thermal power,  $P_{th}$ , as<sup>44</sup>

$$P_{th} = P_p V \epsilon = P_w A_w \epsilon (17.6/14.1) \quad (3)$$

where

$P_p$  = The average fusion power density in the plasma

$V$  = The plasma volume

$\epsilon$  = The energy multiplication factor in the blanket

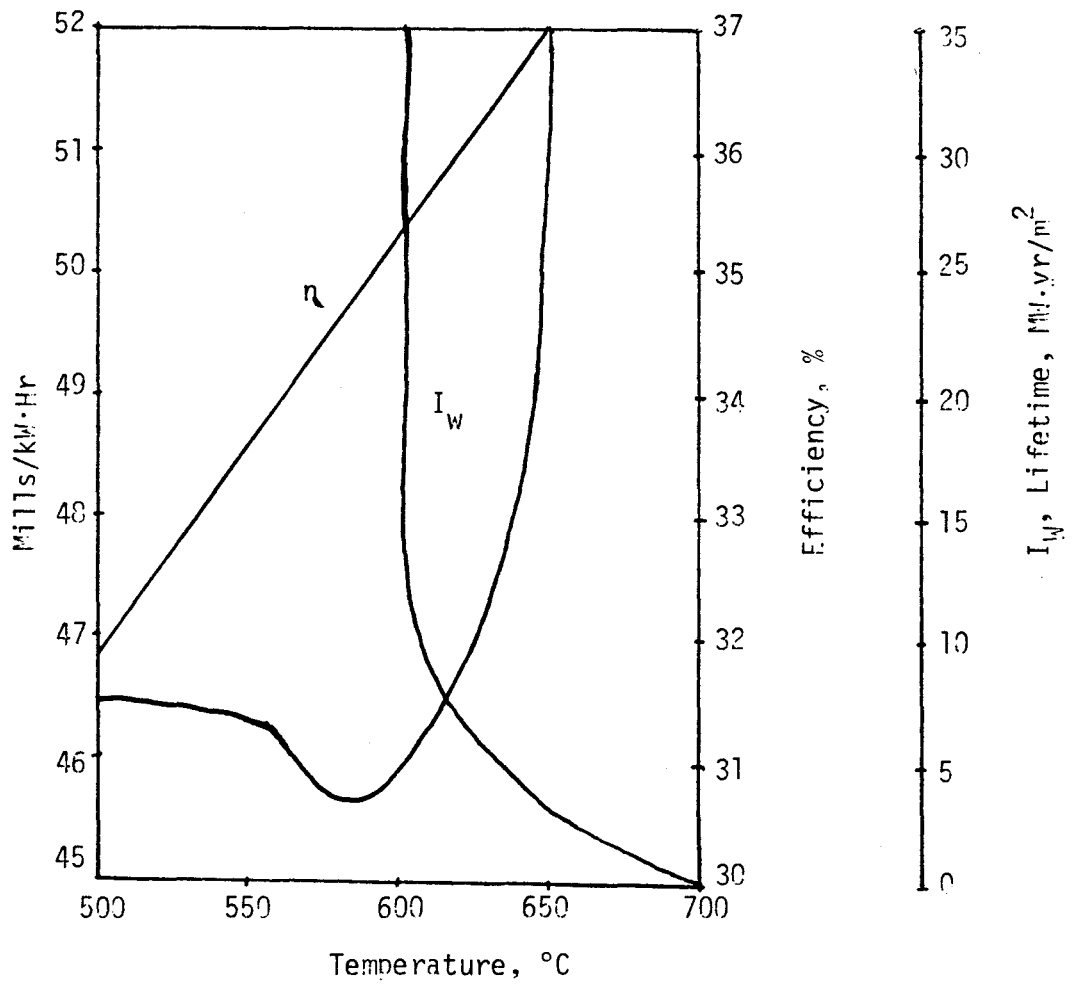
$A_w$  = The surface area of the first-wall

$P_w$  = The neutron wall load

$P_{th}$  = The reactor thermal power

Figure ( 5 )

Ref. (44 )



Variation of lifetime, thermodynamic efficiency and cost of energy with the operating temperature of V-20Ti

For the same power, higher  $P_w$  implies a smaller surface area, higher density and smaller reactor volume. This underlines the motivation for developing designs with higher neutron wall load.

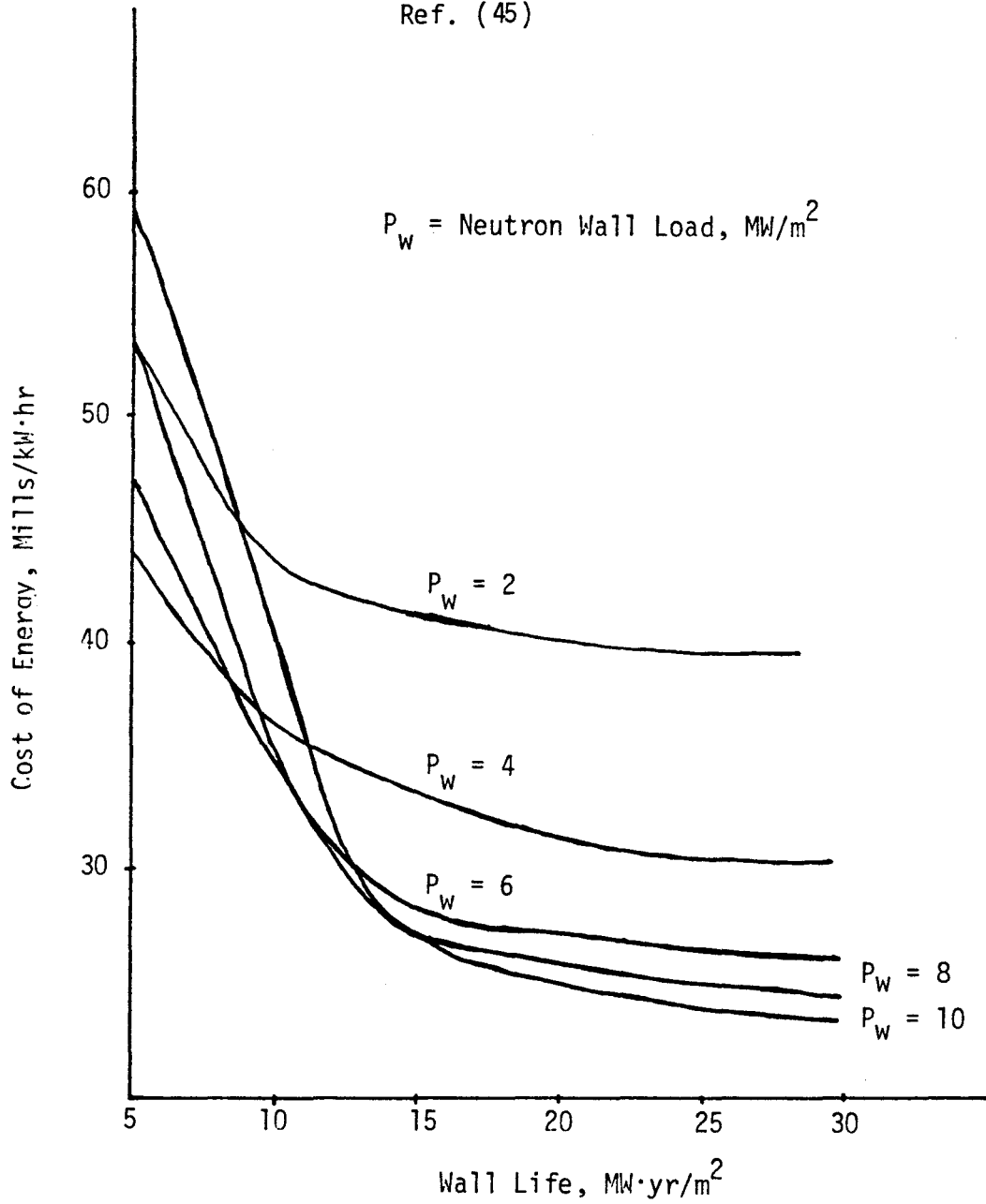
There are limitations, however, on the ability to generate and on the usability of high wall loads. These limits are dictated by:

1. The highest power density,  $P_p$ , achievable in the plasma.  $P_p$  is  $\sim \beta_t^2 B_t^4$  where  $\beta_t$  is a plasma parameter limited by stability considerations and  $B_t$  is the toroidal magnetic field in the plasma center and is limited by technology constraints on the maximum toroidal field as well as reactor geometry considerations.<sup>44</sup>
2. Limitations unique to Tokamaks on the smallness of the reactor size. In order to achieve a reasonable plasma burn-time, the Ohmic heating coil (central core) radius must be greater than a certain minimum. This sets a minimum size for the reactor and hence a maximum value for the wall load for a given reactor power.
3. Structure cooling capability. Constraints on the maximum operating temperature and thermal stresses place an upper bound on the usable wall load.
4. Structure lifetime. For a given fluence lifetime the neutron wall load has to be limited so that the frequency of structure replacement is not excessive.

Investigation of a diversity of Tokamak design concepts and wide range reactor parameters shows that reactors that have favorable economics produce a neutron wall load,  $P_w = 2 - 4 \text{ MW/m}^2$  for a reactor thermal power,  $P_{th} = 3000 \text{ MW}$  and  $P_w = 4 - 5 \text{ MW/m}^2$  for  $P_{th} = 5000 \text{ MW}$ . A condition for the validity of these results is that the lifetime of the structural material is sufficiently long compared to the downtime for replacement of the structure so that Equation (2) given in section (2) is satisfied. Figure (6) shows the effect of the neutron wall loading on the cost of energy.

Figure (6)

Ref. (45)



Effect of neutron wall loading and structural material lifetime on the cost of energy in Tokamaks



COMPARATIVE STUDY IN THE USE OF 316SS, V-20Ti, AND Nb-1Zr AS A STRUCTURAL MATERIAL IN THE FIRST-WALL OF A TOKAMAK REACTOR	العنوان:
Al Morished, Mutlaq Hamad	المؤلف الرئيسي:
Johnson, Ernest F.(Super.)	مؤلفين آخرين:
1981	التاريخ الميلادي:
Princeton	موقع:
1 - 161	الصفحات:
617900	رقم MD:
رسائل جامعية	نوع المحتوى:
English	اللغة:
رسالة ماجستير	الدرجة العلمية:
Princeton University	الجامعة:
School of Engineering and Applied Science	الكلية:
الولايات المتحدة الأمريكية	الدولة:
Dissertations	قواعد المعلومات:
الهندسة النووية، فيزياء البلازما، المفاعلات النووية	مواضيع:
<a href="https://search.mandumah.com/Record/617900">https://search.mandumah.com/Record/617900</a>	رابط:

## CONCLUSION

More experimental work must be done before one can decide which material would be best suited for the first wall of a Tokamak fusion reactor (316SS, V-20Ti or Nb-1Zr).

Based on the comparisons and data reviewed in this thesis, the factors which argue most strongly for the use of refractory metal alloys (V-20Ti and Nb-1Zr) in fusion reactor first-walls are: better surface performance in the presence of a plasma at temperatures of interest, their superior mechanical properties at temperatures above about 600°C, improved radiation resistance, much better physical and thermal properties, and potentially superior operation in liquid lithium cooled systems at high temperatures (especially Nb-1Zr).

Factors for which refractory metal alloys (V-20Ti and Nb-1Zr) are at a disadvantage relative to conventional structural alloys (316SS) include cost, more difficult fabrication and joining requirements, availability (especially in the United States), lack of an established industry, and in the area of gas - metal interactions.

The increased costs associated with the use of V-20Ti and Nb-1Zr (especially V-20Ti), both the raw material costs and fabricated structural costs and any additional costs associated with special hardware or systems which might be required to permit their use must be recoverable by permitting greater system efficiencies. If they are not, V-20Ti and Nb-1Zr will not likely be competitive with 316SS. Other than the possibility of higher operating temperatures which would favor greater efficiency, the only other window which may exist for V-20Ti and Nb-1Zr lies in the possibility of substantially increased lifetimes.

العنوان:  
COMPARATIVE STUDY IN THE USE OF 316SS, V-20Ti, AND Nb-1Zr  
AS A STRUCTURAL MATERIAL IN THE FIRST-WALL OF A TOKAMAK  
REACTOR

المؤلف الرئيسي: Al Morished, Mutlaq Hamad

مؤلفين آخرين: Johnson, Ernest F.(Super.)

التاريخ الميلادي: 1981

موقع: Princeton

الصفحات: 1 - 161

رقم MD: 617900

نوع المحتوى: رسائل جامعية

اللغة: English

الدرجة العلمية: رسالة ماجستير

الجامعة: Princeton University

الكلية: School of Engineering and Applied Science

الدولة: الولايات المتحدة الأمريكية

قواعد المعلومات: Dissertations

مواضيع: الهندسة النووية، فيزياء البلازما، المفاعلات النووية

رابط: <https://search.mandumah.com/Record/617900>

## Chapter Nine

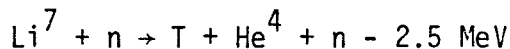
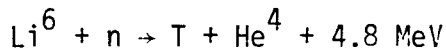
### Appendix

Hazards and Waste of Tokamak

Fusion Reactor

## FUSION AND THE ENVIRONMENT

1. Resources - are there sufficient resources for a large-scale fusion energy system? The two main resources that will be needed as fuel in a Tokamak fusion reactor are tritium (T) and deuterium (D). Tritium has a half life of 12.3 years; therefore, it is almost non-existent in nature (global natural inventory of approximately 70 kg), it must be bred. The main breeding reactions involve the neutron induced fission of lithium.



Because tritium must be bred from lithium, we come to the problem of lithium availability. Lithium resources are summarized in Table (1). Natural lithium is made of 7.4%  $\text{Li}^6$  and 92.6%  $\text{Li}^7$ .

Deuterium can be obtained from the sea water, one in 6700 atoms of hydrogen in seawater is deuterium. This amounts to 33 grams of D per  $\text{m}^3$ , or a total resource of  $4.6 \times 10^{19}$  gm in the oceans of the world.<sup>19</sup>

2. Tritium, which is  $\beta$  radioactive and can be hazardous to operators, is of concern to the fuel economy and its migration due to permeation creates hazards to the population around the reactor site. This will be discussed in great detail later in this appendix. See Table (2) for radiological data.

LITHIUM RESOURCES  
Table ( 1 ) , Ref. (19)

Nature of Deposit	PPM Li by Weight	10 <sup>12</sup> Grams of Contained Li, Range of Estimates
Silver Peak (Nevada) (Briner)	300	0.04 - 0.49
AUU.S briner	35-300	3.9 - 4.8
U.S. pegmatites	6000-7000	0.94 - 1.2
U.S. total	-	4.8 - 6.0
Canadian and African pegmatites	5000-22,000	0.34
Chilean briner	2000	1.1
Non-U.S. world total (except USSR and China)	-	1.4 - 2.0
World oceans	0.17	240,000

## RADIOLOGICAL DATA FOR TRITIUM

Ref. (3 )  
Table (2)

Radioactive half-life	12.3 years	
$\beta$ -particle energy ( $E_{\max}$ )	18.6 keV	
Biological half-life	HTO or T <sub>2</sub> O	T <sub>2</sub>
	12 days	-
Dose limit	500 m rem/yr	3 rem/yr
Critical organ	Body tissue	Skin
Maximum permissible body burden	100 Ci	-
Maximum permissible concentration in air (MPC <sub>a</sub> )	$2 \times 10^{-7}$ Ci/m <sup>3</sup>	$4 \times 10^{-5}$ Ci/m <sup>3</sup>
Maximum permissible concentration in drinking water (MPC <sub>w</sub> )	$3 \times 10^{-3}$ Ci/m <sup>3</sup>	-

3. Radioactivity - of the reactor blanket structure and the auxiliaries - e.g. injectors, resulting from irradiation by the 14.1 MeV neutrons. Some of this radioactivity can appear in other regions of the reactor (e.g. due to corrosion and subsequent transport by the circulating coolants) will be discussed later.

4. Other pollution - particularly thermal pollution. Thermal pollution is the least serious pollution problem out of all the pollution problems (acid rain, air pollution, and water pollution).

In the fusion case, the thermal pollution will be minimized by constructing some chemical processing plants which will use the heat that comes out of the fusion plant. Another approach would be to use atmospheric cooling towers to dissipate heat into the atmosphere. This approach has been used in the fission plants and has been proved to be useful in reducing the thermal pollution to acceptable levels.



RADIOACTIVE INVENTORIES OF A FUSION REACTOR IN GENERAL<sup>19</sup>

1. Tritium in the breeding medium, vacuum pumps, fuel reprocessing system, or that which is held in reserve.
2. Activated metallic structural components in the reactor blanket.
3. Shield material including structure, coolant, neutron and gamma ray absorbers.
4. Blanket coolant including impurities.
5. Breeding medium and its associated impurities.
6. Magnet structures and supports, or laser optical systems.
7. Auxiliary equipment in close proximity to the reactor, such as neutral beam injectors, vacuum pumps, control devices, etc.
8. Neutron multiplier (if required) and impurities in it.
9. Air or other gaseous environment around the reactor.
10. Biological shielding (usually concrete) and building structure.

THE MAJOR DIFFERENCES BETWEEN THE ENVIRONMENTAL IMPACT OF  
A FUSION AND A FISSION PLANT

1. In a fusion plant, there are no fission products that can lead to the release of radionuclides on a continuous basis and there are no fuel reprocessing plants where fission products would be concentrated. Also, there are no very long lived actinides.
  
2. In a fusion plant, there is a great amount of radioactivity in the form of activated structural material, but this is very dependent on what material would be used in the structure. V-20Ti has lowest radioactivity, while 316SS and Nb-1Zr have the highest.
  
3. The rates of tritium release in a fusion plant are intermediate between those for current PWRs (pressurized water reactor), and BWRs (boiling water reactor). The tritium release rates in a plant of 470 MW(e)

Fusion	2.6 Ci/day	<sup>46</sup>
PWR	11 Ci/day	<sup>46</sup>
BWR	0.13 Ci/day	<sup>46</sup>

THE FOUR MAIN SOURCES OF HAZARD TO THE PUBLIC  
OUTSIDE THE FUSION PLANT

1. Release of tritium.
2. Release of radioactive corrosion and sputtered products entrained in the coolant.
3. Release of radioactive structural and breeding material, neutron-multiplying, reflecting, shielding, electrical and organic materials.
4. Release of non-radioactive but toxic materials.

## 1. Release of Tritium

The principal radioactive substance that will be released during routine operation of fusion power plants is tritium. The inventory of tritium in a given fusion plant will vary from 10 kg to 60 kg, depending on the design and the power output of the plant. The release of this tritium or part of it will be hazardous to the public outside the plant.

There are two main pathways by which tritium in a fusion power plant could lead into the environment during normal operations.

1. The first is through the heat exchanger into the steam system, from which the tritium can escape into the condenser-coolant water, and thus into the environment (as liquid  $\text{HTO}$ ).

2. The second is diffusion through the various containment-system boundaries, and eventual escape into the air around the plant as  $\text{HT}$  or gaseous  $\text{HTO}$ .<sup>19</sup>

To solve the problem of tritium leaking into the environment by the two pathways that were mentioned earlier, the typical fusion reactor designs have dealt with the first of these pathways by making the fuel-extraction system (which removes tritium from the primary coolant) large enough and efficient enough to hold the tritium concentration in the primary coolant to very low levels. This low tritium concentration then limits the diffusion of tritium into the intermediate coolant loop (if any e.g. liquid lithium coolant does not need intermediate coolant loop), and from there into the steam system. Design values for tritium release by this pathway for most new designs are on the order of one to two Ci

per day per 1000 MW(th). The second pathway generally has been regarded as being easier to control, and the resulting emissions have been predicted to be significantly smaller. The approaches used to control this pathway include separating hot tritium inventories from cold ones and making every design effort to minimize the former, surrounding hot tritium areas with cold metal walls, and employing copper, aluminum, or ceramic coatings as diffusion barriers. The atmosphere of the plant will be monitored very carefully to detect any tritium leakage into the plant atmosphere, and if there is any, it will be vented through the plant ventilation system which has some kind of tritium getter<sup>46</sup> (e.g. Zr-AL).

By any means, tritium will get to the steam system but in a very small amount, something like 0.6 mg/day, and because of the large volume of water in the steam system (average of  $2.4 \times 10^6$  lt), it would not be worth the processing costs to recover the small quantities of tritium. Therefore, tritium in the steam system is the only thing that has been identified for consideration from the radioactive waste disposal point of view.

There are three methods of approaching this tritium leakage problem:<sup>46</sup>

1. Make the steam system as reliable as possible which will in turn make the losses from the steam system very small and then collect and store any leakage that might occur. When the plant is decommissioned, arrange for the storage or disposal of the tritiated water.

The storage approach has the advantage that under normal conditions the complete tritium inventory can be maintained within the site boundary with no impact on the environment. It also avoids the use of relatively large quantities of water that would be required if the tritiated water were discharged beyond the site boundary. The disadvantages were related to the buildup of the tritium concentration in the system. At the end of one year's operation at a 75% plant capacity factor, the inventory for 6 Ci/day leakage would be 1640 Ci or 684 Ci/l. At the end of 30 year's operation at a 75% capacity factor, the inventory would be 24 k Ci or 10 m Ci/l. With the copper barrier in the steam generator tubes, these quantities would be reduced by a factor of 6. The concentrations given above are high compared to the allowable levels,  $3 \mu$  Ci/l in unrestricted areas and  $100 \mu$  Ci/l in restricted areas - but not excessively so. Care will have to be taken during maintenance of the steam system, but provision can be made for draining the system into the condensers or a special storage tank. The materials in the system will contain absorbed tritium, and special procedures and shielding will be needed when working on the components of the system. Another disadvantage is that after the plant is decommissioned provision will have to be made for storage or disposal of the inventory. The storage method is being considered for use in currently planned pressurized water reactor plants for quantities and concentration similar to that of an average fusion plant. If an allowance of 50% is made for accumulated losses then the storage volume required would be 3.6 million liters or less than one million gallons, which is not an unusually large size of storage facility. However, this

would have to be stored for 145 years before the concentration decayed to the allowable levels to be discharged to a natural body of water.

Another matter that must be considered is the consequences of the accidental release of the tritiated water. To handle the event of release in the form of water, the plant will be designed to contain the release and provide the means for transferring it to the storage tank. Procedures will be developed for cleaning up the plant and restoring it to a safe operating condition. In the event of release as steam, it will be vented to the atmosphere. If the release is in the steam generator building, the venting will be through a 100-meter stack. The atmospheric dispersion factor at a distance of 200 m downwind for release from a 100 m stack under fumigation weather conditions is  $5.2 \times 10^{-4} \text{ sec/m}^3$ . Thus, for a 24 k Ci release, the tritium exposure would be  $12.5 \text{ Ci sec/m}^3$ . The air concentration-to-dose conversion factor for tritium is  $1.7 \times 10^{-7} \text{ (rem/yr)/(p Ci/m}^3\text{)}$  or  $0.054 \text{ rem/(Ci sec/m}^3\text{)}$ . Thus, the dose to an individual at the 200 m site boundary would be 0.675 rem. For average weather conditions, the atmospheric dispersion factor for a 100 m stack has a peak value of  $2.1 \times 10^{-5} \text{ sec/m}^3$  at 600 m. Thus, a more realistic maximum dose to off-site personnel is 0.027 rem. Both of these dosages are well below the guideline of 25 rem whole body dose for accidental releases. Because of uncertainties involved in the doses calculation, engineered safeguards will be used to reduce the credible tritium release. The steam system will be designed with stop valves that under any credible steam line rupture conditions would limit the release to about 25% of

the total inventory. For personnel within the turbine hall, the doses would be significantly higher (of the order of ten times); however, the consequences of their exposure to the high temperature steam would probably be fatal and the radiation exposure of no consequence. Likewise the damage to the plant would be that caused by the steam, and procedures would be used to decontaminate the facility so that it would be repaired and placed back in operation.

2. The second approach would be to dilute and discharge routinely to a body of water the leakages and/or an arbitrary fraction of the steam system inventory.

The approach of routinely diluting and disposing of the tritium leakage into the steam system has the advantages associated with lower inventories. The equilibrium level of the inventory would depend on the fraction of the total steam system inventory that was discharged per day. In pressurized water reactor plants, this discharge rate is of the order of 1.5% per day, which in an average fusion plant would amount to  $3.6 \times 10^4$  liters per day or 9500 gallons per day. This would require the treatment of a similar quantity of raw water as makeup, but this would pose no significant problems. The tritium concentration in the steam system would build up until the amount of tritium in the discharge equaled that diffusing into the system, that is, 6 Ci/day, which gives a concentration of  $167 \mu$  Ci/l. Under these conditions, the tritium inventory would be 400 Ci or less than 2% of the end-of-plant life inventory considered above. The radiological consequences of any accidental releases from the steam



system would be correspondingly reduced. On the other hand, the tritium concentrations are sufficiently high that the radioactive maintenance procedures necessary would not be much less stringent in their requirement than those for the no discharge case considered earlier.

If the continual discharge is handled by release to off-site bodies of water, considerable dilution will be required to reduce the specific activity to acceptable levels. However, it is considered unrealistic to assume that many land based sites would exist at the time any fusion plant might be built at which such large quantities of water would be available.

3. The third would be to release the leakage to the atmosphere by evaporation and blowdown from the plant's cooling towers or by venting steam through an elevated vent.

Probably the most satisfactory method of handling the tritium release would be by direct discharge to the atmosphere. One method to accomplish this would be to dump the discharge from the steam system into the condenser cooling system and allow the tritium to be carried away with the evaporative losses from the cooling towers. However, the magnitude of those losses would depend on the atmospheric conditions and whether the towers were being operated in the set or dry mode. For wet mechanical draft cooling towers at a site with normally low relative humidity, the evaporative losses would be about  $1.4 \times 10^8$  l/day and the blowdown requirements  $0.7 \times 10^8$  l/day. For 6 Ci/day discharge, the equilibrium concentrations would be  $2.9 \times 10^{-2}$   $\mu$  Ci/l, and the blowdown water would

be discharged without dilution. Because of the complexity of the analysis involved, the annual dose to off-site personnel due to tritium in the cooling tower plume has not been estimated. However, it will probably be of the same order of magnitude as that shown below for direct steam release and perfectly acceptable.

A more direct way of discharging the tritium to the atmosphere would be to vent the releases from the steam system through a 100 m high vent. For adverse weather conditions, i.e., fumigation, the atmospheric dispersion factor at 200 m downwind would be  $5.2 \times 10^{-4} \text{ sec/m}^3$ . For release of 6 Ci/day or  $69 \mu \text{ Ci/sec}$ , the tritium concentration would be  $3.6 \times 10^4 \text{ p Ci/m}^3$ , and the dose to an individual at that location would be 61 mrem per full power year or 46 mrem/yr for a plant capacity factor of 75%, which is about 2.3 times the guidelines for the fission reactors. However, for average conditions the atmospheric dispersion factors has a maximum value of  $2 \times 10^{-6} \text{ sec/m}^3$  at 600 m downwind and the corresponding annual dose for a plant capacity factor of 75% would be 0.18 mrem or a factor of about 100 lower than the guidelines.

## 2. Radioactivity in Fusion Reactor Coolants

The primary coolants that have been seriously considered for D-T Tokamak fusion reactors are

1. Helium gas<sup>19</sup>
2. Liquid Lithium<sup>19</sup>

1. The only significant activity induced in pure helium is the  $\text{He}^4 (n, \alpha) \text{He}^5$  reaction. Since  $\text{He}^5$  with half-life of  $10^{-21}$  sec, the activity will build up to approximately 0.5 Ci/W at normal temperatures and pressures of a helium coolant, because of the short half-life. Therefore, radioactivity in helium coolant does not have any importance from the waste generation and disposal point of view. Some impurities in the helium will have some activity, but this can be removed by appropriate clean-up techniques.

2. Liquid lithium generates no significant radioisotopes other than the tritium. However, as with any material, there are normally a large variety of impurities atoms which can become radioactive. Some impurities normally contained in liquid lithium are listed in Table (3). P.J. Persiani has studied the problem in great detail and noticed that activation of such impurities as Fe, Ni, Cr, Ta could lead to some problems, especially when these impurities tend to concentrate in specific parts of the plant such as valves, pumps, or heat exchangers.

Aside from the radioactivity in the lithium coolant, lithium is very reactive with oxygen and could be a fire hazard.

## TYPICAL IMPURITIES FOUND IN HIGH PURITY LITHIUM

Table ( 3 )

Element	Maximum Concentration (PPM per weight)	Approximate Activity After Two Years of Exposure (Ci/kW(th))
Si	50	Low
O	100	Low
N	500	Low
Ca	100	< 1
Na	100	< 2
K	100	< 2
Fe	100	< 1
Ni	100	< 1
Cr	100	< 1
Ta	100	< 0.1
F	3000	< 10
Cl	3000	< 10

Ref. (19)

### 3. Radioactivity in the Metallic Structure

There have been many studies about the hazard of tritium in fusion reactors, but there is hardly any concerning the hazard of the release of neutron-activation products in the first-wall structure.

Release of neutron-activation products in severe hypothetical fusion reactor accidents may constitute a larger health hazard to the public outside the fusion plant than that of the tritium released at the same time. There are many ways that the activation-products could get into the environment, but the most serious ones are:<sup>47</sup>

1. Fire capable of melting activated structure or raising it to temperatures great enough to drive off some of the contained activation products (e.g., lithium fires)
2. Breach of containment, giving air access to heated structural materials to produce volatile oxides of some of the contained activation products (e.g., earthquake, tornado, sabotage, etc.)
3. Combinations of one and two.

The possibility of releasing activation products from structural materials in the event of a lithium fire depends in part on the possibility of actually melting the material (adiabatic flame temperature is 2400°K for the lithium-air reaction and 2100 to 2500°K for the lithium-concrete reaction). The melting point for the material interest is shown in Table (4).

Unfortunately, structural activation products have a potential pathway for release short of gross melting of the structure. Specifically, many of the metals involved form oxides that are volatile - that is, which sublime or evaporate significantly - at temperatures well below the melting point of the metal itself (see Table (4)).

Table (4), Ref. (47)

<u>Materials</u>	<u>Melting Point, °C</u>
316SS	1550
Nb-1Zr	2400
V-20Ti	1900
<u>Oxides</u>	
CrO <sub>3</sub>	237.8
MnO <sub>2</sub>	604.4
NbO	1215.6
ZrO <sub>2</sub>	1632.2
VO <sub>2</sub>	965.6
V <sub>2</sub> O <sub>5</sub>	504.4
TiO <sub>3</sub>	504.4

Table ( 5 ) shows the hazard to human health associated with the releases of various radioactive materials, which was obtained by dividing the number of curies of an isotope assumed to escape by the maximum permissible concentration (MPC) for that isotope in the medium of concern (air or water). Since the MPC can be expressed in curies per cubic meter, the resulting quotient is a volume of air or water sufficient in principle to dilute the released isotope to the permissible level. This dilution volume provides a common unit measure by which the hazards of drastically different isotopes can be compared. It is sometimes called the biological hazard potential (BHP). The BHP in Table ( 5 ) shows how hazardous the release of activation products of a first wall (316SS, Nb-1Zr) compared to that of tritium. Table ( 6 ) shows the boundary doses in the case of 316SS, Nb-1Zr and tritium. See Table ( 7 ) for specific BHP of the three structural materials.

#### 4. Release of Non-Radioactive but Toxic Materials

There are several elements in the current fusion reactor designs which could represent an inhalation hazard if they were to be spread throughout the atmosphere. The probability of such an event is extremely small. These elements are Be, B, Cr, Ca, Pb, Li, Hg, Mo, and Ni. The most toxic of these is Be (beryllium) which has been proposed as a neutron multiplier in a fusion reactor with solid breeding medium. The problem with Be is normally connected to the use of solid breeders, and it is not inherent to fusion power if liquid lithium is used as a breeder.

Table (5), Ref. (47)  
BHP for Severe Fusion Accident

Material	Isotope	Half-Life	Nominal Release Fraction	Inventory for 1.5 GW(e) $10^6\text{Ci}$	Lowest Air MPC, Ci/m <sup>3</sup>	BHP $10^6\text{km}^3$ Air t=0	BHP $10^6\text{km}^2$ Air t=30 days
316SS	$^{51}\text{Cr}$	27.8 days	0.20	500	$8 \times 10^8$	1.3	0.6
	$^{54}\text{Mn}$	313 days	0.20	270	$1 \times 10^9$	54	51
	$^{56}\text{Mn}$	2.68 hr	0.20	1800	$2 \times 10^8$	18	0
	$^{55}\text{Fe}$	2.6 yr	0.04	980	$3 \times 10^8$	1.3	1.3
	$^{58}\text{Co}$	71.3 days	0.20	450	$2 \times 10^9$	45	34
	$^{99}\text{Mo}$	66.7 hr	0.20	140	$7 \times 10^9$	4.0	0
Nb-1Zr	$^{92\text{m}}\text{Nb}$	10.2 days	0.008	3600	-	-	-
	$^{95}\text{Nb}$	35 days	0.008	83	$7 \times 10^9$	0.2	0.1
Tritium	T	12.3 yr	0.80	930	$2 \times 10^7$	3.7	3.7



Table (6), Ref. (47)  
Boundary Doses from Airbourne Isotopes in Severe Fusion Accident

Isotope	Quantity Released $10^6\text{Ci}$	Cloud Dose Conversion, rem per $\text{Ci}\cdot\text{sec}/\text{m}^3$	Inhalation Dose Conversion, rem/Ci	Cloud Dose at Plant Boundary, rem	Inhalation Dose at Boundary, rem	Total Boundary Dose, rem
$^{51}\text{Cr}$	100	$5.7 \times 10^2$	240	310	4800	5100
$^{54}\text{Mn}$	54	$1.5 \times 10^1$	1300	430	14000	14000
$^{56}\text{Mn}$	170	$1.5 \times 10^1$	67	1360	2300	3700
$^{55}\text{Fe}$	39	$4.1 \times 10^2$	26	90	200	290
$^{58}\text{Co}$	90	$1.8 \times 10^1$	800	870	14400	15000
$^{99}\text{Mo}$	27	$3.3 \times 10^2$	125	50	700	750

## Nb-Zr

$^{92\text{m}}\text{Nb}$	29	$1.7 \times 10^1$	900	270	5200	5500
$^{95}\text{Nb}$	0.7	$1.4 \times 10^1$	575	5	80	85

## Tritium

T	740	0.0	42	0	6200	6200
---	-----	-----	----	---	------	------

SPECIFIC BIOLOGICAL HAZARD POTENTIALS OF THE STRUCTURAL  
MATERIALS (316SS, V-20Ti, and Nb-1Zr)  
(URANIUM IS GIVEN FOR COMPARISON)

	BHP <sub>air</sub> (km <sup>3</sup> of air/cm <sup>3</sup> of material) t = 0	BHP <sub>water</sub> (km <sup>3</sup> of water/cm <sup>3</sup> of material)	
		100 years	10,000 years
316SS	2.0	5.4	0.03
V-20Ti	0.2	2x10 <sup>-30</sup>	0
Nb-1Zr	0.36	0.6	0.3
Natural Uranium	1.3 x 10 <sup>-3</sup>	0.2	0.2

Table (7)

Ref. (19)

## LIQUID WASTE IN TOKAMAK

The amount of radioactive liquid waste generated at the fusion plant is expected to be small. No liquids are used directly in the fusion process or come in direct contact with tritium during normal operation.

Demineralized water will be used to cool various components of the plant, but in all cases the water is contained in a closed primary loop, and secondary coolant loops are used to dissipate waste heat to the environment.

Small quantities of liquids may be generated during the servicing and maintenance of equipment that come in contact with tritium. These things will be solidified or collected on an absorbant and packaged as a solid material for off-site disposal.

## CONCLUSION

The hazards and wastes of a fusion plant seems at the present to be less than that of a conventional plant or a fission plant. Under normal operating conditions, there are no gases to be vented to the atmosphere or fuel processing outside of the fusion plant. There are no chances of reactor meltdown because the impurities coming out of the first-wall will tend to cool the plasma to low temperatures where the fusion reaction cannot sustain itself.

The hazards of a fusion plant are like that of any plant that uses high temperatures and high pressures. The presence of tritium in a fusion plant will cause some radiation hazards, but the safeguards which already exist in the fission plants can be used in any fusion plant.

COMPARATIVE STUDY IN THE USE OF 316SS, V-20Ti, AND Nb-1Zr AS A STRUCTURAL MATERIAL IN THE FIRST-WALL OF A TOKAMAK REACTOR	العنوان:
Al Morished, Mutlaq Hamad	المؤلف الرئيسي:
Johnson, Ernest F.(Super.)	مؤلفين آخرين:
1981	التاريخ الميلادي:
Princeton	موقع:
1 - 161	الصفحات:
617900	رقم MD:
رسائل جامعية	نوع المحتوى:
English	اللغة:
رسالة ماجستير	الدرجة العلمية:
Princeton University	الجامعة:
School of Engineering and Applied Science	الكلية:
الولايات المتحدة الأمريكية	الدولة:
Dissertations	قواعد المعلومات:
الهندسة النووية، فيزياء البلازما، المفاعلات النووية	مواضيع:
<a href="https://search.mandumah.com/Record/617900">https://search.mandumah.com/Record/617900</a>	رابط:

## REFERENCES

1. Edwin E. Kintner, The Role of Materials in the Future of Fusion, *Journal of Nuclear Materials*, 85 and 86 (1979) 3.
2. G.L. Kulcinski, Bulk Radiation Damage to First-Wall Materials, *Fusion Reactor Design Problems*, International Atomic Energy Agency, Vienna, (1974).
3. H. Conrads, Radiation Damage in Components of a Fusion Reactor, *Survey of Fusion Reactor Technology*, Commission of the European Communities, Report prepared by the Euratom Fusion Reactor Technology Advisory Group (1972) 99.
4. E.E. Bloom, Mechanical Properties of Materials in Fusion Reactor First-Wall and Blanket Systems, *Journal of Nuclear Materials* 85 and 86 (1979) 795.
5. L.J. Pionke: Technical Assessment of Niobium Alloys Data Base for Fusion Reactor Application, COO-4247-2. U.S. Department of Energy, August 1979.
6. A.D.G. Stewart and M.W. Thompson, *Journal of Material Science* 42 (1971) 1145.
7. M.W. Thompson, *Defects and Radiation Damage in Metals*, p. 113, Cambridge University Press, London (1968).
8. B. Navinsek, Sputtering - Surface Changes Induced by Ion Bombardment, *Progress in Surface Science*, Vol. 7, No. 2 (1976) edited by Professor Sydney G. Davison.
9. J. Lindhard, *Matt. Fys. Medd.* 34 (1965) 14.
10. D.L. Smith, Physical Sputtering Model for Fusion Reactor First-Wall Materials, *Transaction of American Nuclear Society*, No. 27 (1977) 265.
11. D.L. Smith, Physical Sputtering Model for Fusion Reactor First-Wall Materials, *Journal of Nuclear Materials* 75 (1978) 20.
12. G.L. Kulcinski and G.A. Emmert, First-Wall Surface Problems for a D-T Tokamak Reactor, *Journal of Nuclear Materials* 53 (1974) 31.
13. J. Roth, R. Behrisch and B.M.U. Scherzer, Blistering of Niobium Due to 0.5 to 9 keV Helium and Hydrogen Bombardment, *Journal of Nuclear Materials* 53 (1974) 147.
14. S.K. Das and M. Kaminsky, Comparative Study of Blistering in Nb, V, and V-20Ti.

15. G.J. Thomas and W. Bauer, Surface Deformation in He and H Implanted Metals, *Journal of Nuclear Materials* 53 (1974) 134.
16. S.K. Das and M.K. Kaminski, Radiation Blistering of Structural Materials for Fusion Devices and Reactors, *Journal of Nuclear Materials* 53 (1974) 115.
17. K.M. Zwilsky, Materials Research Programme for Fusion Reactors, Fusion Reactor Design Problems, International Atomic Energy Agency, Vienna, 1974.
18. The Fusion Reactor Materials Program Plan, COE-ET-0032/1, U.S. Department of Energy, July 1978.
19. W. Hafele, J.P. Holdren, G. Kessler, and G.L. Kulcinski, Fusion and Fast Breeder Reactors, p. 381, International Institute for Applied Systems Analysis, Laxenburg 1977.
20. F.W. Wiffen and E.E. Bloom, Effect of High Helium Content on Stainless Steel Swelling, ORNL-TM-4541, U.S. Atomic Energy Commission, May 1974.
21. H. Tang and J. Moteff, The Influence of Neutron Irradiation Temperature on the Void Characteristics of Niobium and Nb-1Zr Alloy, Radiation Effects and Tritium Technology for Fusion Reactors, Vol. I, 1976, edited by J.S. Watson and F.W. Wiffen, Nuclear Metallurgy Committee of Aime.
22. A.D. Brailsford and R. Bullough, The Rate Theory of Swelling Due to Void Growth in Irradiated Metals, *Journal of Nuclear Materials* 44 (1972) 121.
23. A. Kothe, Proceedings, Defects in Refractory Metals, p. 125, Mol. Belgium, 1972.
24. R.E. Gold, D.L. Harrod, R.L. Ammon, R.W. Buckman, Jr., and R.C. Svedberg, Technical Assessment of Vanadium-Base Alloys for Fusion Reactor Applications, COO-4540-1 (Vol. 1). U.S. Department of Energy, April 1978.
25. F.W. Wiffen, The Effect of Alloying and Impurity on the Formation and Ordering of Voids in BCC Metals, ORNL-TM-3496. U.S. Atomic Energy Commission, September 1971.
26. R.F. Mattas and D.L. Smith, Model for Life-Limiting Properties of Fusion Reactor Structural Materials, *Nuclear Technology* 39 (1978) 186.
27. Nuclear Systems Materials Handbook, Vol. I, Design Data. TID-26666.

28. R.E. Gold and D.L. Harrod, Refractory Metal Alloys for Fusion Reactor Applications, *Journal of Nuclear Materials* 85 and 86 (1979) 805.
29. R.F. Mattas and D.L. Smith, Modeling of Life-Limiting Properties of Fusion Reactor Structural Materials, ANL/FPP/TM-84, May 1977.
30. W.F. Vogelsang, G.L. Kulcinski, R.G. Lott, and T.Y. Sung, Transmutation, Radioactivity, and Afterheat in D-T Tokamak Fusion Reactor, *Nuclear Technology* 22 (1974) 379.
31. J.H. Devan, Compatibility of Structural Materials With Fusion Reactor Coolant and Breeder Fluids, *Journal of Nuclear Materials* 85 and 86 (1979) 249.
32. S. Timoshenko and D.H. Young, *Element of Strength of Materials*, D. Van Nostrand Co., New York, 1968.
33. F.W. Wiffen, Creep and Tensile Properties of Helium Injected Nb-1Zr, ORNL/TM-5397, May 1976.
34. Horst Bohm, The Effect of Neutron Irradiation on the High Temperature Mechanical Properties of Vanadium-Titanium Alloys, Defects and Defect Clusters in B.C.C. Metals and Their Alloys, *Nuclear Metallurgy*, Vol. 18, edited by R.J. Arsenault.
35. F.W. Wiffen, The Effect of CTR Irradiation on the Mechanical Properties of Structural Materials, ORNL/TM-5624, November 1976.
36. J.B. Conway, R.H. Stentz and T.T. Berling, Fatigue, Tensile, and Relaxation Behavior of Stainless Steels, Technical Information Center, Office of Information Services, U.S. Atomic Energy Commission, 1975.
37. C.R. Brinkman, G.E. Karth, and T.M. Beeston, Influence of Irradiation on the Creep/Fatigue Behavior of Several Austenitic Stainless Steel and Incoley 800 at 700°C, TSTM-STP 529.
38. K.C. Liu, Mechanical Properties Testing of Unirradiated Path C Alloys, Alloy Development for Irradiation Performance DOE/ET-0058/1, U.S. Department of Energy, August 1978.
39. R.W. Conn, Tokamak Reactors and Structural Materials, *Journal of Nuclear Materials*, 85 and 86 (1979) 9.
40. J.W. Davis, Economic Impact of Using Refractory Metals in Fusion Reactors, COO-4247-1, McDonnell Douglas Astronautics Company (1977).
41. Leonard F. Xntema and Alan L. Percy, Tantalum and Columbium, *Rare Metals Handbook*, Edited by Clifford A. Hampel, Reinhold Publishing Corporation, New York, 1956.



42. H.E. Dunn, D.L. Edlund, and T.G. Griffin, Vanadium, Rare Metals Handbook, Edited by Clifford A. Hampel, Reinhold Publishing Corporation, New York, 1956.
43. H.R. Ogden and Bruce W. Gonser, Titanium, Rare Metals Handbook, Edited by Clifford A. Hampel, Reinhold Publishing Corporation, New York, 1956.
44. M.A. Abdou and Z. El-Derini, A. Comparative Study of the Performance and Economics of Advanced and Conventional Structural Materials in Fusion Systems, Journal of Nuclear Materials 85 and 86 (1979) 57.
45. S.D. Harkness and B. Cramer, A. Review of Lifetime Analysis for Tokamaks, Journal of Nuclear Materials 85 and 86 (1979) 135.
46. A. Fusion Power Plant, R.G. Mills, ed., Princeton Plasma Physics Laboratory Report MATT-1050 (1974).
47. John P. Holden, Contribution of Activation Products to Fusion Accident Risk, Nuclear Technology/Fusion, 1 (1981) 79.